Forschungszentrum Jülich
in der Helmholtz-Gemeinschaft

Institut für Werkstoffe und Verfahren der Energietechnik
Institut 3: Energieverfahrenstechnik

Grundlagenuntersuchungen und neue Entwicklungen von Brennstoffzellen-Membranen

72. AGEF-Seminar

04. Dezember 2002 in Jülich
Tagungsband

herausgegeben von Detlef Stolten und Klaus Wippermann

Jül-4013

Grundlagenuntersuchungen und neue Entwicklungen von Brennstoffzellen-Membranen

72. AGEF-Seminar

04. Dezember 2002 in Jülich
Tagungsband

herausgegeben von Detlef Stolten und Klaus Wippermann

Berichte des Forschungszentrums Jülich ; 4013
ISSN 0944-2952
Institut für Werkstoffe und Verfahren der Energietechnik
Institut 3: Energieverfahrenstechnik Jül-4013

Zu beziehen durch: Forschungszentrum Jülich GmbH · Zentralbibliothek
D-52425 Jülich · Bundesrepublik Deutschland
☎ 02461/61-5220 · Telefax: 02461/61-6103 · e-mail: zb-publikation@fz-juelich.de

VORWORT:

Das **72. AGEF-Seminar** fand am 4. Dezember 2002 im Forschungszentrum Jülich statt und wurde dort vom Institut für Werkstoffe und Verfahren der Energietechnik IWV-3 (http://www.fz-juelich.de/iwv/d-iwv3.html) in Zusammenarbeit mit der Arbeitsgemeinschaft Elektrochemischer Forschungseinrichtungen e.V., AGEF e.V. (http://agef.uni-duesseldorf.de) organisiert. Die AGEF bemüht sich seit Jahren, in ihren Seminaren aktuelle Themen der elektrochemischen Forschung und Entwicklung in wissenschaftlichen Vorträgen aufzugreifen. Dabei bildet die Brennstoffzellentechnik einen Forschungsschwerpunkt in der AGEF. Das IWV-3 ist auf dem Gebiet der Elektrochemie und Verfahrenstechnik für Brennstoffzellen aktiv (www.fuelcells.de).

Das Thema dieses Seminars, ‚Grundlagenuntersuchungen und neue Entwicklungen von Brennstoffzellen-Membranen', schlägt den Bogen von der Modellierung von Membraneigenschaften bis zur Entwicklung fluorfreier Membranen, Hochtemperaturmembranen und Kompositmembranen, wobei der Schwerpunkt auf dem Gebiet der Polymermembran-Brennstoffzellen (H_2-PEFC und Direktmethanol-PEFC) liegt. Ein grundlegendes Verständnis der Membraneigenschaften und daraus resultierende innovative Ideen zur Entwicklung neuer oder modifizierter Membranmaterialien und Schichtstrukturen sind von essentieller Bedeutung für den technischen Erfolg von Brennstoffzellen.

Der Tagungsband enthält Kopien der Folien, die bei diesem Seminar präsentiert wurden. Wir danken allen Autoren, die mit ihren Beiträgen zum erfolgreichen Gelingen des Seminars und des vorliegenden Bandes beigetragen haben. Herrn Markus Stähler danken wir für seine Mithilfe bei der Erstellung der Druckvorlage.

Dezember 2002 Detlef Stolten und Klaus Wippermann (Hrsg.)

TAGUNGSPROGRAMM:

Aachen Bonn Bielefeld Bochum Dortmund Düsseldorf Duisburg Iserlohn Jülich Münster

AGEF Arbeits-Gemeinschaft Elektrochemischer Forschungsinstitutionen e.V.

72. AGEF-Seminar

"Grundlagenuntersuchungen und neue Entwicklungen von Brennstoffzellen-Membranen"

04. Dezember 2002

Forschungszentrum Jülich
52425 Jülich
IFF Hörsaal (Gebäude 04.8, Eingang E 2, II. Etage)

Vorbereitung: D. Stolten, K. Wippermann, FZ Jülich / IWV-3 (FSP 4)

Zeitraum	Thema / Vortragende(r)
09:00 – 09:10	***Begrüßung und Einführung*** D. Stolten, Jülich
09:10 - 09:50	***Polymermembranen für Brennstoffzellen*** S. Pereira Nunes, GKSS Geesthacht
09:50 - 10:30	***Fortschritte in der Entwicklung protonenleitender Elektrolyte für Brennstoffzellen*** K.D. Kreuer, MPI für Festkörperforschung, Stuttgart
10:30 - 11:10	***Wasserfreie protonenleitende Polymere – Materialien für PEMFCs ?*** W.H. Meyer, MPI für Polymerforschung, Mainz
11:10 - 11:30	*Kaffeepause*
11:30 - 11:50	***Entwicklung fluorfreier Polymerblendmembranen für Brennstoffzellen*** J. Kerres, ICVT, Stuttgart
11:50 - 12:10	***Überblick über die Membrananforderungen aus Fahrzeugsicht und aktueller Stand der Technik*** G. Frank, Daimler Chrysler AG, Ulm
12:10 - 12:30	***Strahlengepfropfte Membranen für H_2- und Methanol-Brennstoff-zellen-Präparation und* ex situ- *und* in situ-*Charakterisierung*** G. Scherer, Paul-Scherrer-Institut, Villigen / Schweiz
12:30 - 13:30	*Mittagessen, Seekasino*

13:30 - 13:50	***Neue Protonenaustauschermembranen durch strahlungsinduziertes Pfropfen*** G. Schmidt, TU Clausthal, Clausthal-Zellerfeld
13:50 - 14:10	***Anionen-Austauschermembranen als Polymer-Ionenleiter*** J. Jörissen, Universität Dortmund
14:10 - 14:30	***Herstellungsstrategien und Eigenschaftsspektrum bei anorganisch-organischen perfluorierten Hybridmembranen für die DMFC*** M. Willert-Porada, Universität Bayreuth
14:30 – 15:00	*Kaffeepause*
15:00 – 15:20	***Molekulare Aspekte des Protonen-Transports in Polymer-Elektrolyt-Membranen*** M. Eikerling, TU München
15:20 – 15.40	***Stofftransportprozesse in PEM für die DMFC: Modellierung auf Basis des vollständigen Maxwell-Stefan Ansatzes*** Thorsten Schultz, MPI für Dynamische Komplexe Technische Systeme, Magdeburg
15.40 – 16.00	***Molekulardynamische Simulationen des Protonentransports in PEM Membranen*** E. Spohr, FZ Jülich
16.00	*Ende des Seminars*
16.00 ff	*Mitgliederversammlung der AGEF*

INHALT:

S. Pereira Nunes, GKSS Geesthacht
Polymermembranen für Brennstoffzellen..... 1.1 - 25

K.D. Kreuer, MPI für Festkörperforschung, Stuttgart
Fortschritte in der Entwicklung protonenleitender Elektrolyte für Brennstoffzellen..... 2.1 - 10

W.H. Meyer, MPI für Polymerforschung, Mainz
Wasserfreie protonenleitende Polymere – Materialien für PEMFC ?..... 3.1 - 19

J. Kerres, ICVT, Stuttgart
Entwicklung fluorfreier Polymerblendmembranen für Brennstoffzellen... 4.1 - 22

G. Frank, Daimler Chrysler AG, Ulm
Überblick über die Membrananforderungen aus Fahrzeugsicht und aktueller Stand der Technik..... 5.1 - 8

G. Schmidt, TU Clausthal, Clausthal-Zellerfeld
Neue Protonenaustauschermembranen durch strahlungsinduziertes Pfropfen..... 6.1 - 11

J. Jörissen, Universität Dortmund
Anionen-Austauschermembranen als Polymer-Ionenleiter..... 7.1 - 2

M. Willert-Porada, Universität Bayreuth
Herstellungsstrategien und Eigenschaftsspektrum bei anorganisch-organischen perfluorierten Hybridmembranen für die DMFC..... 8.1 - 15

M. Eikerling, TU München
Molekulare Aspekte des Protonen-Transports in Polymer-Elektrolyt-Membranen..... 9.1 - 13

Thorsten Schultz, MPI für Dynamische Komplexe Technische Systeme, Magdeburg
Stofftransportprozesse in PEM für die DMFC: Modellierung auf Basis des vollständigen Maxwell-Stefan Ansatzes..... 10.1 - 10

E. Spohr, Forschungszentrum Jülich
Molekulardynamische Simulationen des Protonentransports in PEM-Membranen..... 11.1 - 12

Membranes for Fuel Cell

Suzana Pereira Nunes

GKSS Research Center

Membrane requirements

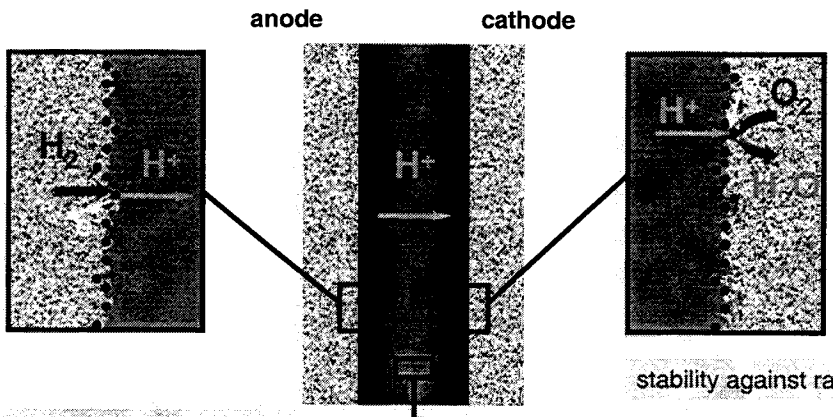

stability against radical

Membrane-Electrode Interface (anode or cathode):
- free access fuel (or O_2)to catalyst (effective reaction)
- optimal contact between catalyst and ionomeric membrane material (rapid proton delivery)
-good adhesion membrane/catalyst/ electrode
-electron conductivity (rapid electron transport)

Membrane Bulk
- low electron conductivity (avoid short circuit)
-high proton conductivity
- low fuel and O_2 crossover

Low cost

Nunes

Membranes for fuel cell

GKSS

Fluorinated polymers, composite membranes

Non fluorinated polymers

- sulfonated polymers
- phosphonated polymers
- imidazol containing polymers

Polymer blends

Crosslinking

Organic-inorganic polymer composites

Nunes

Commercial fluorinated membranes for fuel cell

GKSS

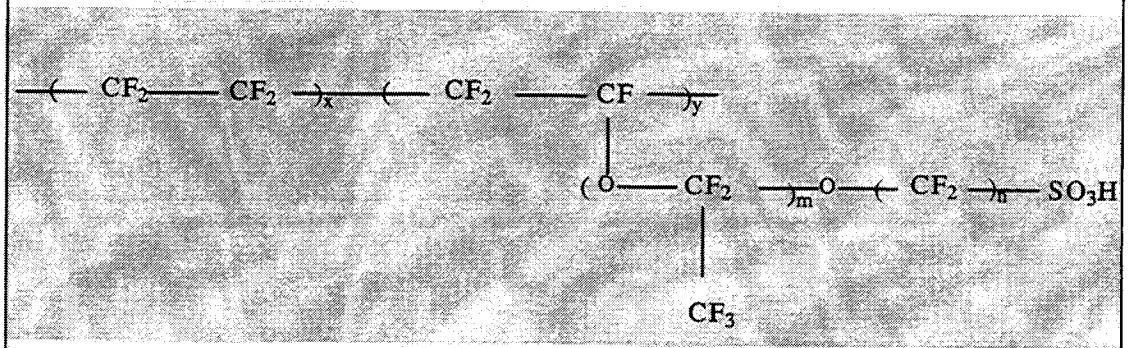

Nafion® 117	m>1, n=2, x=5-13.5, y=1
Flemion ®	m=0, n=1-5
Aciplex ®	m=0,3, n=2-5,x=1.5-14
Dow ®	m=0, n=2, x=3.6-10

Nunes

Fluorinated membranes Radiation-grafted membranes

GKSS

$$-CF_2-CF_2-CH_2-CH_2-$$

electron beam
or gamma irradiation

FEP-g-PS (γ irradiation)

Gupta et al. Solid State Ionics 61 (1993) 213
Büchi et al. Electrochimica Acta 40 (1995) 345

PVDF-g-PS (electron irradiation

S. D. Flint and C. T. Slade Solid State Ionics 97 (1997) 299
D. I. Ostrovskii et al. Solid State Ionics 97 (1997) 315

grafting

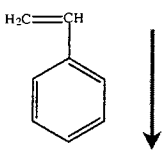

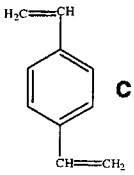

crosslinking

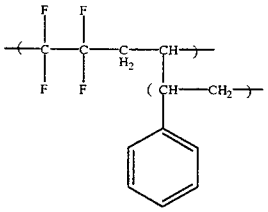

chlorosulfonic acid

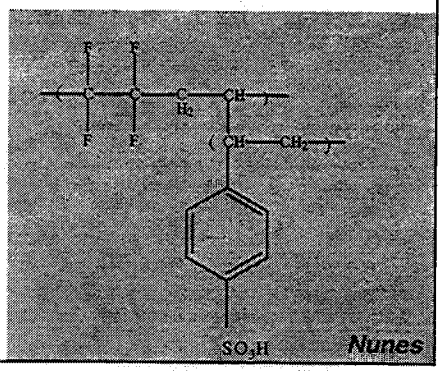

Nunes

Fluorinated membranes

GKSS

Fuel cell performance of proton irradiated and subsequently sulfonated poly(vinyl fluoride) membranes

Preben Vie[a,*], Mikael Paronen[b], Monica Strømgård[a], Eero Rauhala[c], Franciska Sundholm[b]

Journal of Membrane Science 204 (2002) 295–301

PVF

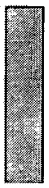

Irradiation
with protons

Chlorsulfonic Acid
1.5 % in CH2Cl2

3 % H2O2

PVF matrix with sulfonated clusters

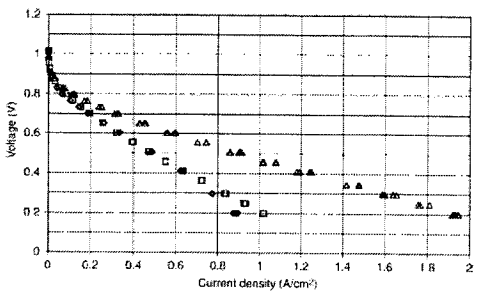

Fig. 3. Polarisation characteristics of the tested membranes, PVF-SA (25 μm) (□), Nafion® 117 (○) and Nafion® 112 (△), at close to optimal fuel cell temperatures for the PVF-SA membrane. The gas pressure was 2 bar and the temperatures varied slightly around 50 °C. The mechanical pressure was 10 bar.

Nunes

Fluorinated membranes

GKSS

Ballard Advanced Materials

BAM1G
Poly(phenylquinoxaline)

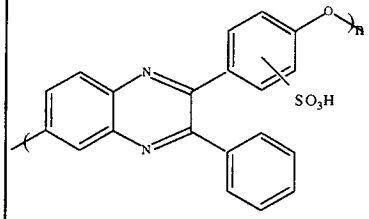

Life time 350 h

BAM2G
Poly (aryl ether sulfone)
Poly(2,6 diphenyl-4 phenylene oxide)

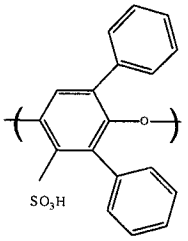

Life time 500 h

BAM3G
Polytrifluorostyrene

Life time 15000 h

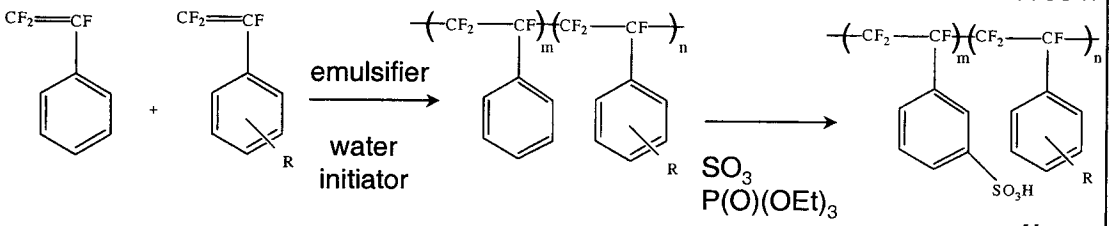

Stone et al. US Pat 5773480

Nunes

Fluorinated membranes with support

GKSS

Supported membranes: Gore-Select

Gore US Pat. 5547551 and 5599614

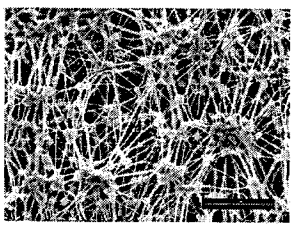

PTFE microporous support (20 μm)
Treated with nonionic surfactant and covered with Nafion NR-50 (1100EW)

Advantage:
Improving the mechanical strengh without decreasing the conductance

Conductance

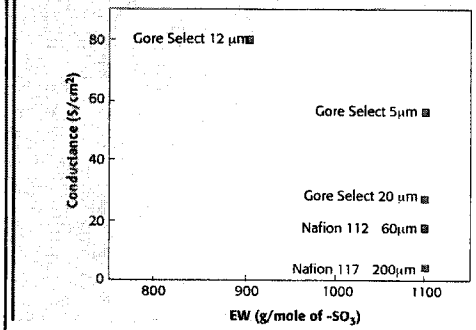

Ionic Conductivity

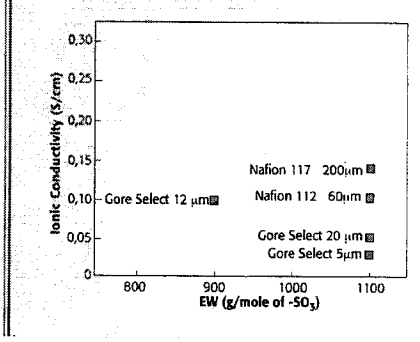

Membranes with support

GKSS

Ion conductive polymer/ glass fibers

Denton et al. (Johnson Matthey) US 6042958 (2000)

Ion conductive polymer in porous polymer support (PBO or PES)

Formato et al. (Foster-Miller) US 6248469 (2001)

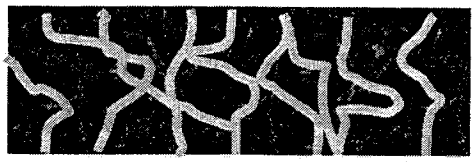

(PEEK)

Wilson et al. (Victrex) WO 01/19896 A1 (2001)

Asymmetric membrane for fuel cell

Biegert et al. (DaimlerChrysler) DE 19926353 A1 (2000)

Nunes

Non-fluorinated sulfonated polymers

GKSS

Sulfonated polysulfone

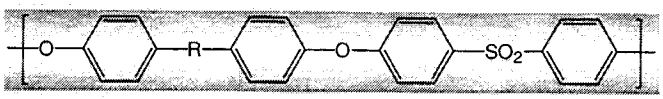

Sulfur trioxide:
- very reactive
- inexpensive

<u>but:</u>
- heterogeneous
- cross-linking

Chlorosulfonic acid:
- inexpensive

<u>but:</u>
- heterogeneous
- chain cleavage
- cross-linking

Lithiation route:
- sulfonation of electron-deficient rings

<u>but:</u>
- expensive

SO_3-TEP-complex:
- minimization of cross-linking

<u>but:</u>
- low reactivity (with high TEP content)

Chlorosulfonic acid, trimethylsilyl ester:
- homogeneous
- good reaction control

<u>but:</u>
- relatively expensive

Nunes

Non-fluorinated sulfonated polymers

GKSS

Sulfonated polyphenylsulfone

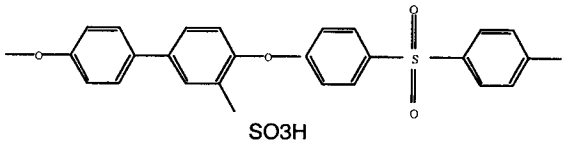

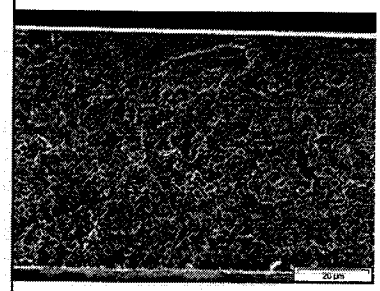

Methanol permeability 1/9 Nafion

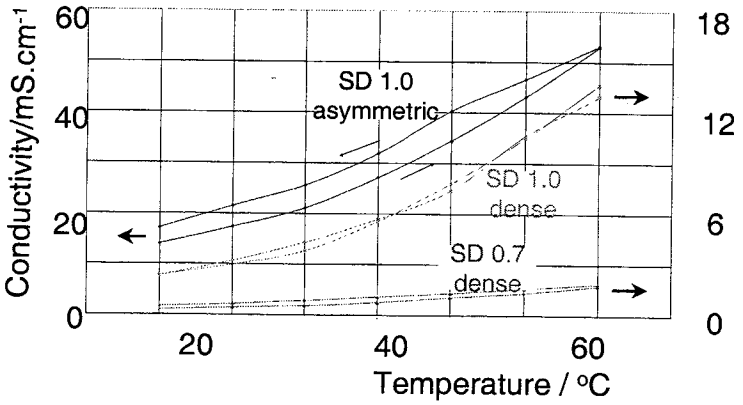

A. Dyck, D. Fritsch, S. P. Nunes J. Appl. Polym. Sci 2002

Nunes

Non-fluorinated sulfonated polymers

GKSS

Polyarylene ether sulfone

Direct polymerization of sulfonated poly(arylene ether sulfone) random (statistical) copolymers: candidates for new proton exchange membranes

Feng Wang[a], Michael Hickner[a], Yu Seung Kim[a], Thomas A. Zawodzinski[b], James E. McGrath[a,*]

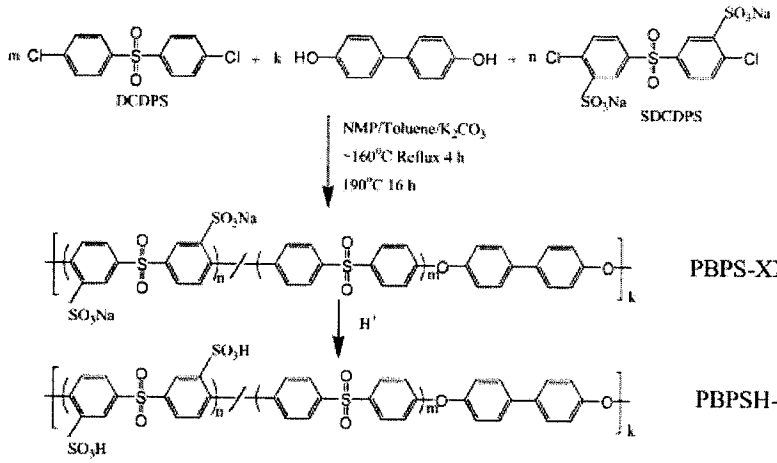

(n+m)/k = 1.01 (in mole); XX = 100n/(n+m)

Journal of Membrane Science 197 (2002) 231–242

Nunes

Non-fluorinated sulfonated polymers

GKSS

Sulfonated polyetherketone

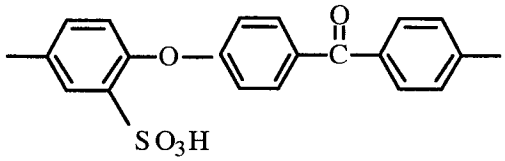

SPEK

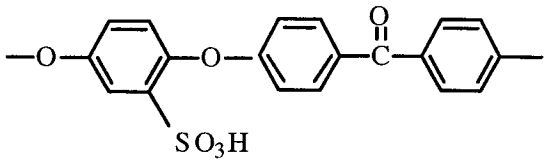

SPEEK

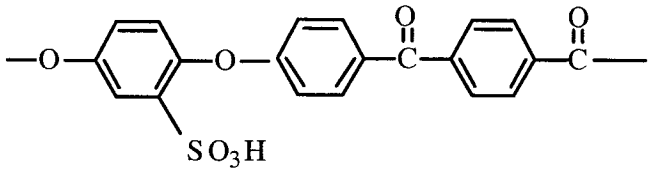

SPEEKK

Nunes

Non-fluorinated sulfonated polymers

GKSS

S-PEEK

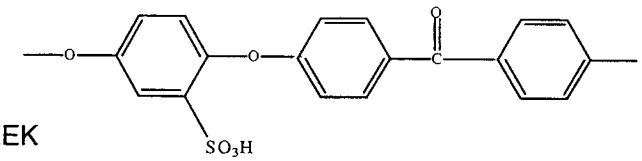

S-PPBP

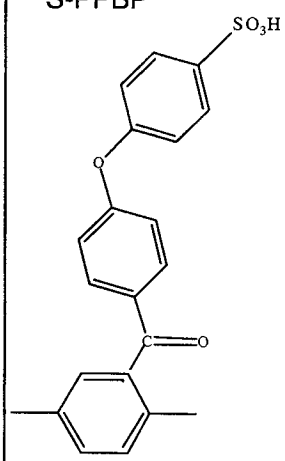

Poly(phenoxy benzoyl phenylene)

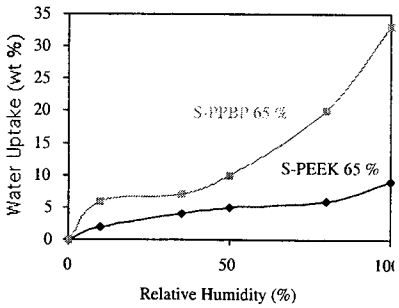

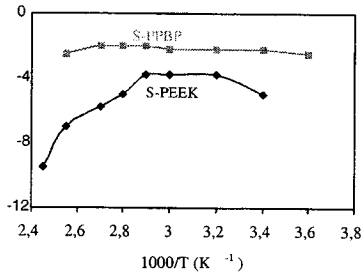

Rikukawa and Sanui 2000

Nunes

Non-fluorinated sulfonated polymers

GKSS

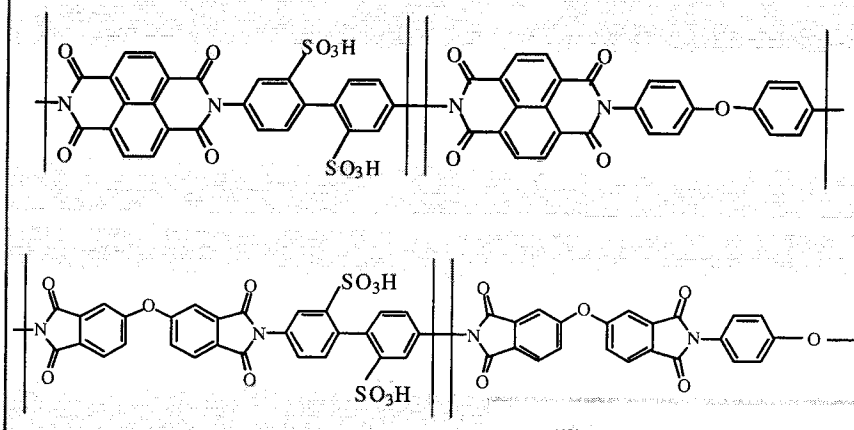

Sulfonated Polyimide

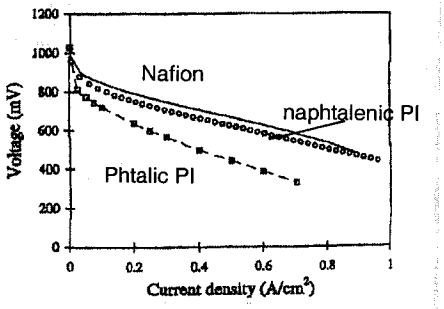

Pineri et al. J. Membrane Sci. 1999
Genies et al. Polymer 42 (2001) 5097

Nunes

Non-fluorinated sulfonated polymers

GKSS

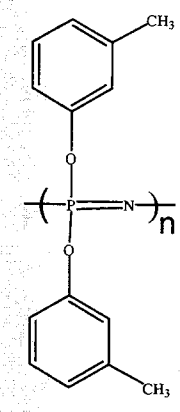

Sulfonated polyphosphazene

Sulfonation with SO_3
in dichlorethane at 0°C

Crosslinking with
UV/benzophenone

Proton conductivity:
40 mS/cm (25° C) 30 % lower than Nafion®
82 mS/cm (65° C)

Methanol diffusion coefficient (30 °C)

Crosslinked POP (IEC=1.4 mmol/g)	1.62 x 10^{-8} cm^2/s
Nafion 117 (IEC = 0.9 mmol/g)	6.6 x 10^{-6} cm^2/s

Pintauro et al. J. Membrane Sci. 1999

Nunes

Phosphonated polymers

GKSS

Phenyl phosphonic acid functionalized poly[aryloxyphosphazenes] as proton-conducting membranes for direct methanol fuel cells

Harry R. Allcock[a,*], Michael A. Hofmann[a], Catherine M. Ambler[a], Serguei N. Lvov[b,c,1], Xiangyang Y. Zhou[b], Elena Chalkova[b], Jamie Weston[b]

Journal of Membrane Science 201

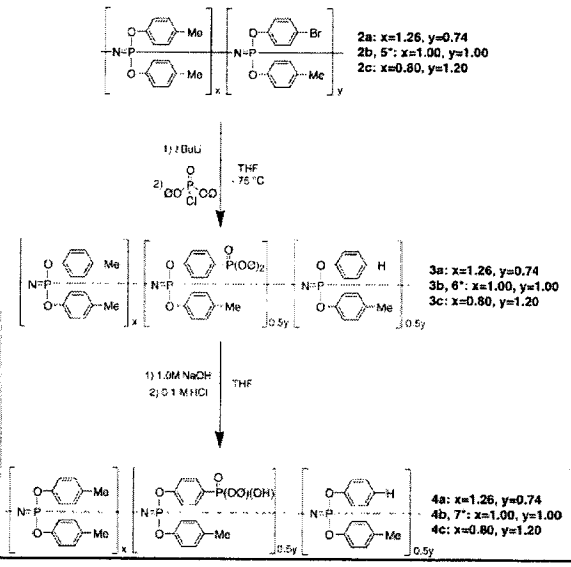

Membrane	IEC (meq.g-1)	Ion conductivity (mScm-1)
P-Poyphosphazene	1.17	38
	1.34	45
	1.43	54
S-Polyphosphazene	1.07	11
Nafion 117	0.91	60-100

Nunes

Phosphonated polymers

GKSS

Xu and Cabasso Polym. Mat. Sci. Eng. 68 (1993) 120

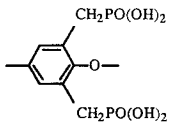

Stone et al. (Ballard) 2J. New. Materials Electrochem. System. 3 (2000) 43

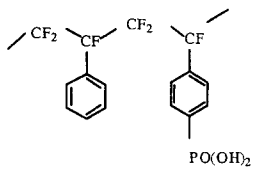

Yamabe et al. (Asahi) European Polym. J. 36 (2000) 1035

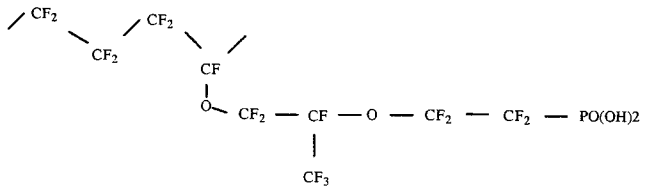

Nunes

Phosphonated polymers

GKSS

Miyatake and Hay J. Polym. Sci. 39 (2001) 3770

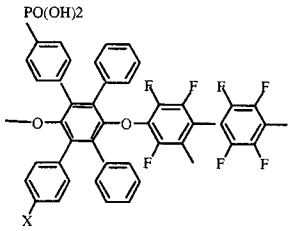

Kotov et al. J. Fluorine Chemistry 82 (1997) 13-19

Copolymer	Proton conductivity (mS/cm) (80°C)
TFE/ CF_2=$CFO(CF_2)_3P(O)(OC_2H_5)_2$	76
TFE/ CF_2=$CFO(CF_2)_2P(O)(OC_2H_5)_2$	69
TFE/ CF_2=$CFOCF_2CF(CF_3)(CF_2)_2P(O)(OC_2H_5)_2$	6
Nafion	70-80

Nunes

Phosphonated polymers

Radel

GKSS

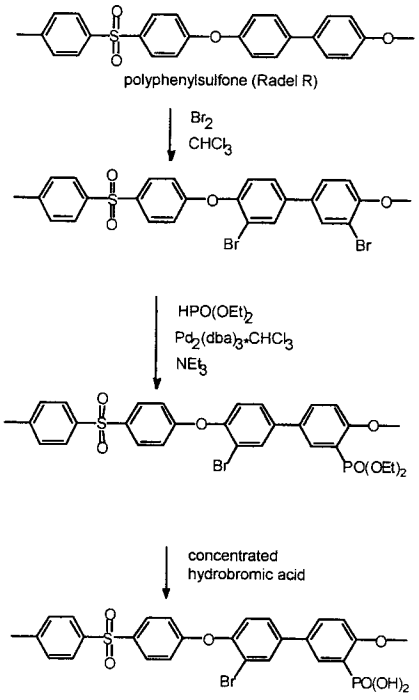

90 %

Jacoby, Peinemann and Nunes Patent Application 2001
Jacoby et al. Macromolecular Chemistry andPhysics

Nunes

Polybenzimidazole (PBI)

GKSS

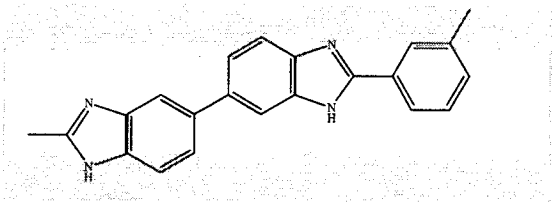

Polymer	Solvent	Dopping acid/ molecules per polymer unit	T (°C)	Proton conductivity (mS/cm)
Nafion			80	70
			120 (400 torr)	3.6
PBI	DMAc	H_2SO_4/ 2.5	170 (400 torr)	20
PBI	DMAc	H_3PO_4/ 2.5	180 (400 torr)	10
PBI	DMAc	H_3PO_4/ 5	190	40
PBI	TFA	H_3PO_4/ 5.8	130	52-72
PBI	TFA	H_3PO_4/ 5.8	190	60

TFA = trifluoroacetic acid

Savinell and Litt US Pat. 5525436 and 5716727

Nunes

PBI

GKSS

PBI solution

↓

coagulation bath

DMAc/methanol
NMP/methanol
DMAc/water

30/20/50 wt%
Methanol/DMAc/H_3PO_4

porous structure

H_3PO_4

Drying at 80-120 °C

colapsed pores
Dense film

Advantages
- fast acid incorporation
- higher acid loadings
- improved mechanical properties
-better retention of the acid

Hoechst Celanese WO 98/14505

Alkylsulfonated PBI

GKSS

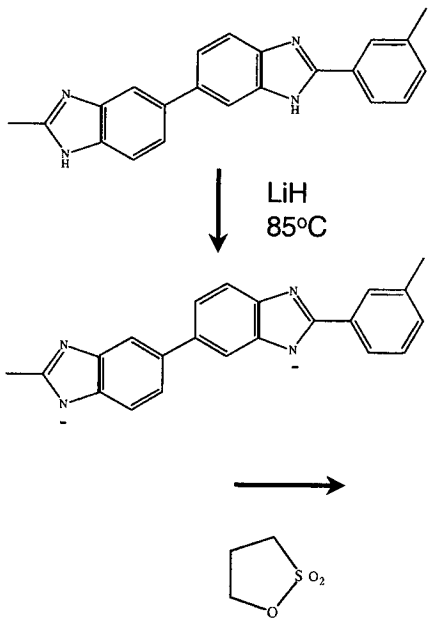

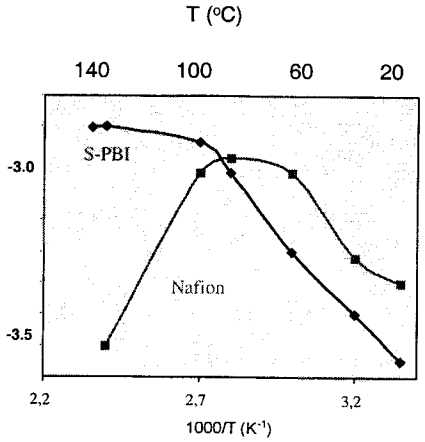

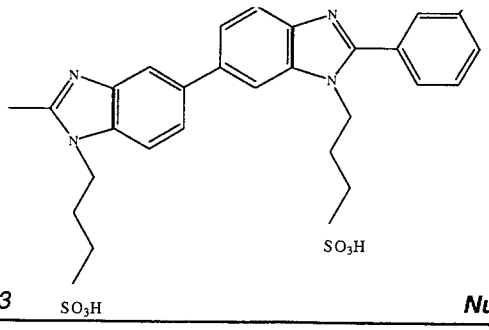

Rikukawa and Sanui Prog. Polym. Sci. (2000) 1463

Nunes

Sulfonated PBI

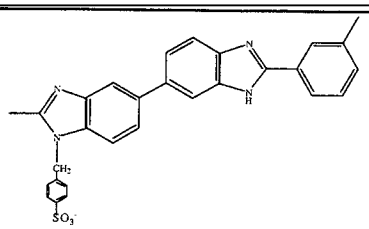

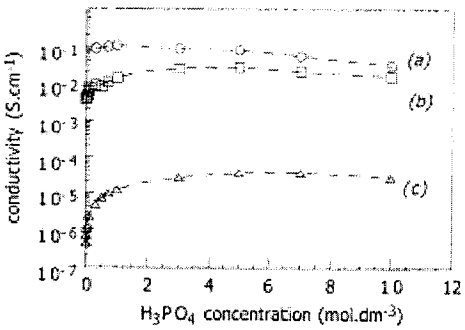

Fig. 3. Conductivity at 25°C of: (a) Nafion^{TM}-117; (b) benzylsulfonate-grafted PBI and (c) PBI as a function of the H_3PO_4 concentration (immersion time 8 h) [46,47].

Table 3
Conductivity (25°C/100% RH) of benzylsulfonate grafted (85% sites sulfonated) PBI following dehydration and immersion in basic solutions (1 M, 15 min, 25°C) [46,47]

Membrane	Conductivity ($S cm^{-1}$)
PBI-S	4.2×10^{-4}
PBI-S/NH_4OH	1.5×10^{-2}
PBI-S/$(CH_3)_4OH$	8.2×10^{-3}
PBI-S/imidazole	7.9×10^{-3}
PBI-S/DABCO[a]	1.2×10^{-2}
PBI-S/LiOH	1.2×10^{-2}
PBI-S/NaOH	1.2×10^{-2}
PBI-S/KOH	1.7×10^{-2}
PBI-S/CsOH	1.7×10^{-2}

[a] 1,4-Diazabicyclo[2.2.2]octane.

D.J. Jones, J. Rozière / Journal of Membrane Science 185 (2001) 41–58

PBI

GKSS

A. Schechter, R.F. Savinell / Solid State Ionics xx (2002) xxx–xxx

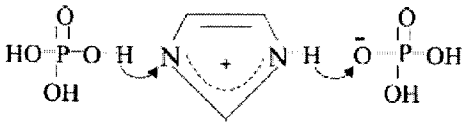

Fig. 4. Proton conduction paths between imidazole and phosphoric acid molecules.

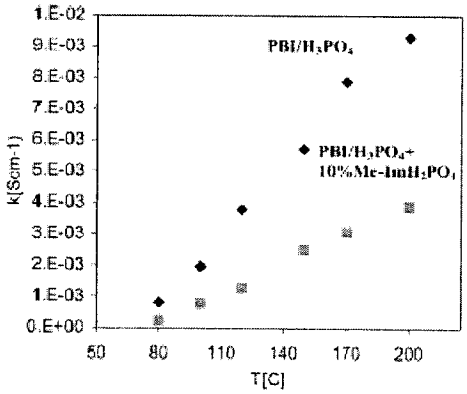

Fig. 5. Conductivity of PBI/H_3PO_4 600% (M) with and without addition of $Me\text{-}ImH_2PO_4$ salt (10% molar in acid), measured at dry conditions.

Nunes

Blockcopolymers

GKSS

Non Ionic block

Ionic block

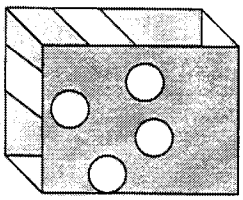

Mechanical strength

Water repellency
(avoid flooding)

Rapid proton transport

Lehmann, Meier-Haack, Paul, Peinemann, Jakoby, Nunes Patent Application 2001

Blockcopolymers

GKSS

Sulfonated SEBS

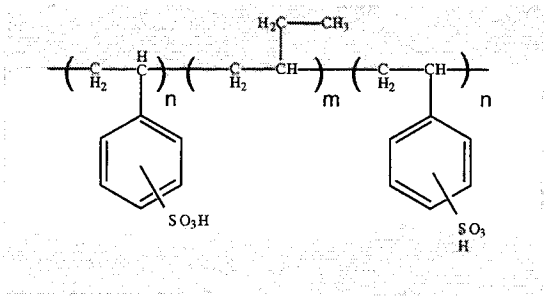

Proton conductivity
> 90 mS/cm

Water uptake (25 °C)
200 % (55-60 % sulf.)

1/5 to 1/3 than Nafion
methanol crossover

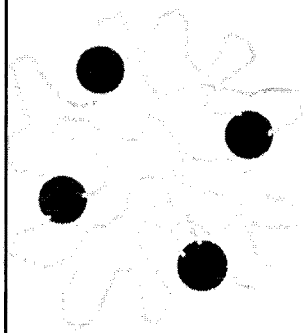

Lamellar morphology
d-spacing ca. 37 nm
(63 nm in water)

28-31 % S
40-60 % sulfonation

Dais US Pat 5679482, 1997 ***Nunes***

Blockcopolymers

GKSS

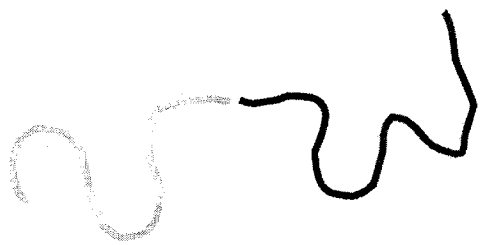

Fluorinated block
Water repellency

Sulfonated block
Ion conductivity

avoid flooding

rapid proton transport

Ex: TFE/PPVE-TFE/PSVE
TFE=tetrafluoroethylene
PPVE=perfluorvinylether

Watanabe and Eriguchi (Asahi Glass) US Patent Application 2001/0018144 A1

Nunes

Blockcopolymers

GKSS

Influence of the structure of sulfonated polyimide membranes on transport properties

N. Cornet [a], G. Beaudoing [b], G. Gebel [a,*]

Separation and Purification Technology 22-23 (2001) 681–687

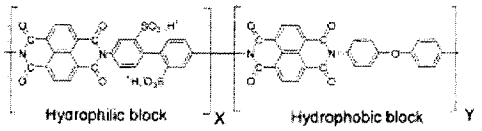

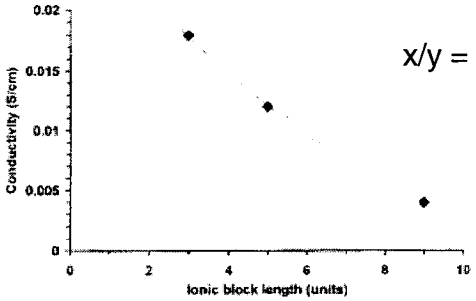

x/y = 30/70

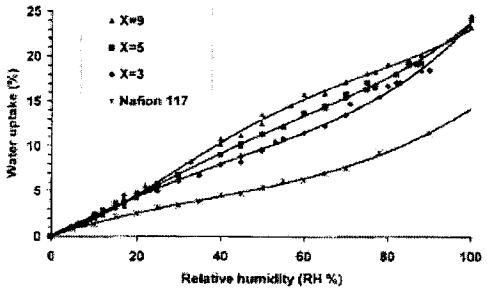

Nunes

Polyimides

GKSS

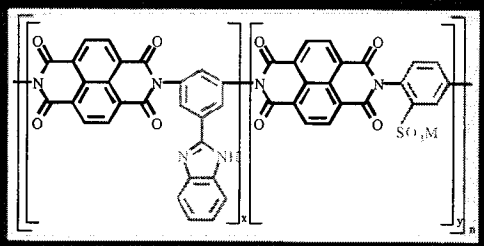

x/y: 50/50
EW = 876 g/eq
I = 17.0 mS/cm

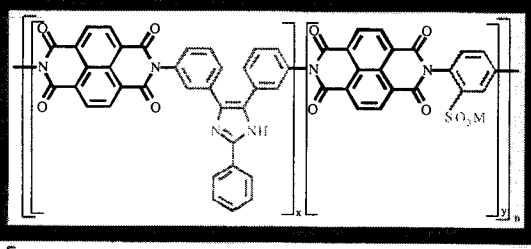

x/y: 50/50
EW = 978 g/eq
I = 1.5 mS/cm

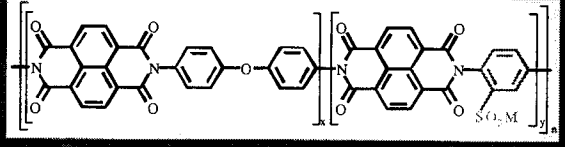

x/y: 30/70
EW = 605 g/eq
I = 5.4 mS/cm

GKSS

Polyoxazoles

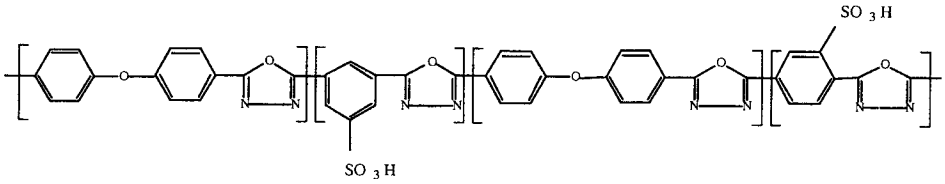

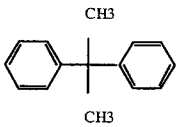

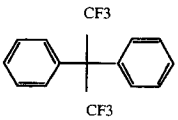

GKSS

Perfluorinated Ionomer Membrane-Ionic Liquid Composites

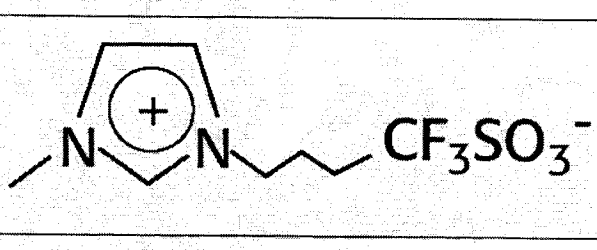

Ionic conductivity:
0.06 to 0.11 s/cm
at 150°C to 180°C

	solvent uptake (%)	
Ionomer membrane	23 °C	100 °C
N177-H^+	9	54
890 EW-Nafion H^+	13	120

from: M. Doyle, S.K. Choi, G. Proulx, J. Electrochem. Soc. 147(1) 34-37, 2000

Nunes

Polymer blends

GKSS

ACID/BASE

J.A. Kerres / Journal of Membrane Science 185 (2001) 3–27

PPO/PVDF

Cabasso and Yuan US 6103414 (2000)

Nafion/Teflon

O' Brien (du Pont) US 6294612

PBO/PSU

Formato et al. (Foster Miller) Pat. Appl. US 2002/0045085 A1

PVDF/PSSA

Prakash et al. WO 98/22989 (1998)

S-PSU/S-PEEK

M. Mulder J. Membrane Sci. 2002

Nunes

Organic/Inorganic membranes

GKSS

Nafion/Inorganic moisture absorbing particles

Nafion/SiO_2

Antonucci et al. Solid States Ionics 125 (1999) 431
Antonucci and Arico EP 0926754A1 1999
5% Nafion 3 % SiO2, operation up to 155°C

Nafion/P2O5 1.6-2.6 proton conductivity increase

Arimura et al. Solid State Ionics 118 (1999) 1

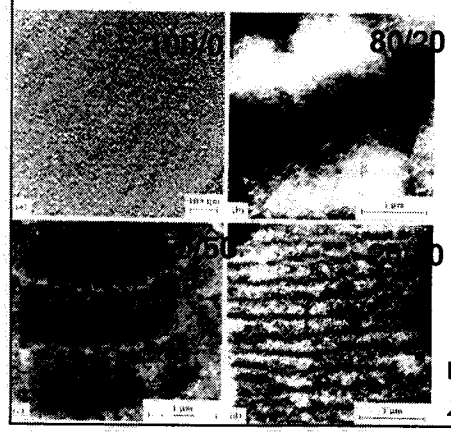

Nafion /TEOS

Zoppi, Yoshida, Nunes 39 (1998) 1309

Nunes

Organic/Inorganic membranes

GKSS

Ionomer/Silica particles by hydrolysis of silanes

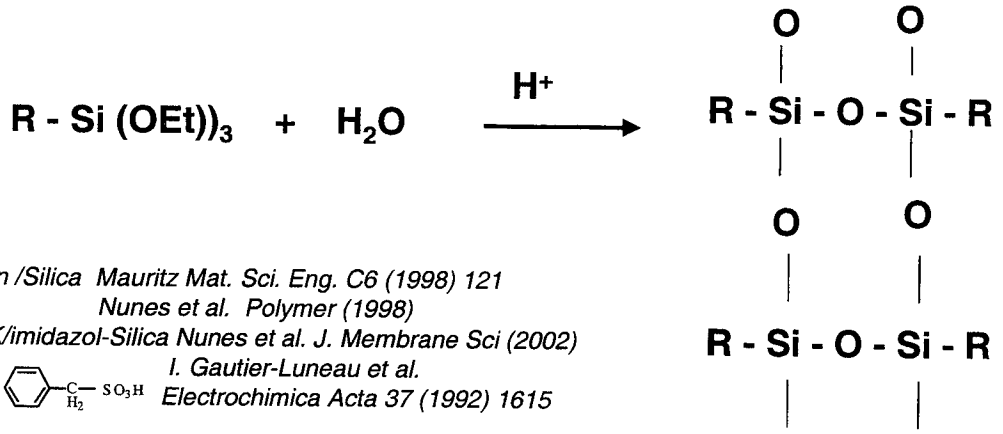

Nafion /Silica Mauritz Mat. Sci. Eng. C6 (1998) 121
Nunes et al. Polymer (1998)
SPEK/imidazol-Silica Nunes et al. J. Membrane Sci (2002)
R = *I. Gautier-Luneau et al. Electrochimica Acta 37 (1992) 1615*

R = $(CH_3O)_3Si$ 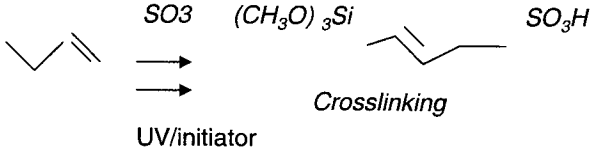 *$(CH_3O)_3Si$* *SO_3H*

Depre et al. Electrochimica Acta 43 (1992) 1305

Nunes

Organic/Inorganic membranes

GKSS

PVDF/ SiO_2 or TiO_2/ aqueous electrolyte

Porous of ca. 8 nm
Electrolyte : KOH, H2SO4, trifluoromethane sulfuric acid
Proton Conductivity
SiO_2/KOH 74-113 mS/cm
8 % SiO2//decane/H_2SO_4 440 mS/cm

Peled et al. *WO 99/44245*
Electrochemical and Solid-State Letters 3 (2000) 525

Nunes

Polymer/Phosphates

GKSS

Nafion/ Zirconium Phosphate	*DuPont US Patent 5919583 1999*
PTFE/ Zirconium Phosphate	*Lynthech US Patent 6059943 2000*
Layered Phosphates and Phosphonates	*Alberti et al. Adv. Mat. 8 (1996) 291*
Zirconium sulfophenylphosphonate	*Alberti et al. J. Membrane Sci. 185 (2001) 73*
SPEEK/Zirconium Phosphate	*Jones and Roziere J. Membrane Sci. 185 (2001) 41*
SPEK/Zirconium Phosphate	*Nunes et al. J. Membrane Sci. 2002*

Nunes

Organic/Inorganic membranes

GKSS

Layered Phosphates and Phosphonates

G. Alberti, M. Casciola / Solid State Ionics 97 (1997) 177–186

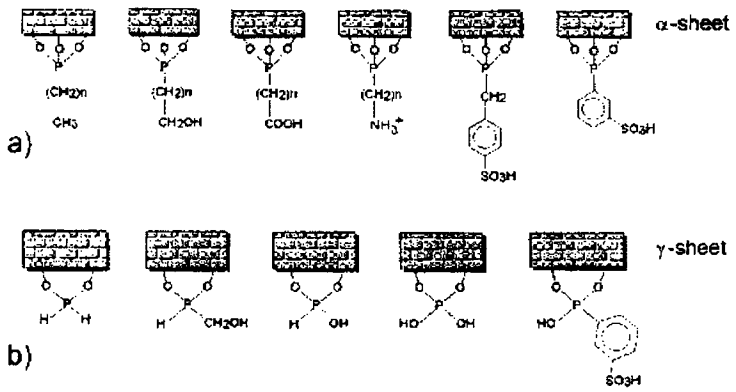

Fig. 2. Schematic representation of (a) some α-derivatives containing pendant groups of increasing acidity; (b) some γ-derivatives containing pendant groups of increasing acidity. In both α- and γ-derivatives the proton conductivity can range from nearly zero to 2×10^{-5} and 5×10^{-2} S cm^{-1}, respectively.

Nunes

ELSEVIER Solid State Ionics 97 (1997) 177–186

GKSS

Layered metal^{IV} phosphonates, a large class of inorgano-organic proton conductors

G. Alberti*, M. Casciola

Compound	σ (S cm^{-1})
γ-$Zr(PO_4)(H_2PO_4)$	4×10^{-5}
α-$Zr(O_3POH)_2$	1.3×10^{-6}
	1×10^{-7}
pellicular α-$Zr(O_3POH)_2$	1×10^{-4} (parallel)
	3×10^{-7} (perpend.)
α-$Zr(O_3PCH_2COOH)_2$	2×10^{-9}
α-$Zr(O_3P(CH_2)_2COOH)_2$	$<10^{-10}$
α-$Zr(O_3P(CH_2)_3COOH)_2$	1.6×10^{-8}
α-$Zr(O_3P(CH_2)_4COOH)_2$	$<10^{-10}$
α-$Zr(O_3P(CH_2)_5COOH)_2$	1.4×10^{-7}
α-$Zr(O_3P(CH_2)_2NH_3)_2\cdot0.1HCl$	2×10^{-5}
α-$Zr(O_3PCH_3)_{1.0}(O_3PC_6H_4SO_3H)_{0.9}$	5×10^{-6}–1.2×10^{-3}

Nunes

Organic/Inorganic membranes

GKSS

SPEK/Zirconium Phosphate Composites

Polymer modification with

Zirconium phosphates → Proton conduction

and oxides → Low methanol and water transport

Nunes, Ruffmann, Rikowski, Vetter J. Membrane Sci. 203 (2002) 215

500 nm

Organic/Inorganic membranes

GKSS

Flux and conductivity of composite membranes

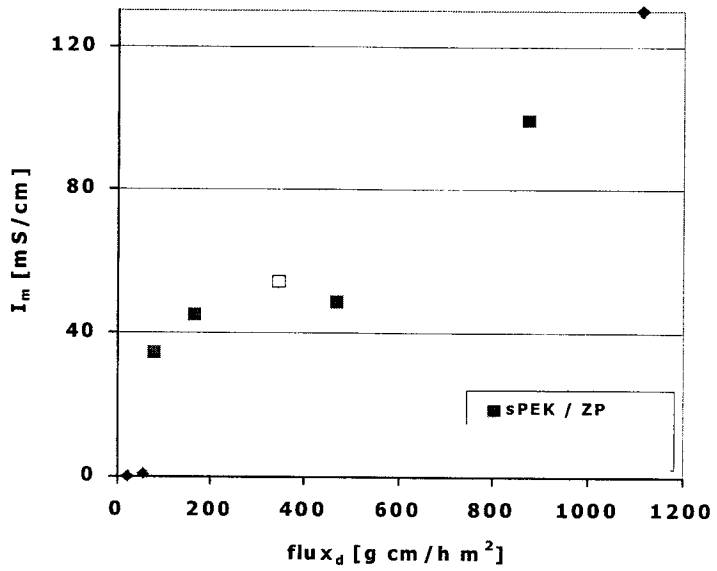

Organic/Inorganic membranes

GKSS

SPEEK/BPO4

Mikhailenko, Zaidi and Kaliaguine

Catalysis Today 67 (2001) 225

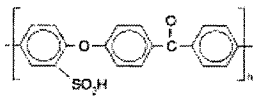

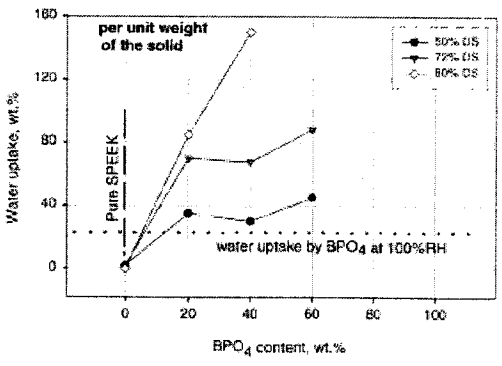

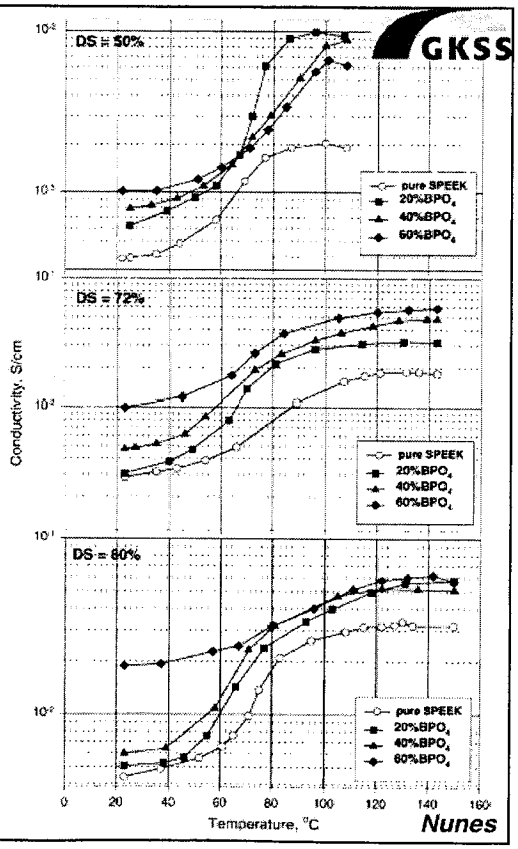

Nunes

Organic/Inorganic membranes

GKSS

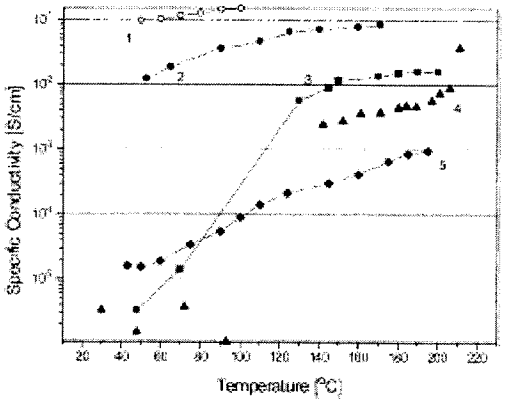

J. Power Sources 103 (2001) 1-9

Fig. 4. Membrane conductivity for water-independent membranes: (1) (○) fully-hydrated Nafion membrane at 100% RH; (2) (●) recast Nafion/imidazole membrane; (3) (■) Nafion 115 membrane swollen with molten imidazole; (4) (▲) cesium hydrogen sulfate membrane; (5) (◆) Nafion 115 membrane swollen with methanol/imidazole solution.

Nunes

Organic/Inorganic membranes

GKSS

Modification of SPEK with heteropolyacids

Improvement of conductivity with heteropolyacids

Fixation of heteropolyacids in the polymer matrix

Reduction of permeability with oxides

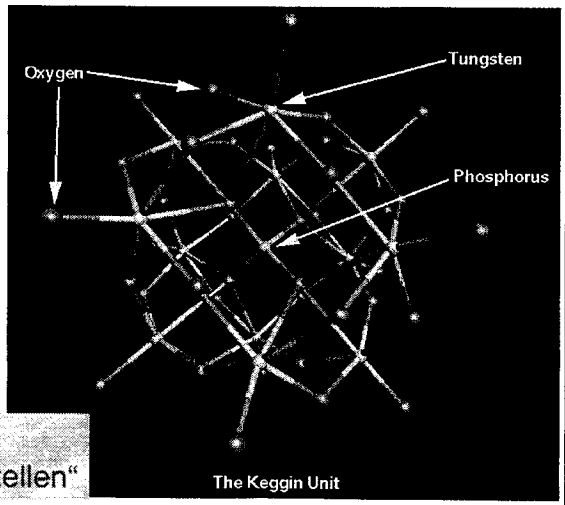

The Keggin Unit

DFG Schwerpunktprogramm:
„Neue Schichtstrukturen für Brennstoffzellen"

Ponce, Prado, Richau, Mohr, Nunes J. Membrane Sci., in press

Organic/Inorganic membranes

GKSS

Polymer/ Heteropolyacid

Nafion/silicotungstic acid/thiophene
Tazi and Savadogo Electrochem. Acta 45 (2000) 4329

SPEEK/ tungsto- and molibdophosphonic acid
Zaidi et al. J. Membrane Sci. 173 (2000) 17

PBI/ phosphotungstic acid/ SiO2
Staiti et al. J. Power Sources 90 (2000) 231

PBI/silicotungstic acid
Staiti and Minutoli J. Power Sources 94 (2001) 9

PBI/silicotungstic acid /silica (TEOS) /H_3PO_4
Saiti J. New. Mat. Electrochem. Systems 4 (2001) 181

Nafion/silica /silicotungstic and phosphotungstic acid (DMFC)
Saiti J. New. Mat. Electrochem. Systems 4 (2001) 181

SPSF/phosphatoantimonic acid
Poinsignon et al. J. Membrane Sci. 185 (2001) 59

SPEK/modified phosphotungstic, silicotungstic, phosphomolybidic acid
Ponce et al. J. Membrane Sci. (2002)

Nunes

Polymer/ Heteropolyacid

GKSS

$SPEK/H_3P(W_3O_{10})_4$

Pervaporation of 20 % methanol at 55°C

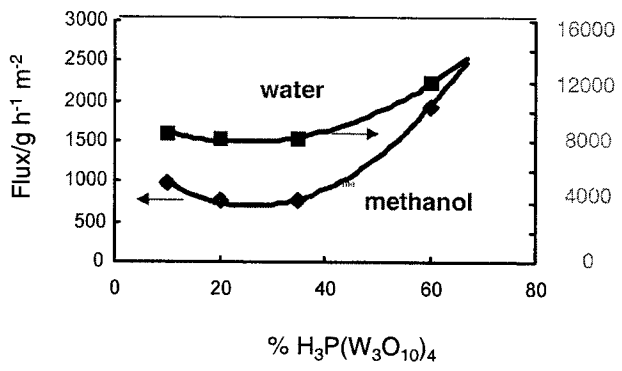

Ponce et al. J. Membrane Sci. 2002, in press

Organic/Inorganic membranes

GKSS

Polymer/ Heteropolyacid

$SPEK/H_3P(W_3O_{10})_4/ZrO_2$

Pervaporation 20 % Methanol at 55°C

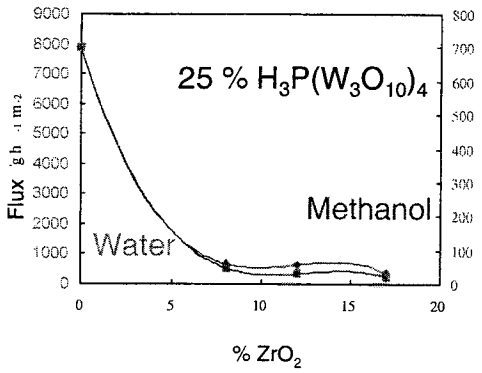

SPEK/ $H_3P(W_3O_{10})_4/ ZrO_2$	Conductivity mS/cm
100/0/0	50
90/10/0	82
40/60/0	112
56/25/7	86
40/25/13	3

Ponce et al. J. Membrane Sci., in press

Organic/Inorganic membranes

GKSS

SPEK/ Heteropolyacid

Heteropolyacid	Inorganic	Solvent	% extraction
$H_3PMo_{12}O_{40}$ aq			>80
$H_3(RSi)_2OPSiMo_{11}O_{39}$ aq	ZrO_2	DMSO	23
$H_5PNiMo_{11}O_{39}$ aq	ZrO_2	NMP	9
$H_3PMo_{12}O_{40}$ aq	$R\ SiO_{3/2}$	DMSO	20
$H_3(RSi)_2OPMo_{11}O_{39}$ aq	$R\ SiO_{3/2}$	DMSO	18
$H_3PNiMo_{11}O_{40}$ aq	$R\ SiO_{3/2}$	NMP	7

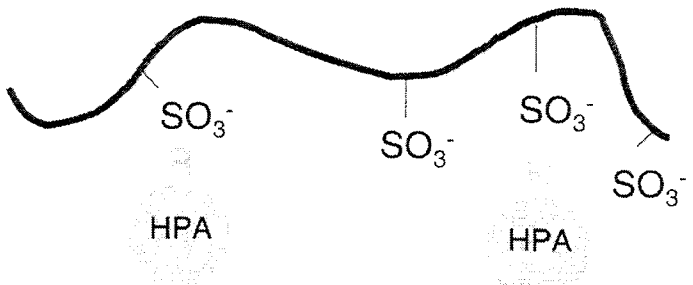

Ion channels

An open and shut case

Maria Schumacher and John P. Adelman

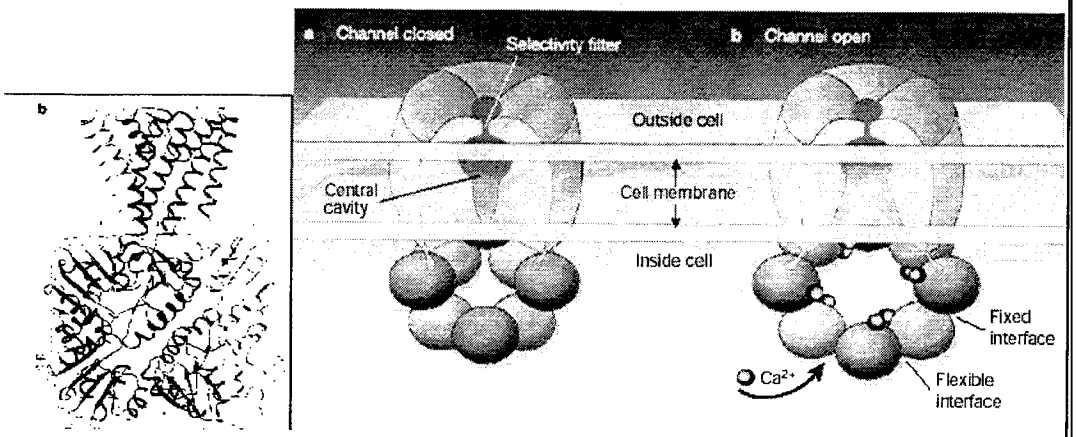

Figure 1 Schematic model for the gating and opening of a bacterial Ca^{2+}-gated K^+ channel, based on the new papers by MacKinnon and colleagues[1,2]. a, The closed conformation; b, the open conformation. Three of the four subunits of a K^+ channel are shown in brown. The purple and red circles represent the eight RCK domains, which, after binding Ca^{2+}, are thought to reorientate with respect to each other, causing changes in the pore in the centre of the channel.

Jiang et al. Nature 417 (2002) 515-526 *Schumacher and Adelman Nature 417 (2002) 501*

Max-Planck-Institut für Festkörperforschung, Stuttgart

Max-Planck-Institute for Solid State Research

Recent advanced in the development of proton conducting electrolytes for fuel-cell applications

K.D. Kreuer

Max-Planck-Institut für Festkörperforschung
Heisenbergstr.1, D-70569 Stuttgart
K.D.kreuer@FKF.mpg.de

high water/methanol "cross-over" in proton conducting membranes (NAFION®)

proton-conducting polymers with low electroosmotic drag: a microstructure approach

low proton conductivity of conventional membranes at medium T (120°-200°C) and low humidification

heterocycles as proton solvents: from monomers to polymers

high operation-T of SOFCs based on oxide ion conducting electrolytes (YSZ)

oxides combining high stability and high proton conductivity at T = 500°-800°C: from elementary reactions to 1st fuel-cell tests

K.D. Kreuer, 2002

Max-Planck-Institut für Festkörperforschung, Stuttgart

Max-Planck-Institute for Solid State Research

• proton conducting polymers with low electroosmotic drag: a microstructural approach

Nafion 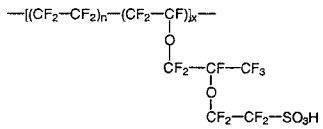

S-PEK 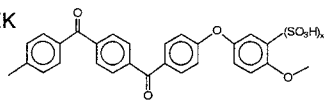

⟶ hydrophobic/hydrophilic nano-separation (especially in the presence of water)

microstructure from SAXS

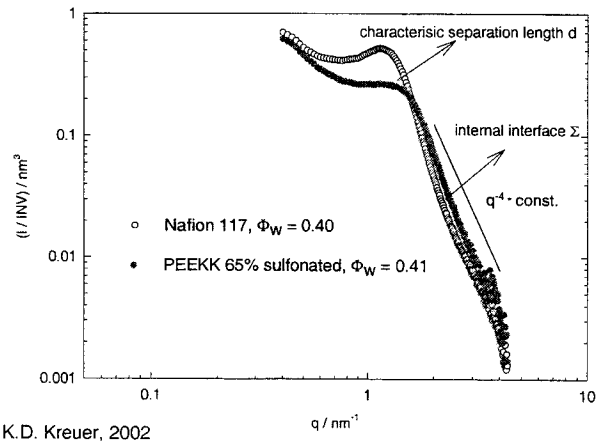

$$d = \frac{2\pi}{q}$$

$$\Sigma = \lim_{q\to\infty} \frac{q^4 I(q)}{INV} \cdot \pi \cdot \Phi_w \cdot (1-\Phi_w)$$

$$INV = \int_0^\infty I(q) \cdot q^2 dq \quad : \text{scattering invariant}$$

Φ_w : volume fraction of absorbed water

M. Ise; Dissertation, Uni-Stuttgart (2000)
K.D. Kreuer, J.Membrane Science 185, 29 (2001)

K.D. Kreuer, 2002

Max-Planck-Institut für Festkörperforschung, Stuttgart

Max-Planck-Institute for Solid State Research

An artists view

NAFION

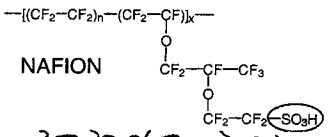

S-PEK

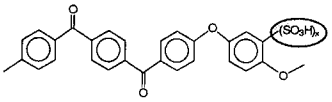

Nafion

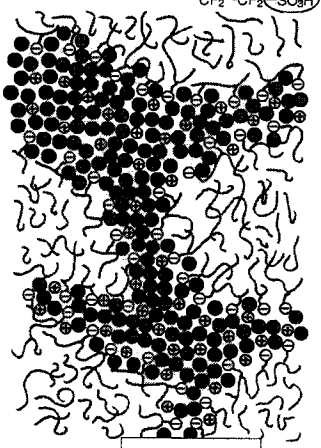

1 nm

⊖ : $-SO_3^-$

⊕ : protonic charge carrier

● : H_2O

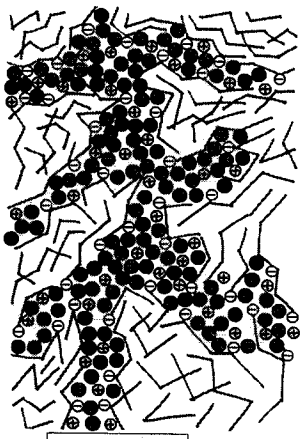

S-PEK

- wide channels
- more separated
- less branched
- good connectivity
- small $-SO_3^-$ / $-SO_3^-$ separation
- pK_a ~ -6

- narrow channels
- less separated
- highly branched
- dead-end channels
- large $-SO_3^-$ / $-SO_3^-$ separation
- pK_a ~ -1

K.D. Kreuer, 2002

K.D.Kreuer, J.Membrane Science 185, 29 (2001)

Max-Planck-Institut für Festkörperforschung, Stuttgart

Max-Planck-Institute for Solid State Research

transport matrix

$$\begin{pmatrix} j_{H^+} \\ j_{H_2O} \\ j_{CH_3OH} \end{pmatrix} = \begin{pmatrix} L_{11} & L_{12} & L_{13} \\ L_{21} & L_{22} & L_{23} \\ L_{31} & L_{32} & L_{33} \end{pmatrix} \begin{pmatrix} \nabla\mu_{H^+} + F\nabla\Phi \\ \nabla\mu_{H_2O} \\ \nabla\mu_{CH_3OH} \end{pmatrix} \quad \text{with } L_{ij} = L_{ji}$$

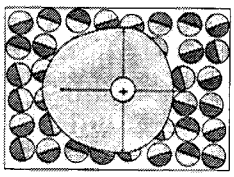

proton conductivity — driving force $F\nabla\Phi$ — method: ac impedance

$$\sigma = F^2 L_{11}$$

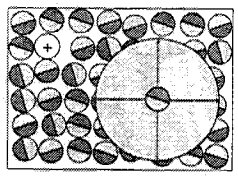

self-diffusion — RT — PFG-NMR

pulsed magnetic field gradient NMR

$$D_{H_2O} = \frac{RT}{c_{H_2O}^2} \frac{dc_{H_2O}}{d\ln a_{H_2O}} L_{22}$$

$$D_{CH_3OH} = \frac{RT}{c_{CH_3OH}^2} \frac{dc_{CH_3OH}}{d\ln a_{CH_3OH}} L_{33}$$

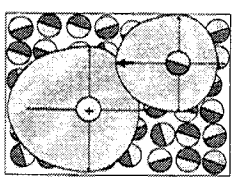

electroosmotic drag — $F\nabla\Phi$ — E-NMR

electrophoretic NMR

$$K_{H_2O} = \frac{F^2}{\sigma} L_{12} = \frac{L_{12}}{L_{11}}$$

$$K_{CH_3OH} = \frac{F^2}{\sigma} L_{13} = \frac{L_{13}}{L_{11}}$$

K.D. Kreuer, 2002

Max-Planck-Institut für Festkörperforschung, Stuttgart

Max-Planck-Institute for Solid State Research

transport coefficients as a function of water volume fraction (proton mobility (L_{11}) and water self-diffusion(L_{22}))

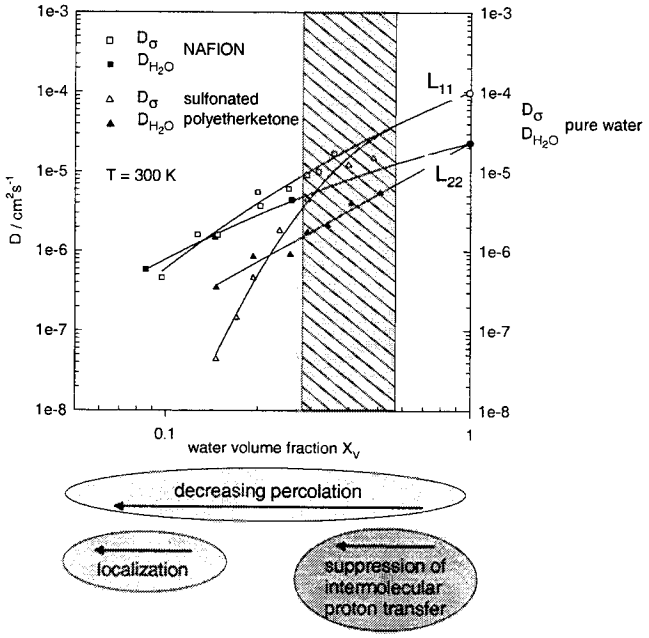

K.D. Kreuer, 2002

K.D.Kreuer, J.Membrane Science 185, 29 (2001)

Max-Planck-Institut für Festkörperforschung, Stuttgart

Max-Planck-Institute for Solid State Research

electroosmotic water/methanol drag $\left(\frac{L_{12}}{L_{11}}, \frac{L_{13}}{L_{11}}\right)$

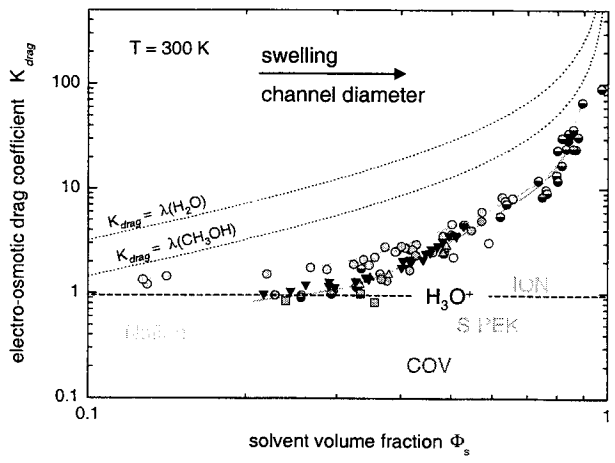

M.Schuster, M.Ise, A.Fuchs, K.D.Kreuer, J.Maier, in preparation

electroosmotic drag:

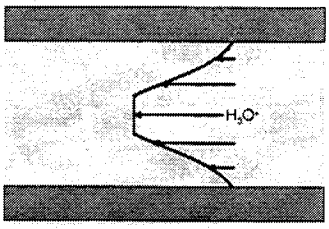

- lower limit given by primary hydration of proton (H_3O^+)
- otherwise electroosmotic drag may be described as hydrodynamic process controlled by *water/water* and *water/polymer interaction*, *microstructure* and *swelling*

- reduce *hydrophobic/hydrophilic separation*
- reduce *swelling* (methanol, T)
- increase *polymer/water interaction*

K.D. Kreuer, 2002

Max-Planck-Institut für Festkörperforschung, Stuttgart

Max-Planck-Institute for Solid State Research

covalently crosslinked S-PEK (J.Kerres, Stuttgart)

swelling in water/methanol

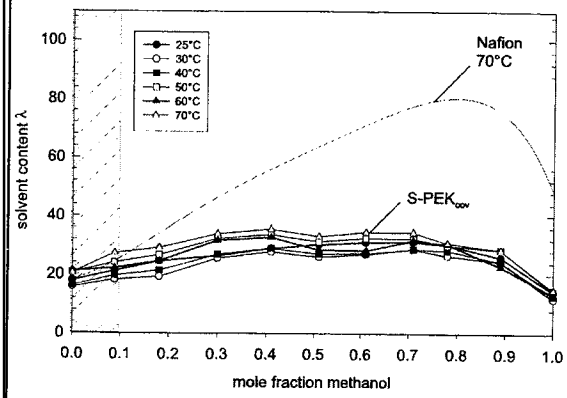

swelling in water

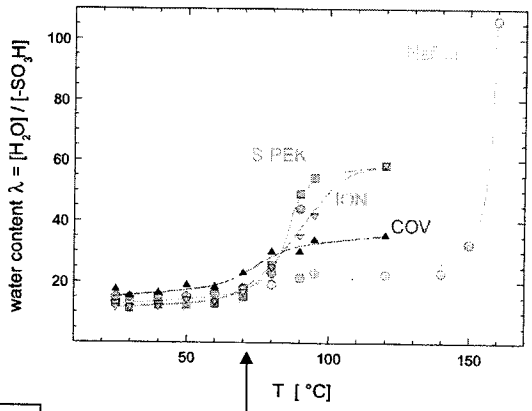

	K_{drag}
Nafion	2.5
S-PEK$_{cov}$	1.1!

T = 70°C

M.Schuster, M.Ise, A.Fuchs, K.D.Kreuer, J.Maier, in preparation

K.D. Kreuer, 2002

Max-Planck-Institut für Festkörperforschung, Stuttgart

Max-Planck-Institute for Solid State Research

- heterocycles as proton solvents: from monomers to polymers (colaboration with MPI-P)

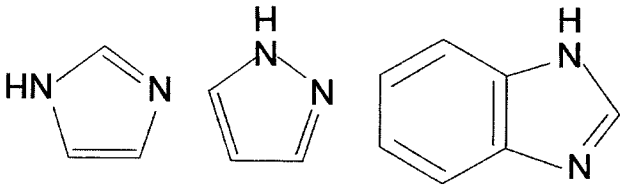

imidazole	pyrazole	benzimidazole
	< 200°C	< 250°C
T_m = 90°C	T_m = 80°C	T_m = 170°C

→ form similar hydrogen bond networks as water

transport coefficients similar to those of water for a given temperature relative to melting point

K.D. Kreuer, 2002

K.D.Kreuer, A.Fuchs, M.Ise, M.Spaeth, J.Maier; Electrochim. Acta 43, 1281 (1998)

Max-Planck-Institut für Festkörperforschung, Stuttgart

Max-Planck-Institute for Solid State Research

structure diffusion in liquid imidazole

proton mobility and imidazole self-diffusion

ab - initio - MD

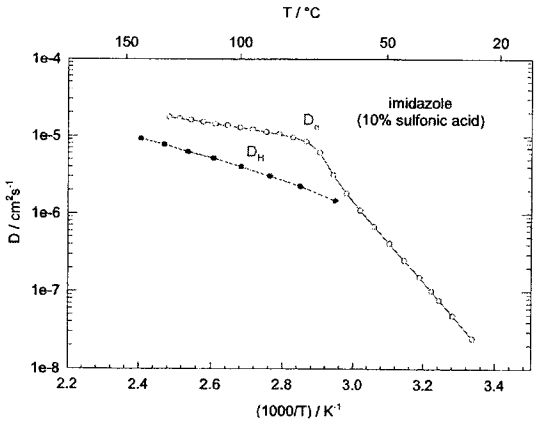

K.D.Kreuer, A.Fuchs, M.Ise, M.Spaeth, J.Maier; Electrochim. Acta 43, 1281 (1998)

W.Münch, K.D.Kreuer, W.Silverstri, J.Maier, G.Seifert; Solid State Ionics 145, 295 (2001)

K.D. Kreuer, 2002

Max-Planck-Institut für Festkörperforschung, Stuttgart

Max-Planck-Institute for Solid State Research

how can heterocycles be immobilized without loosing the local dynamics assisting "structure diffusion"

approach:

σ-bond in symmetrical position

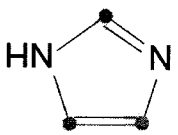

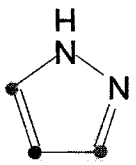

teminated soft side-chains

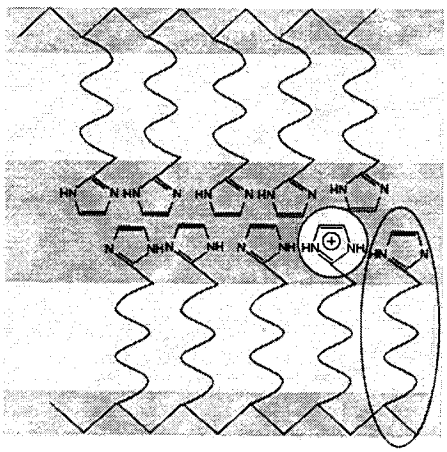

K.D.Kreuer, J.Membrane Science 185, 29 (2001)

rigid polymer backbone

soft spacer

liquid - like proton solvent

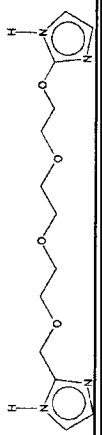

K.D. Kreuer, 2002

Max-Planck-Institut für Festkörperforschung, Stuttgart

Max-Planck-Institute for Solid State Research

a polymeric model system

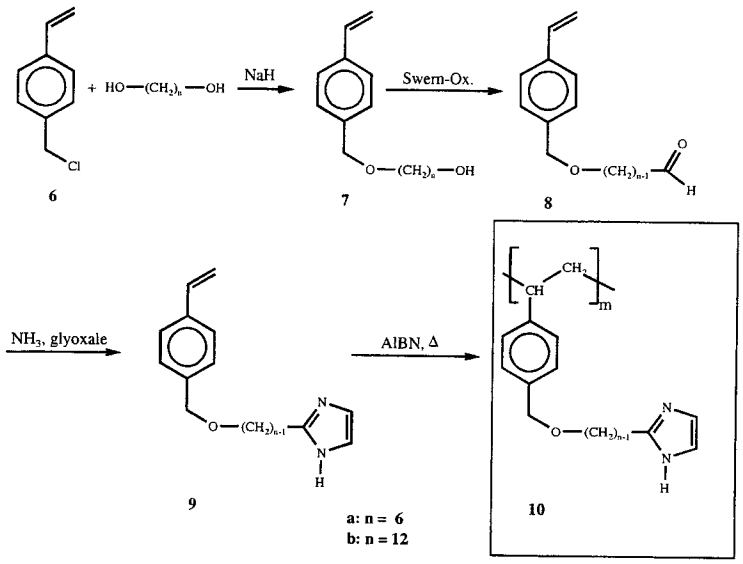

H.G.Herz, K.D.Kreuer, J.Maier, G.Scharfenberger, M.F.H.Schuster, W.H.Meyer; Electrochimica Acta (2002), in press

K.D. Kreuer, 2002

Max-Planck-Institut für Festkörperforschung, Stuttgart

Max-Planck-Institute for Solid State Research

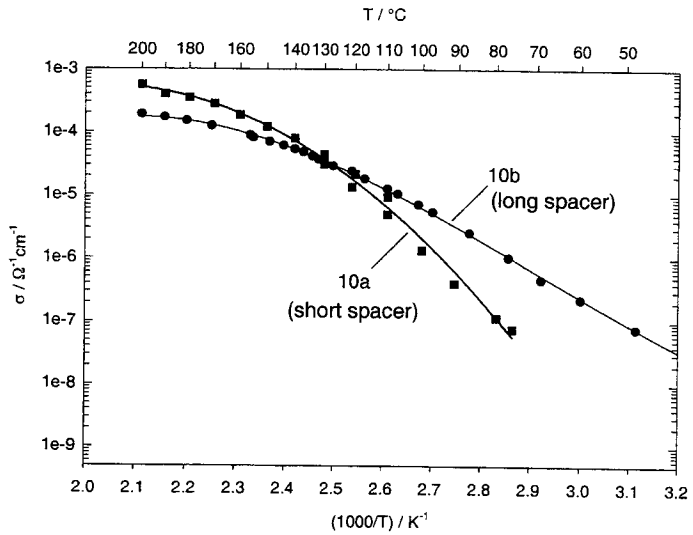

high proton mobility in fully polymeric systems based on soft-spacers terminated by heterocycles has been demonstrated *(prove of concept)*

H.G.Herz, K.D.Kreuer, J.Maier, G.Scharfenberger, M.F.H.Schuster, W.H.Meyer; Electrochimica Acta (2002), in press

K.D. Kreuer, 2002

Max-Planck-Institut für Festkörperforschung, Stuttgart
Max-Planck-Institute for Solid State Research

- oxides combining high stability and high proton conductivity at T=500°-800°C:
  from elementary reactions to 1st fuel-cell tests

formation of protonic charge carriers

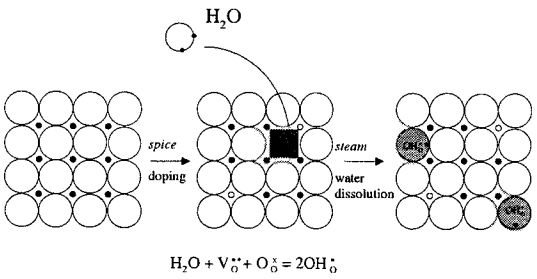

K.D.Kreuer; Solid State Ionics 125, 285 (1999)

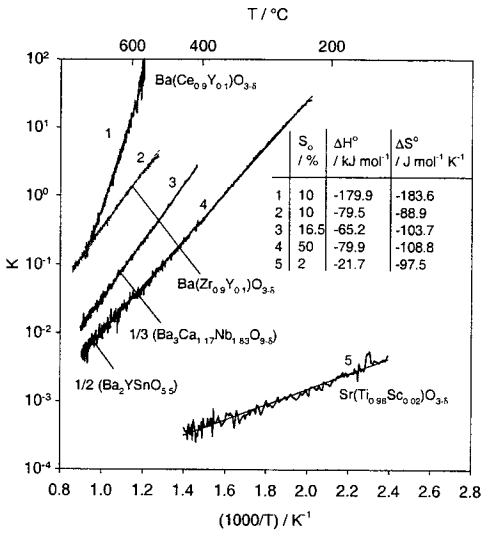

	S_o / %	ΔH° / kJ mol^{-1}	ΔS° / J mol^{-1} K^{-1}
1	10	-179.9	-183.6
2	10	-79.5	-88.9
3	16.5	-65.2	-103.7
4	50	-79.9	-108.8
5	2	-21.7	-97.5

titanate → niobate → stannate → zirconate → cerate

K.D. Kreuer, 2002

Max-Planck-Institut für Festkörperforschung, Stuttgart
Max-Planck-Institute for Solid State Research

mobility of protonic defects

fluctuating hydrogen bond

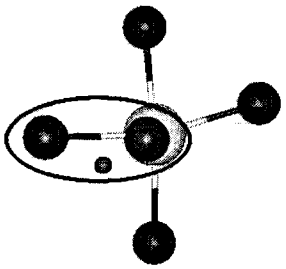

$SrTiO_3$ (T=1800K)

proton dynamics in high energy hydrogen bond

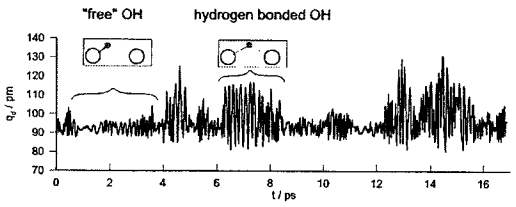

→ variation of hydrogen bond strength leads to configurations which favors bond breaking and situations which favors proton transfer

K.D.Kreuer; Solid State Ionics 136-137, 149 (2000)

K.D. Kreuer, 2002

Max-Planck-Institut für Festkörperforschung, Stuttgart

Max-Planck-Institute for Solid State Research

optimization of proton conductivity and stability

→ $Y:BaZrO_3$

bulk proton conductivity

stability

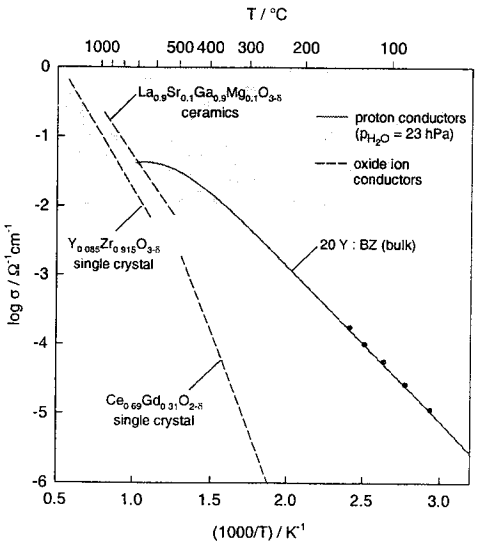

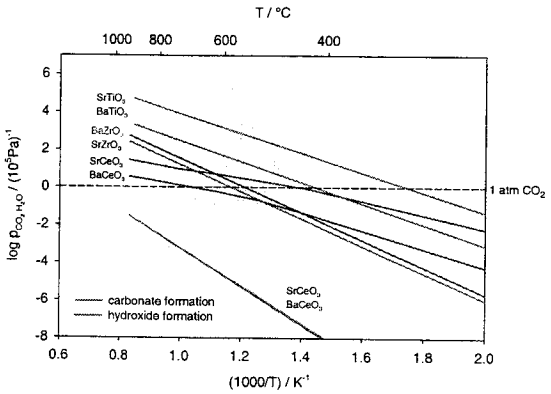

cerate → zirconate → titanate

K.D.Kreuer; Solid State Ionics 125, 285 (1999)

K.D. Kreuer, 2002

Max-Planck-Institut für Festkörperforschung, Stuttgart

Max-Planck-Institute for Solid State Research

transport beyond the bulk

current constriction and grain boundary impedance

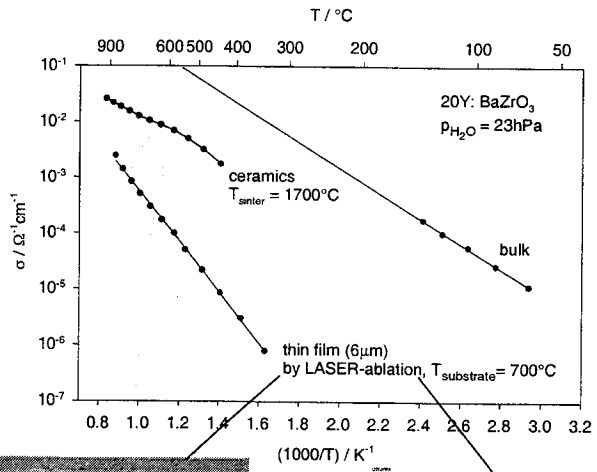

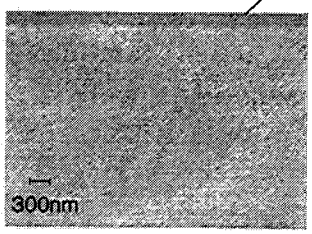

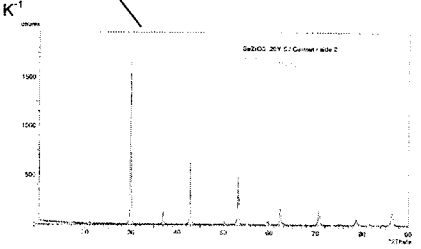

K.D. Kreuer, 2002

Max-Planck-Institut für Festkörperforschung, Stuttgart

Max-Planck-Institute for Solid State Research

CeO_2 as sintering aid

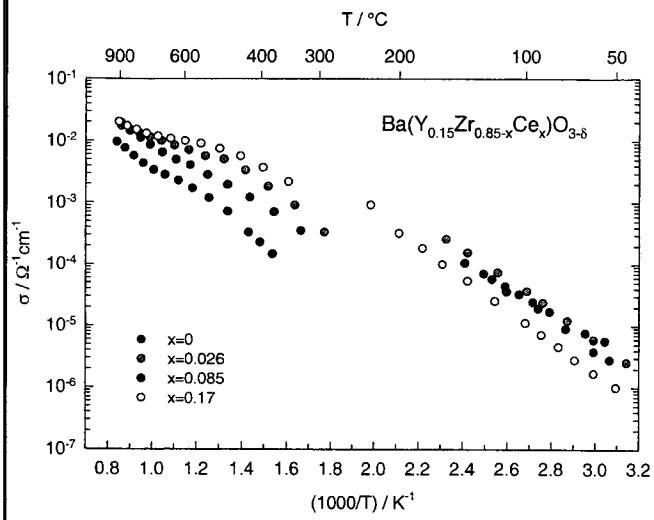

micro-cracks

X=0

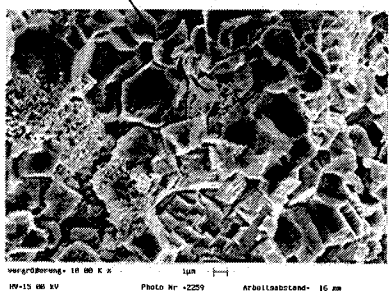

X=0.17

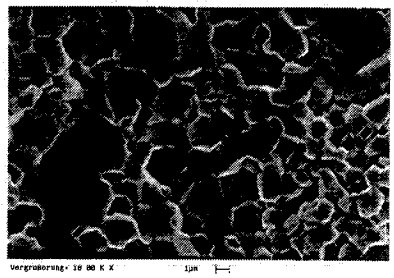

K.D. Kreuer, 2002

Max-Planck-Institut für Festkörperforschung, Stuttgart

Max-Planck-Institute for Solid State Research

preliminary FC - test

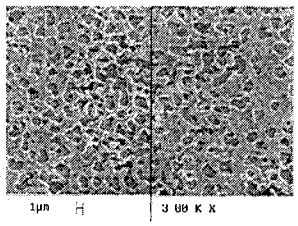

d = 1mm

5% H_2 in Ar
p_{H2O} = 23hPa

O_2
p_{H2O} = 23hPa

electrolyte	electrodes	fuel	T	max. power	
Yb: $SrCeO_3$	Pt	H_2	800°C	35 mW	Iwahara 1988
Nd: $BaCeO_3$	Pt (Ni)	H_2 (CH_4)	800°C	80 mW	Iwahara et al 1990
Gd: $BaCeO_3$	Ag, Pt	H_2	600°C 800°C	18 mW 85 mW	Bonanos et al 1991
Gd: $BaCeO_3$	Pt	H_2	600°C 800°C	120 mW 230 mW	Taniguchi et al 1992
Sm: $BaCeO_3$	Pt (Ni, $La_{0.6}Ba_{0.4}O_{3-\delta}$)	H_2	1000°C	220 mW	Iwahara et al 1993

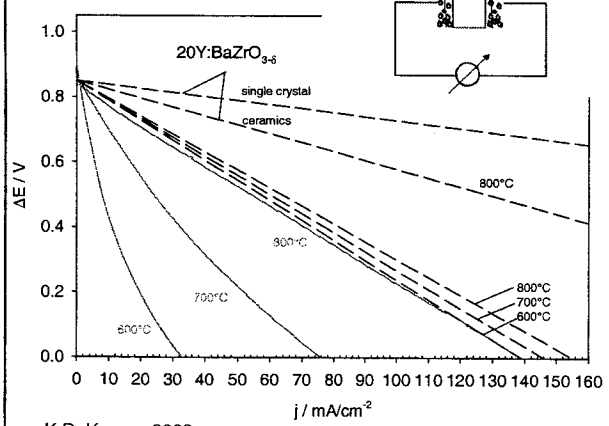

\+ the bulk of Y-doped $BaZrO_3$ combines very high proton conductivity and a wide ionic domaine with high thermodynamic stability

−
- brittleness (cracks)
- current constriction and grain boundary impedance
- low adherence of nobel metal electrodes (high overpotential)
- high sintering - T

K.D. Kreuer, 2002

Max-Planck-Institut für Festkörperforschung, Stuttgart

Max-Planck-Institute for Solid State Research

DMFC
(liqiud)

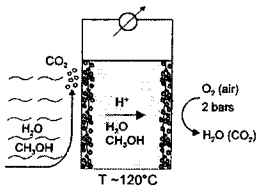

reduced electroosmotic water/methanol drag by microstructural control and reduced swelling
(prove of concept for T< 80°C)

DMFC
(gaseous)

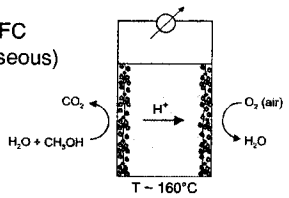

high proton mobility of fully polymeric proton solvents based on flexible spacers terminated by heterocycles
(demonstrated for model compounds, T< 200°C)

SOFC

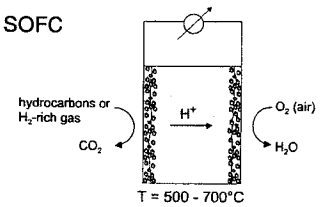

Y:$BaZrO_3$ combines high bulk proton conductivity and thermodynamic stability

(high grain boundary impedance and electrode overpotentials)

K.D. Kreuer, 2002

Max-Planck-Institut für Festkörperforschung, Stuttgart

Max-Planck-Institute for Solid State Research

A. Fuchs
U. Traub
M. Ise
M. Schuster
H.G. Herz
W. Münch
J. Maier (head of department)

G. Seifert, Dresden
W.H. Meyer, MPI-P

R. Bauer, FuMaTech
M. Waidhas, Siemens

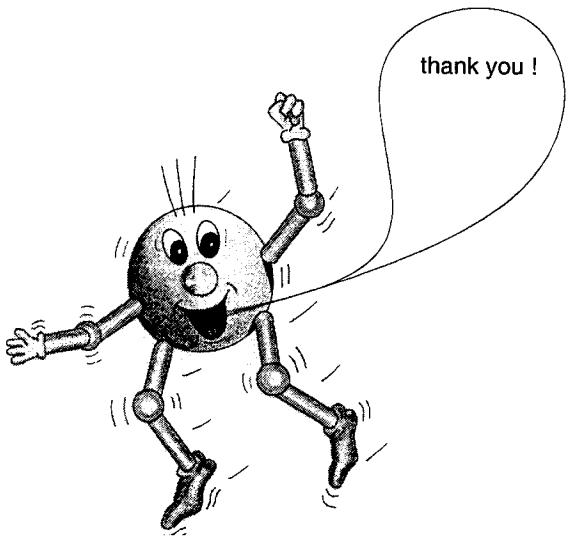

K.D. Kreuer, 2002

Wasserfreie protonenleitende Polymere

- Materialien für PEMFCs?

Wolfgang H.Meyer

Max-Planck-Institut für Polymerforschung
Max Planck Institute for Polymer Research

New Approaches for PEMFC Membranes

waterfree proton conducting polymers

alternative proton solvents
H_3PO_4, H_2SO_4
sulfamide, imidazole
and alternative polymers
PEO, PEI, PAMA...
PBI

immobilized proton solvents
N-heterocycles
models and mechanism
intrinsically H^+ conducting polymers

Wolfgang H.Meyer

Max-Planck-Institut für Polymerforschung
Max Planck Institute for Polymer Research

Disadvantages of Traditional Separator Membranes

water containing

low temperatur operation

electro-osmotic water drag

CO - poisening

water management

high cooling

low efficiency

Wolfgang H.Meyer

Max-Planck-Institut für Polymerforschung
Max Planck Institute for Polymer Research

alternative proton solvent: H_3PO_4

H_3PO_4 is a weak acid: pKa = 2.16 ↷ ~ 8mol% H^+ present at 25°C

Tm_{H3PO4} = 42°C

dissociation: $5\ H_3PO_4 \Leftrightarrow 2\ H_4PO_4^+ + H_2PO_4^- + H_3O^+ + H_2P_2O_7^{2-}$

mol/l at 311 K :	16.815	0.890	0.429	0.461	0.461

(R.A.Munson, J.Phys.Chem., 1968, 68, 3374)

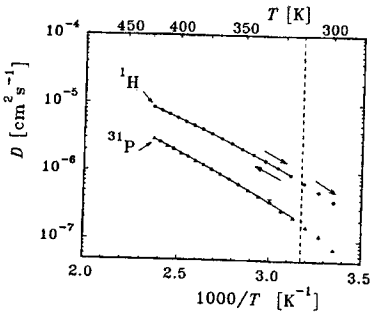

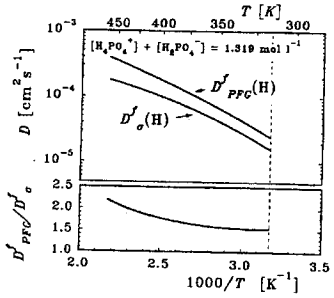

proton transport almost exclusively based on **structure diffusion** ($D^{1H}_{(struc)}$ derived from QENS) (Kreuer et al., Solid State Ionics 1993, 61, 41)

Wolfgang H.Meyer

Polymer - Acid Complexes

—CH_2–CH_2–O— PEO

—CH_2–CH_2–NH— PEI

—CH_2–CH(OH)— PVA

—CH_2–CH(C=ONH_2)— PAam

—CH_2–CH(N-C=O)— PVP

—CH_2–CH(N)— P4VP

polymers with "basic" sites have been blended with H_3PO_4 (H_2SO_4) and applied in electrochromic devices, hydrogen sensors and fuel cells

sufficient conductivities, e.g.:
$\sigma_{(PMMA\text{-}PEO/0.2H3PO4)} = 2.7 \times 10^{-2}$ S/cm (50°C)

however: materials are insufficiently stable

reviews

Lassègues et al.:
- Solid State Ionics 2001, 145, 37;
- p 311-28 in : "Proton conductors.." P. Colomban Ed., Cambridge University Press, N.Y. 1992

Wieczorek et al., Synth. Metals, 1991, 45, 323-33

Nafion - H_3PO_4

substitution of water by phosphoric acid in Nafion gives rise for high σ at 175°C, reduced MeOH crossover and long-term stability

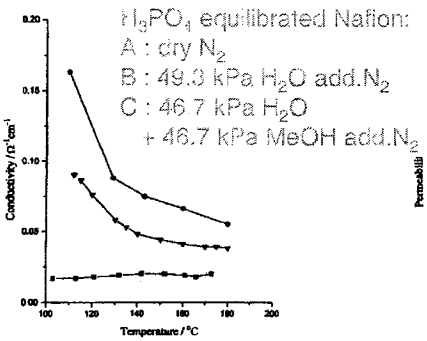

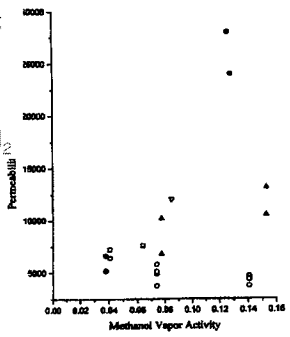

for comparison:
Nafion 125:
250mA/cm² (50°C)

1 Barrer = 7.5×10^{-18} m³ (STP) m/m² s Pa

(Savinell et al.,J.Electrochem.Soc.,1994, 141, L46)

Nafion - H_3PO_4 and other solvents

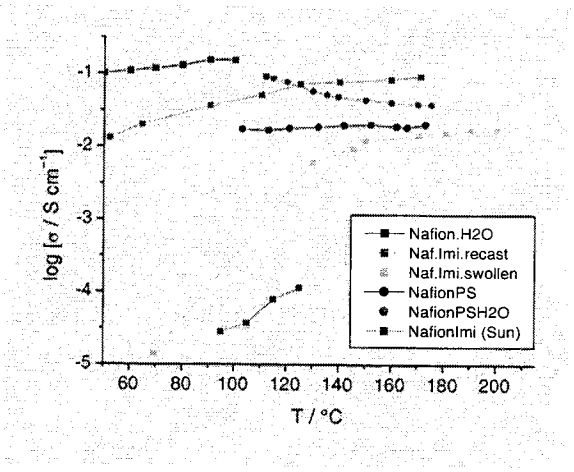

M.Schuster, Dissertation University of Mainz, 2002, Germany
http://ArchiMeD.uni-mainz.de/pub/2002/0017/diss.pdf

PEO - H_3PO_4

maximum conductivities at 20 mol% H_3PO_4(relative to PEO content):
corresponds to eutectic composition of PEO-H_3PO_4 ⟹ **phase diagram**

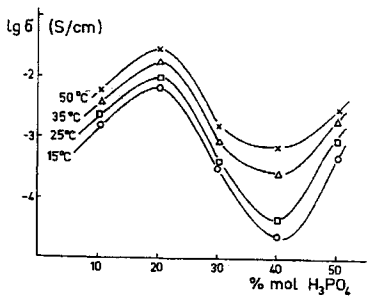

conductivity isotherms of
PEO-PMMA (8:2) blends

(Przyluski et al., SSI 1993, 60, 141)

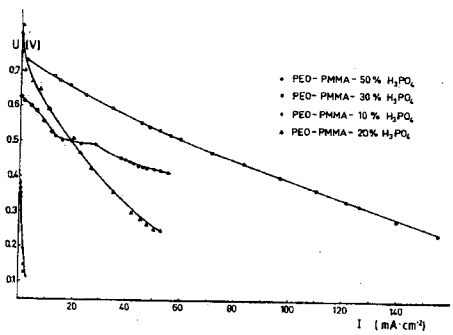

high electrode/electrolyte resistance cause
low voltage efficiency,
no long term stability

PEI - H_3PO_4

conductivities in poly(ethyleneimine)/phosphoric acid blends
are strongly concentration dependent : **type of charge carriers change**

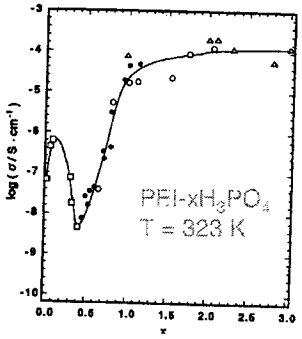

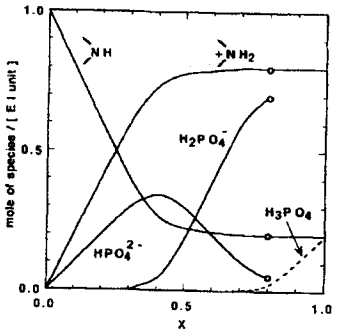

at 0<x 0.4 conductivity is based on hopping of H^+ over basic sites NH_2^+
at 0.4<x<0.8 HPO_4^{2-} is depleted by salt formation ⟹ minimum
(PEI can be protonated only to a maximum of about 80%)
at x>0.8 conductivity increases due to $H_2PO_4^-$ and free H_3PO_4

Wolfgang H.Meyer

(Tanaka et al., Electrochim.Acta, 2000, 45, 1385; 40, 2421)

Poly-4-Vinylimidazole - H_3PO_4

P4VI blends with H_3PO_4 (x = moles H_3PO_4 per repeat unit)
(Pu et al., Macromol. Chem. & Phys., 2001, 202, 1478)

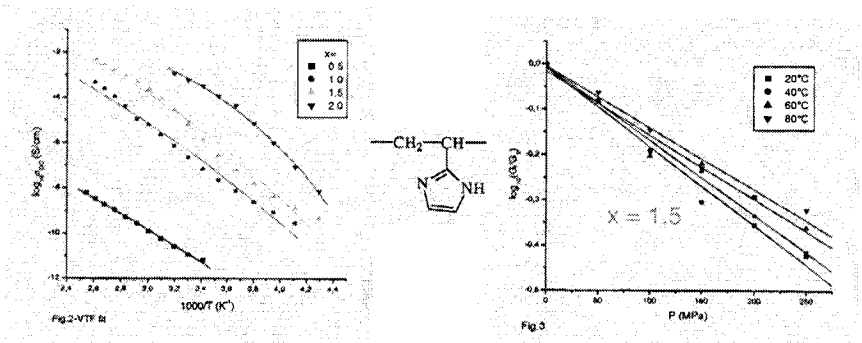

activation volumes from pressure dependent σ data : 8 - 10 cm^3/mol
much smaller than free volume controlled ion motion (20-60) but higher than "H^+-hopping" in PBI/H_3PO_4 (4-6) ; **change in mechanism** at T_g

Wolfgang H.Meyer

Max-Planck-Institut für Polymerforschung
Max Planck Institute for Polymer Research

$PAMA^+H_2PO_4^- / H_3PO_4$

poly(diallyldimethylammonium-dihydrogenphosphat)
blends with H_3PO_4 ⟹ **immobilization of proton solvent**

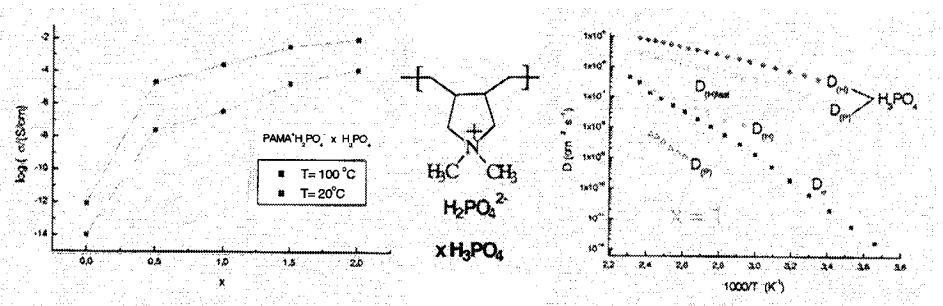

1. conductivities are lower than in pure H_3PO_4 because D_H and D_P are lower in the blends
2. not all proton hopping contributes to proton conductivity ($D_{fast} > D_\sigma$)
   (Bozkurt et al., SSI 1999, 125 , 225)

Wolfgang H.Meyer

Max-Planck-Institut für Polymerforschung
Max Planck Institute for Polymer Research

$PAMA^+H_2PO_4^- / H_3PO_4$

poly(diallyldimethylammonium-dihydrogenphosphat) blends with H_3PO_4

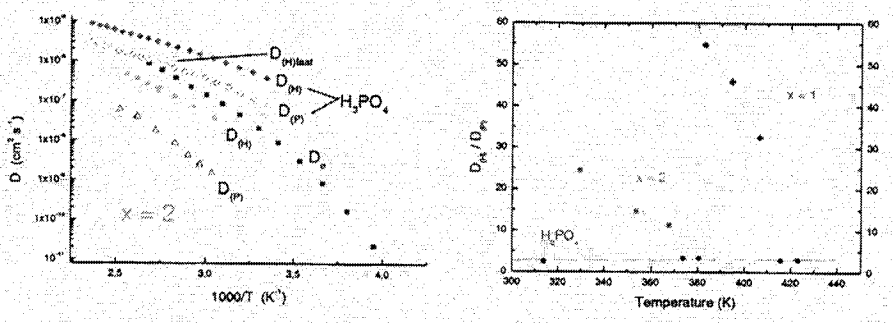

D_H and D_P are not only smaller in the blends than in H_3PO_4, but the ratio D_H/D_P is much higher (x- and T-dependent)

the phosphate moieties are distinctly **immobilized** by coulombic interactions

(Bozkurt et al., SSI 1999, 125 , 225)

Wolfgang H.Meyer

Max-Planck-Institut für Polymerforschung
Max Planck Institute for Polymer Research

PBI / Polybenzimidazole

Synthesis: melt condensation from diaminobenzidine and dicarboxylic acid derivative

problem: purification of tetramine (side products, high Mw)
postcondensation at 400°C / vacuum

(H.Vogel, C.S.Marvel, J.Polym.Sci., 1961,50, 511; 1963, 1, 1953)

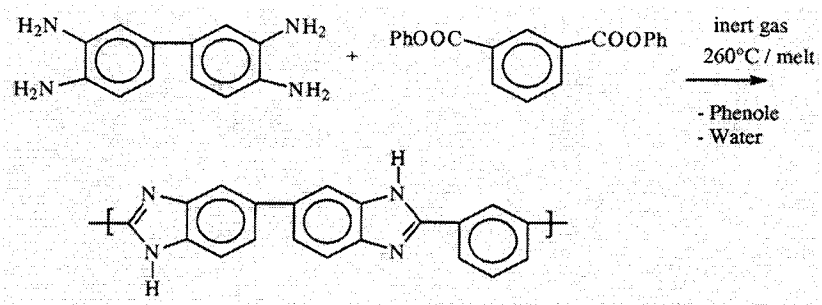

pK_a =5.5 ; T_g = 430°C; soluble in formic acid, DMSO, H_3PO_4, thermally stable up to 500°C in air, cheaper than Nafion, but at present exclusively produced by Celanese, only MEAs

Wolfgang H.Meyer

Max-Planck-Institut für Polymerforschung
Max Planck Institute for Polymer Research

PBI / H_3PO_4

"doping" of PBI can be achieved via casting both, PBI and H_3PO_4 from solution or via swelling of the preformed PBI-membrane in H_3PO_4 (solutions in water)

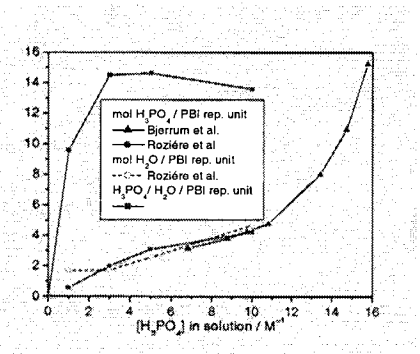

after long exposure to the swelling solution H_3PO_4 is enriched over H_2O in PBI

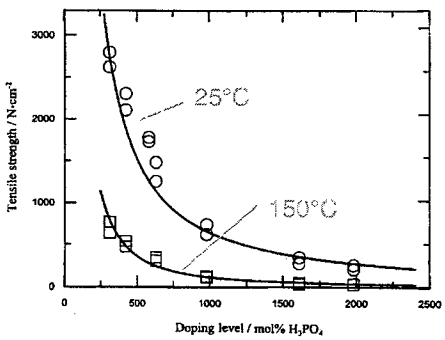

swelling of PBI with H_3PO_4 leads to a dramatic decrease of tensile strength

Roziére et al., J.Mater. Chem. 1999, 9 (12), 3045
Bjerrum et al., J.Appl. Electrochem., 2001, 31(7), 773;

Wolfgang H.Meyer

Max-Planck-Institut für Polymerforschung
Max Planck Institute for Polymer Research

PBI / H_3PO_4

H_3PO_4 doped PBI membranes appear to be very promising for elevated temperature application in fuel cells

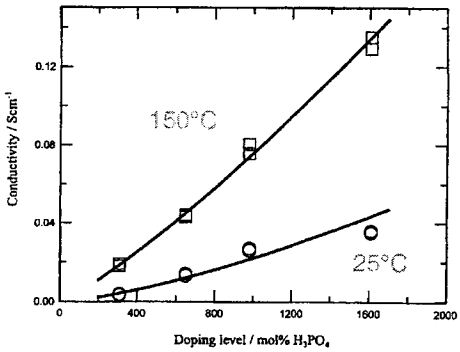

strong doping level dependent conductivity, water drag coefficient almost zero

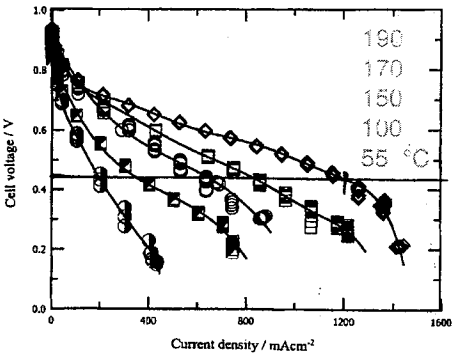

fuel cell performance at different T and normal p with H_2 / O_2 // rate 32 mlmin^{-1} cm^{-2}

Wolfgang H.Meyer

Bjerrum et al., J.Appl. Electrochem., 2001, 31(7), 773

Max-Planck-Institut für Polymerforschung
Max Planck Institute for Polymer Research

PBI / H_3PO_4

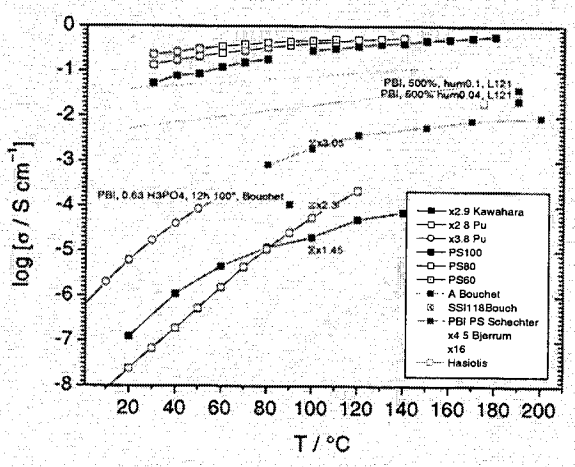

however:

different compositions / different preparation pathways:

dry H_3PO_4 / cast from TFA: $\sigma_{200°C}$=9.10^{-3} S/cm (Savinell)

swelling from aqueous solutions: $\sigma_{200°C}$= 0.02 -0.04 S/cm (Wainright)

gas humdification increase σ and current densities, $\sigma_{160°C}$= 0.13 S/cm (16 H_3PO_4/ PBI; 85 r.h.) (Qingfeng)

Savinell et al., SSI 2002, 147 (1-2), 181;
Wainright et al., J.Electrochem. Soc, 1995, 142(7), L121;
Qingfeng et al., J.Electrochem.Soc., 2001, 148(5), A513;

Wolfgang H.Meyer

Max-Planck-Institut für Polymerforschung
Max Planck Institute for Polymer Research

PBI / H_3PO_4

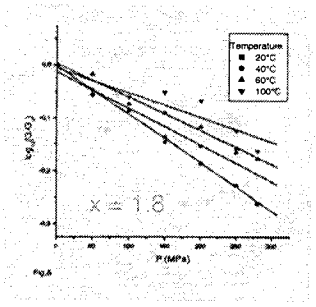

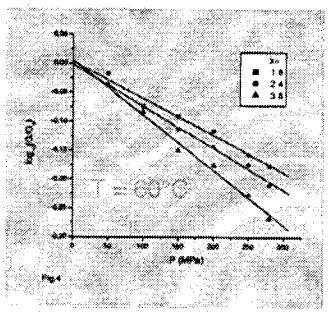

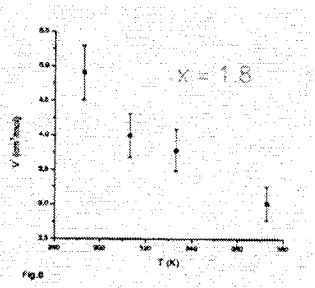

pressure dependent conductivity data reveal a temperature and composition dependent activation volume for proton transport in H_3PO_4 doped PBI; the values are typical for hopping transport; water content is crucial

Pu et al., J.Polym.Sci B, 2002, 40, 663

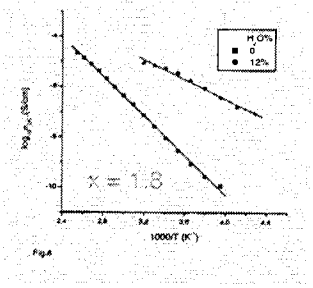

Wolfgang H.Meyer

Max-Planck-Institut für Polymerforschung
Max Planck Institute for Polymer Research

PBI / H_3PO_4 containing MEA

fuel cell performance with PBI/H_3PO_4 - MEAs appears to be promising:

Wang et al. report power densities of 0.1 W/cm^2 at 200°C for a DMFC and 0.25 W/cm^2 at 150°C for a H_2/O_2 cell (Electrochim. Acta,1996,41,193)

Quingfeng et al.established power densities of 0.55 W/cm^2 at 190°C for DMFC without further humidification, 3 vol% CO caused voltage losses from 0% to 20% (1.2 Acm^{-2}) (J.Appl.Electrochem. 2001, 31, 773)

Quingfeng et al. recently reported about the use of a PBI (75%) blend with sulfo-PSU, 500% H_3PO_4, 0.54 W/cm^2 for H_2/O_2 and 0.49 W/cm^2 for methanol reformate (3 vol% CO) at 200°C , stable 3 days (Electrochem. Solid State lett., 2002, 5, A125)

finally:
Celanese announced the production of PBI-based MEAs for up to 200°C

long-term performance needs to be proven

Wolfgang H.Meyer

Max-Planck-Institut für Polymerforschung
Max Planck Institute for Polymer Research

PEO - Sulfamide ($H_2NSO_2NH_2$)

IR- and Raman studies prove eutectic PEO-sulfamide compositions at (PEO)/ $H_2NSO_2NH_2$ = 2,4 and 30 : **H-bond fluctuations**

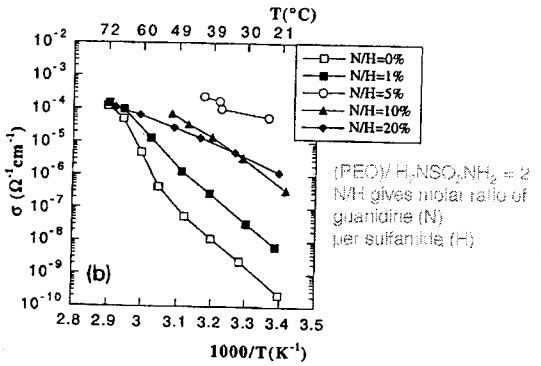

(PEO)/ $H_2NSO_2NH_2$ = 2 N/H gives molar ratio of guanidine (N) per sulfamide (H)

sulfamide is a proton solvent with pKa ~ 10:

$2\ H_2NSO_2NH_2 \rightleftharpoons [H_2NSO_2NH_3]^+ + [H_2NSO_2NH]^-$

Grotthus transport via H-bonds?

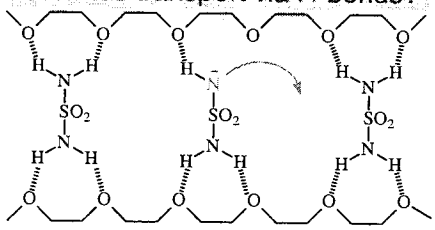

"doping" with guanidine $HN=C(NH_2)_2$ leads to proton vacancy transport (Bermudez et al., SSI 1993, 61, 219)

Wolfgang H.Meyer

Max-Planck-Institut für Polymerforschung
Max Planck Institute for Polymer Research

Concept of Immobilized Proton Solvents

why? to warrant proton solvent retention in the membrane even at high temperatures

approaches:
1. immobilization via covalently tethering
2. immobilization via coulombic interactions (Bozkurt et al., Celanese etc.)

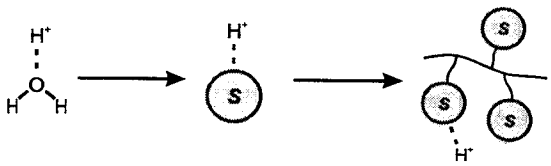

1. in two steps: choice of appropriate proton solvent tethering to polymer backbone

Wolfgang H.Meyer

N-Heterocycles as Proton Solvents

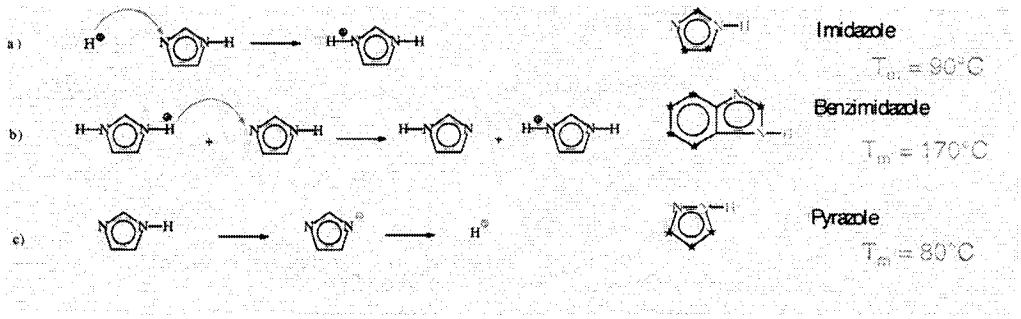

imidazole, benzimidazole and pyrazole are weak bases (pKa ~ 3) which exhibit amphoteric behaviour (a and c), autoprotolysis (b), H-bond formation and exhibit similar transport coefficients as water at a given T relative to T_m. The pure materials show moderate proton conductivity (Kreuer et al., Electrochim. Acta, 1998, 43, 1281)

Imidazole as Proton Solvent

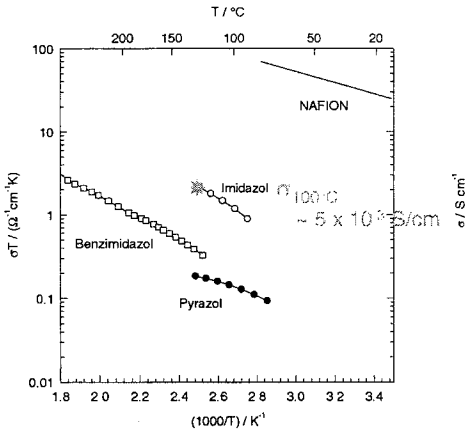

conductivity of pure heterocycles in comparison to Nafion (Kreuer et al., Proc. ISPE-5, Uppsala 1996)

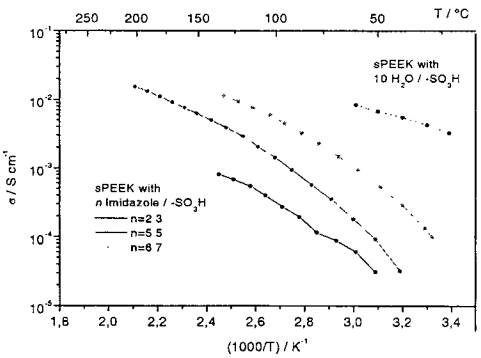

imidazole as proton solvent substituting water in sulfo-PEEKK (Kreuer et al., Electrochim. Acta, 1998, 43, 1281)

Imidazole as Proton Solvent

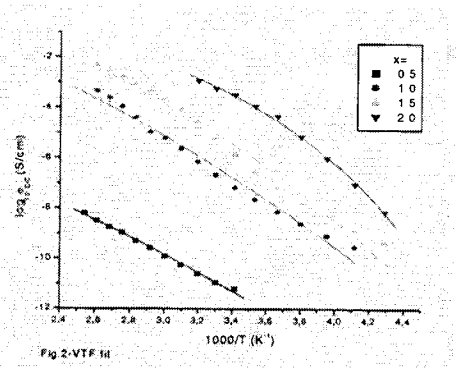

imidazole immobilized in
P4VI x H_3PO_4
(Pu et al., Macromol. Chem. & Phys., 2001, 202, 1478;
Bozkurt et al., SSI, 2001, 138, 259)

if
proton solvent is immobilized
then
proton transport must be based on "structure diffusion"
(Grotthus type transport)

parameters?

H-bond fluctuations?

local mobility?

⟹ **model compounds**

Wolfgang H.Meyer

Immobilization of N-Heterocycles chemical tethering

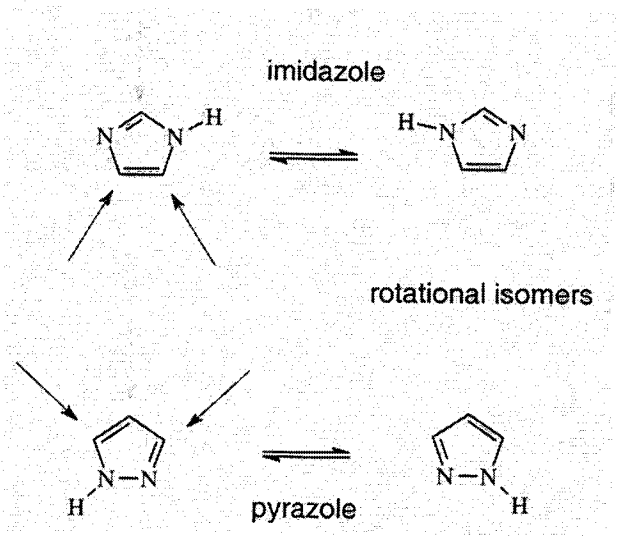

Wolfgang H.Meyer

Max-Planck-Institut für Polymerforschung
Max Planck Institute for Polymer Research

Proton Transport in Model Compounds

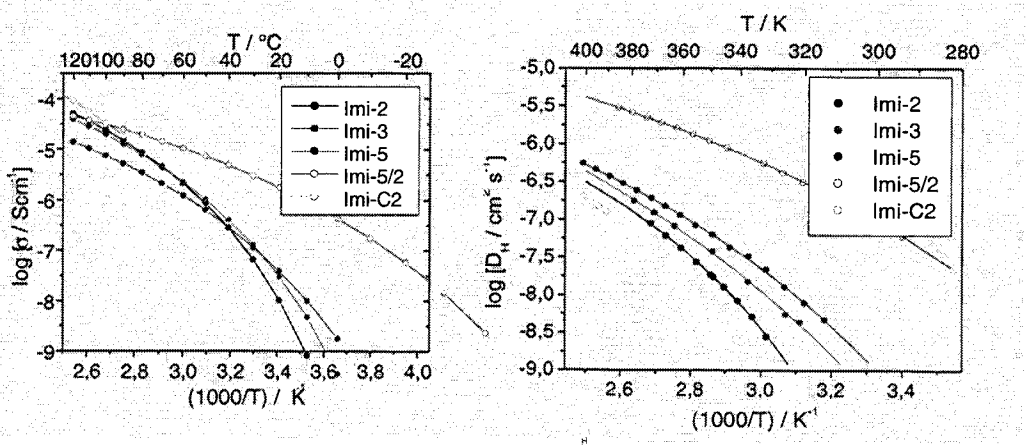

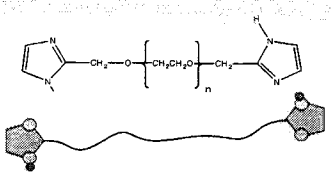

"Imi-n"

Wolfgang H.Meyer

Max-Planck-Institut für Polymerforschung
Max Planck Institute for Polymer Research

Proton Transport in Model Compounds

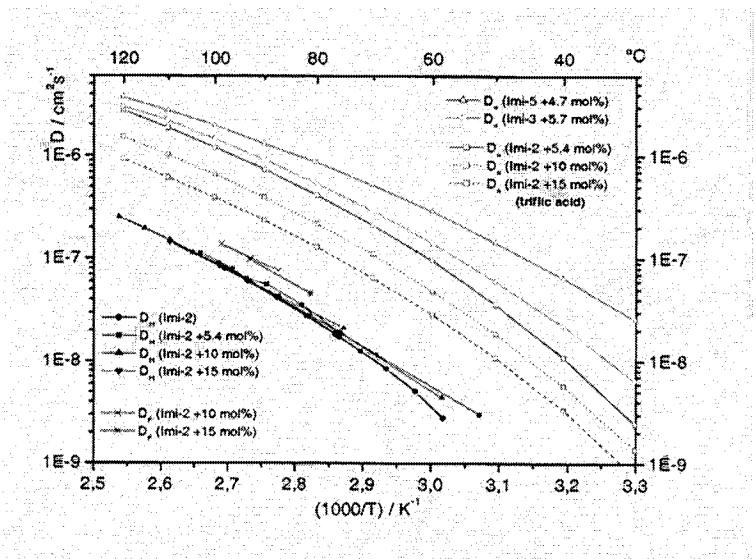

Wolfgang H.Meyer

Max-Planck-Institut für Polymerforschung
Max Planck Institute for Polymer Research

Proton Transport in Model Compounds

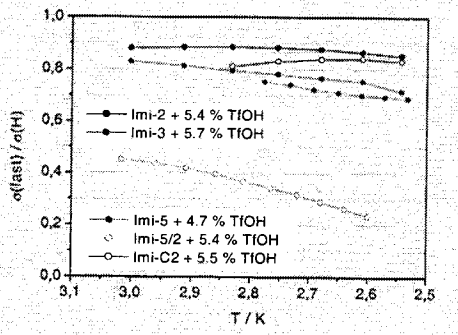

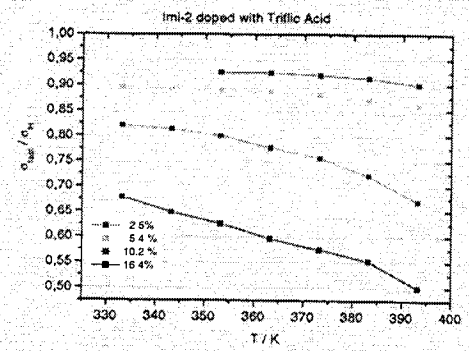

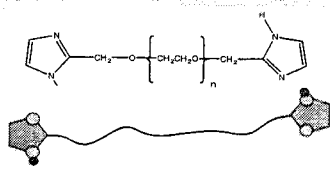

"Imi-n"

Wolfgang H.Meyer

Max-Planck-Institut für Polymerforschung
Max Planck Institute for Polymer Research

Proton Transport in Model Compounds

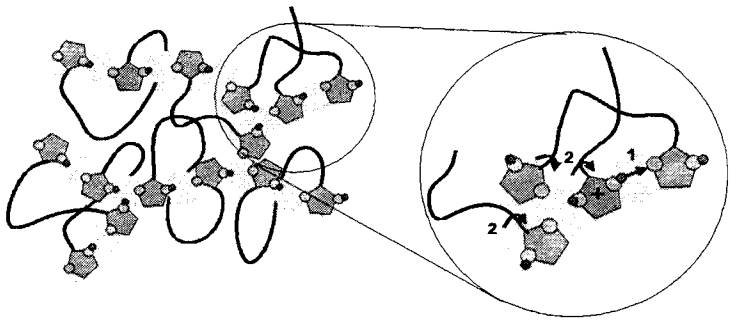

1. ~ 0.3 ps
2. ~ 30 ps
(W.Münch, SSPC-11 / Guildford 2002)

"structure diffusion" in Imi-n

Wolfgang H.Meyer

Structure - vs. Selfdiffusion - a Comparison of Materials

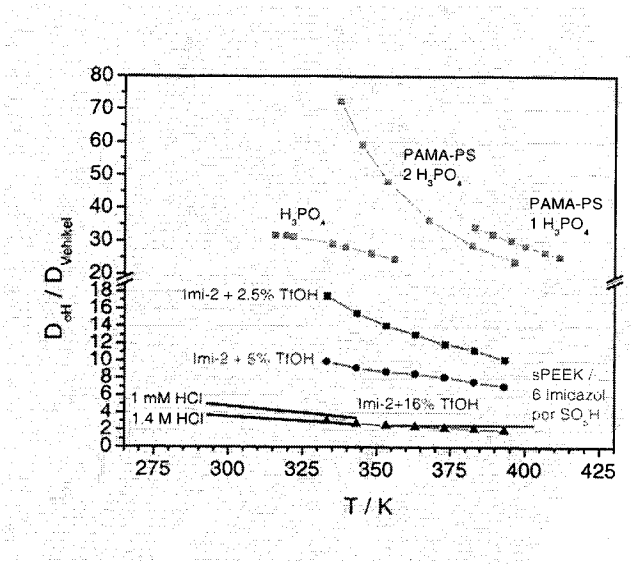

Wolfgang H.Meyer

M.Schuster, Dissertation University of Mainz, 2002, Germany
http://ArchiMeD.uni-mainz.de/pub/2002/0017/diss.pdf

Max-Planck-Institut für Polymerforschung
Max Planck Institute for Polymer Research

Fully Polymeric Proton Conductor with Immobilized Imidazole as Proton Solvent

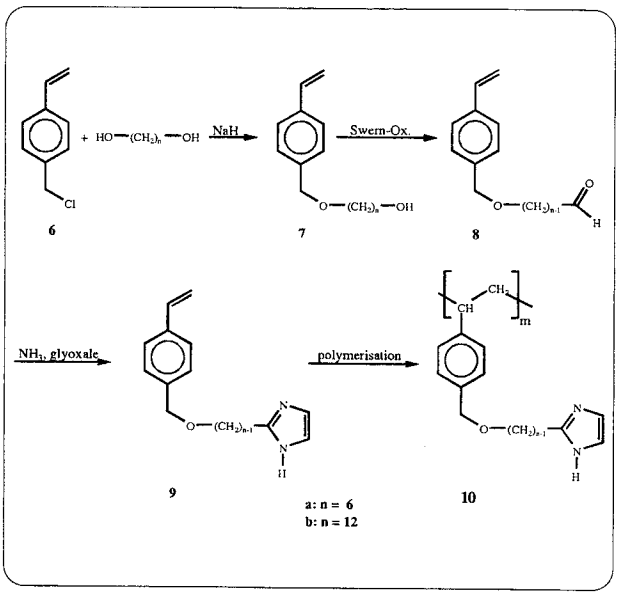

Wolfgang H.Meyer

Max-Planck-Institut für Polymerforschung
Max Planck Institute for Polymer Research

Fully Polymeric Proton Conductor with Immobilized Imidazole as Proton Solvent

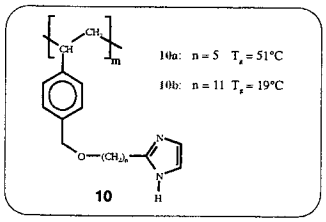

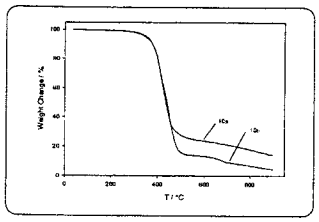

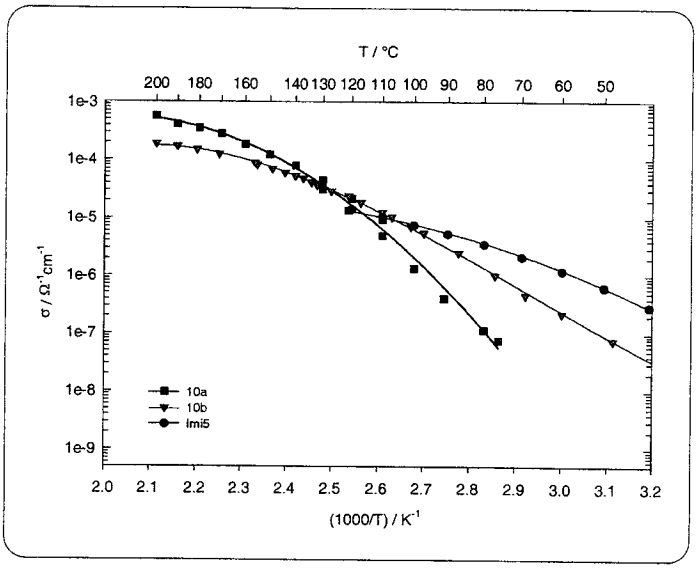

Wolfgang H.Meyer

Herz et al., Electrochim. Acta, 2002 submitted

Max-Planck-Institut für Polymerforschung
Max Planck Institute for Polymer Research

Fully Polymeric Proton Conductor with Immobilized Imidazole as Proton Solvent

Cyclic oligomer : ClmS

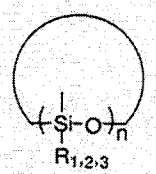

Linear polymer : PlmS

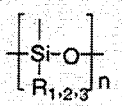

Nanoparticles : AlmS

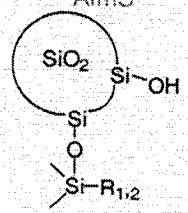

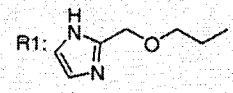

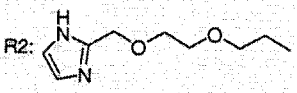

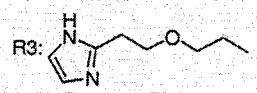

- (poly)siloxane backbone
- flexible ether type spacer
- variation of spacer length
- silicagel nanoparticle

Wolfgang H.Meyer

Max-Planck-Institut für Polymerforschung
Max Planck Institute for Polymer Research

Fully Polymeric Proton Conductor with Immobilized Imidazole as Proton Solvent

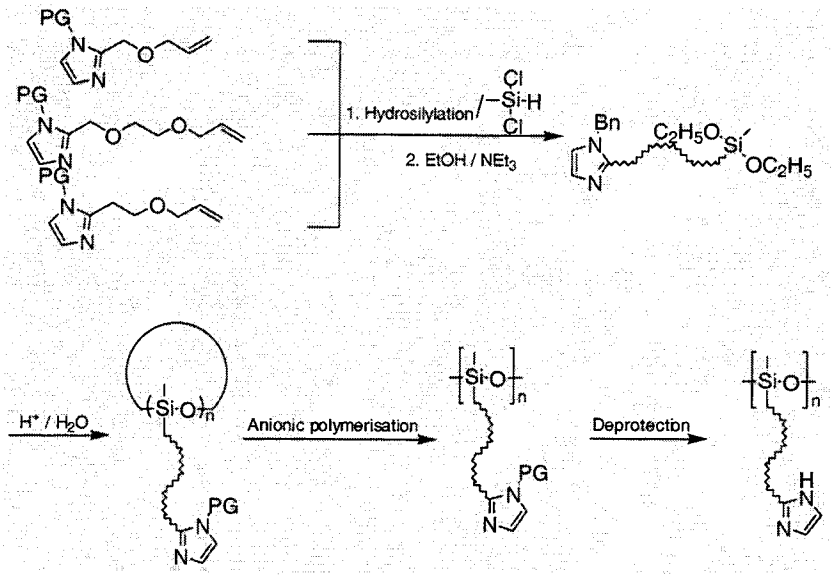

Wolfgang H.Meyer

Max-Planck-Institut für Polymerforschung
Max Planck Institute for Polymer Research

Fully Polymeric Proton Conductor with Immobilized Imidazole as Proton Solvent

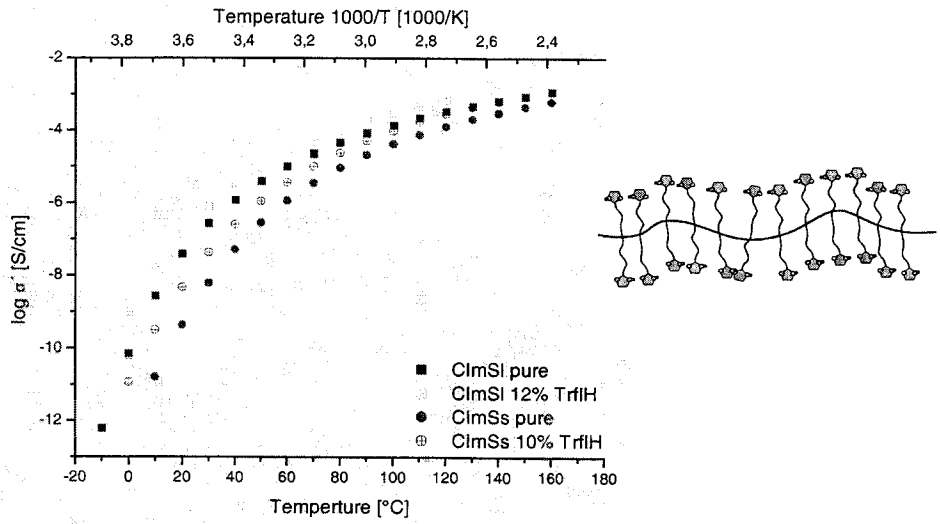

	ClmSs	ClmSI	ClmSstab
Glass transition, Tg	8,8 °C	-1 °C	0°C
Decomposition, Td	170 °C	220°C	225°C

Wolfgang H.Meyer

Max-Planck-Institut für Polymerforschung
Max Planck Institute for Polymer Research

Nano Powders with Tethered Proton Solvents

The following nanopowders have been surface-modified :

A 300 (D_{50} = 7nm, BET = 288m²/g, aerosil/Degussa) and
OX-50 (D_{50} = 44nm, BET = 44m²/g, aerosil/Degussa)

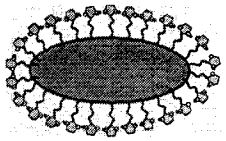

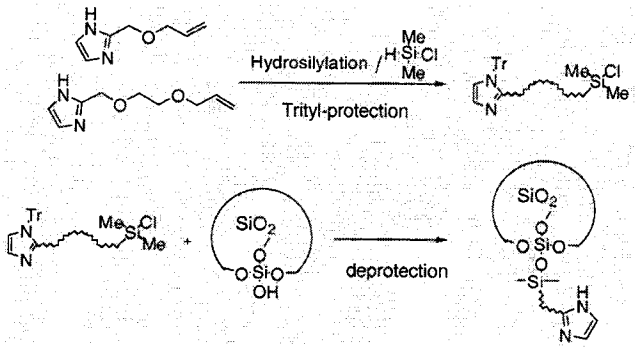

AlmSs	OX 50	A 300
Grafting density	62,5 µmol / g	376,5 µmol / g
	12,3 mg / g	74,3 mg / g
Grafting distance	1,21 nm	1,27 nm

AlmSI	OX 50	A 300
Grafting density	59,8 µmol / g	355,7 µmol / g
	14,5 mg / g	86,4 mg / g
Grafting distance	1,25 nm	1,31 nm

Wolfgang H.Meyer

Max-Planck-Institut für Polymerforschung
Max Planck Institute for Polymer Research

Nanocomposites with Tethered Proton Solvents

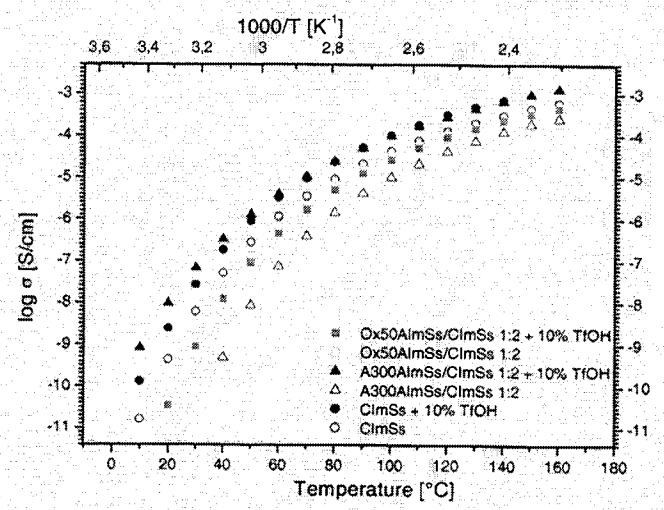

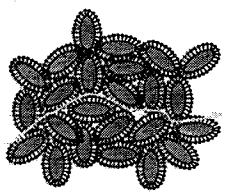

Wolfgang H.Meyer

Conclusions

phosphoric acid and **N-heterocycles** are good alternatives for water as **proton solvent**

PBI is a very stable matrix polymer

blends of H_3PO_4 / PBI appear promising, however proton solvent retention needs to be proven (long term stability)

the concept of **proton solvent immobilization** has been proven both, with model oigomers and polymers

proton conduction in polymers only on the basis of structure diffusion is possible!

materials as yet have only model character
nanocomposites are a promising approach towards stable membranes

Max-Planck-Institut für Polymerforschung
Max Planck Institute for Polymer Research

Acknowledgement

MPI for Solid State Research
(Stuttgart /Germany):

Klaus-Dieter Kreuer
Hans-Georg Herz
Michael Schuster
Joachim Maier

MPI for Polymer Research
(Mainz/Germany):

Martin Schuster
Gunter Scharfenberger
Angelika Manhart
Christoph Sieber
Gerhard Wegner

German Science Foundation
ME 1495 / 2-4

Wolfgang H.Meyer

Entwicklung fluorfreier Polymerblendmembranen für Brennstoffzellen

Jochen Kerres, Wei Zhang, Andreas Ullrich, Chy-Ming Tang, Martin Hein
*Institut für Chemische Verfahrenstechnik (**ICVT**), Universität Stuttgart, Stuttgart*

Viktor Gogel, Thomas Frey, Ludwig Jörissen
*Zentrum für Sonnenenergie- und Wasserstoff-Forschung (**ZSW**), Ulm*

© Jochen Kerres 2002

Ziele

Entwicklung von Membranen mit...

- hoher H^+-Leitfähigkeit
- niedriger Wasser-/Methanolaufnahme (Quellung)
- niedriger Methanol-Permeabilität
- Brennstoffzellen-Anwendbarkeit bei T>100°C
- niedriger Preis

© Jochen Kerres 2002

Arten der Vernetzung

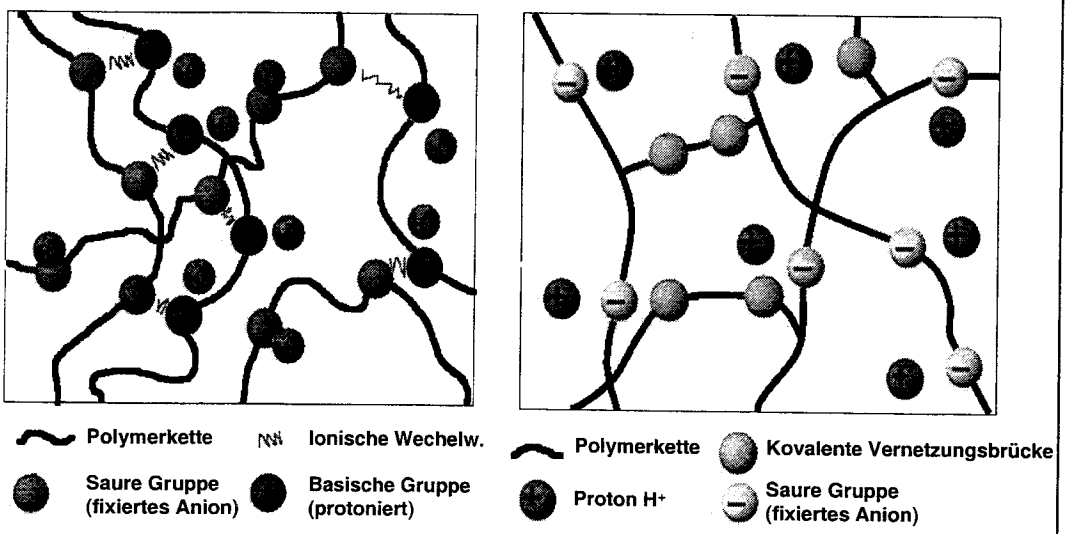

© Jochen Kerres 2002

Blendmembranherstellung

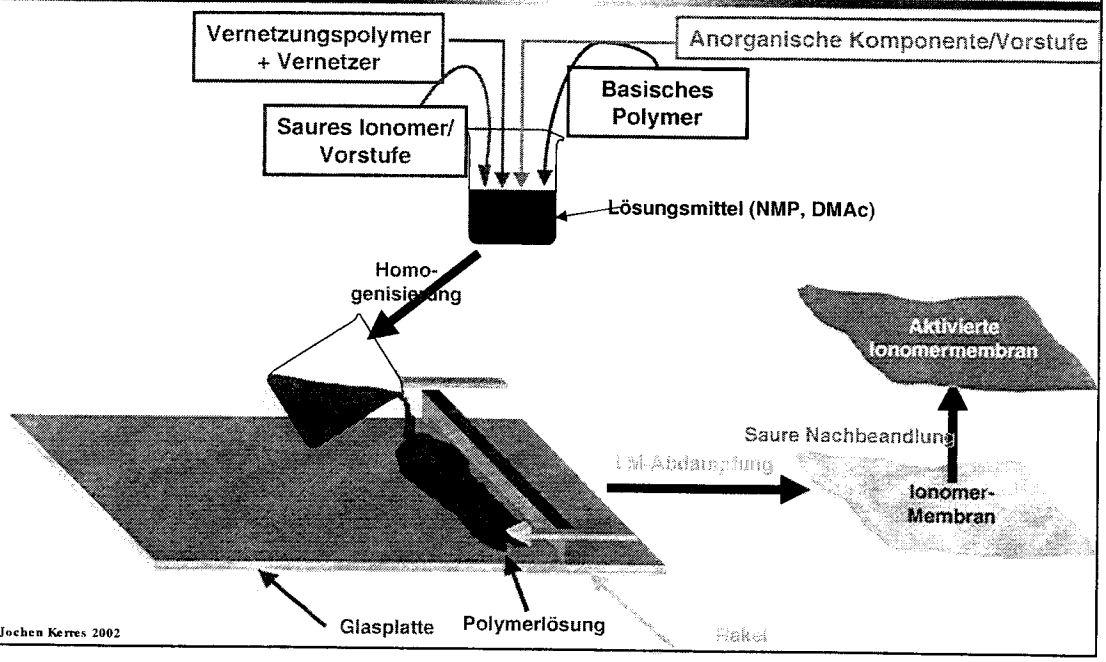

© Jochen Kerres 2002

Typ I: Ionisch vernetzt

Säure-Base-Blend = Polymersulfonat + Polymeramin

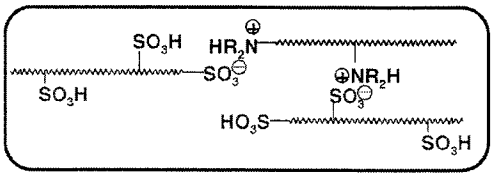

☺ Flexibilität ➔ verringerte Sprödigkeit

☺ Viele Kombinationen Säure/Base

☹ Ionische bindungen lösen sich ab T=70-90°C

© Jochen Kerres 2002

Typ II: Kovalent vernetzt

Kovalent vernetzt =
Polymere Sulfinate + Vernetzer + Sulfopolymere

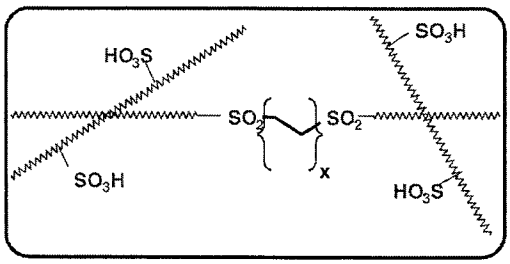

☺ begrenzte Wasseraufnahme

☺ leichte Herstellung

☹ Polysulfonat-Makromoleküle können bei T>100°C ausbluten

© Jochen Kerres 2002

Saure Polymere...

...und ihre nichtionischen Vorstufen

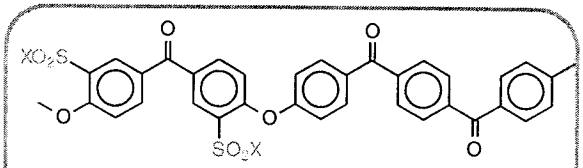

sulfoniertes PEKEKK Ultrapek
X=Cl oder OH

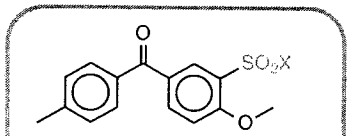

sulfoniertes PEK Victrex
X=Cl oder OH or OLi

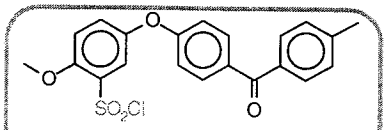

sulfochloriertes PEEK Victrex

© Jochen Kerres 2002

Vernetzungspolymere

Sulfinierte Poly(ethersulfon)e

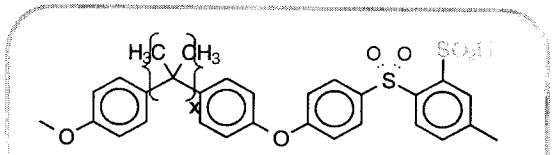

sulfiniertes Polyethersulfon, 1 Gruppe pro WE
x=0: PPhSU Radel R
x=1: PSU Udel

© Jochen Kerres 2002

Basische Polymere

Selbstentwickelt

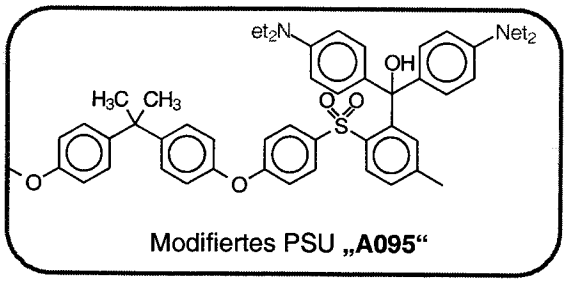

Modifiertes PSU **„A095“**

Kommerziell

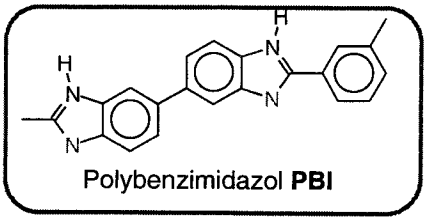

Polybenzimidazol **PBI**

© Jochen Kerres 2002

Membranzusammensetzung und -eigenschaften

Ionisch vernetzte Membranen

Membran [Nr.]	Zusammensetzung [g]	IEC exp.(ber.) [meq/g]	R_{sp}^{H+} [Ω*cm]	SW 25°C(90°C) [%]
504H	4.5 $PEK(SO_3H)_{0.4}$, 1.5 ml $C_3H_7NH_2$ 0.3 A095*, 0.3 PBI	1.12(1.11)	23.7	28.8(73.6)
504Li	4.5 $PEK(SO_3Li)_{0.4}$ 0.3 A095, 0.3 PBI	1.34(1.11)	23.9	35.7(133.7)
504Si	4.5 $PEK(SO_3H)_{0.4}$, 3 ml $C_3H_7NH_2$ 0.3 A095, 0.3 PBI 0.3 SiO_2 Aerosil A380	1.16(1.06)	18.9	35.4(79.9)
565H	12 $PEK(SO_3H)_{0.4}$, 2 ml $C_3H_7NH_2$ 0.6 A095, 0.6 PBI	1.2(1.32)	35	22.2(90)

© Jochen Kerres 2002

Membranmorphologie

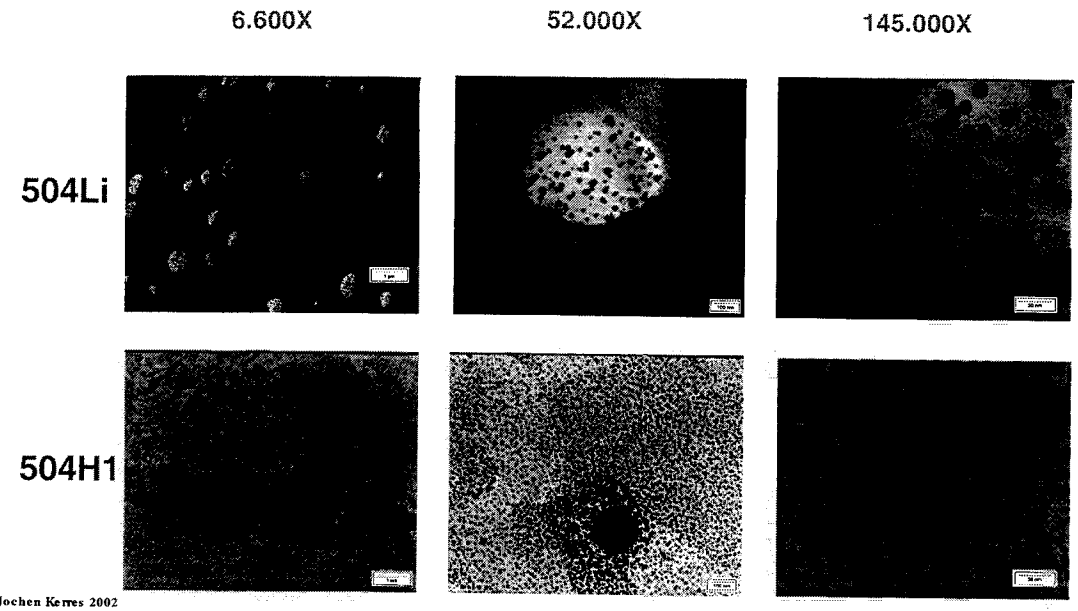

© Jochen Kerres 2002

Membranzusammensetzung und –eigenschaften

Kovalent vernetzte Ionomermembranen

Membran [Nr.]	Zusammensetzung [g]	IEC exp.(ber.) [meq/g]	R_{sp}^{H+} [Ω*cm]	SW 25°C(90°C) [%]
1049	3.1 PEK$(SO_2Cl)_{0.4}$ 1.33 RadelR-SO_2Li, 0.19 ml CL*	1.18(1.23)	9.8	42(72)
1055	2.1 PEEK$(SO_2Cl)_1$ 2.29 RadelR-SO_2Li, 0.32 ml CL*	1.12(1.23)	10.13	37.5(59.4)
1105K	2.11 PEKEKK$(SO_2Cl)_{2.9}$ 2.61 PSU-SO_2Li, 0.34 ml CL	1.2(1.23)	14.04	25.3(42.2)
1228	1.5 PEK $(SO_2Cl)_{1.3}$ 2.49 RadelR-SO_2Li, 0.35 ml CL	1.24(1.23)	9.5	31.7(42.3)

© Jochen Kerres 2002

*CL: Vernetzer 1,4-Diiodbutan

Membraneigenschaften: Ionisch vernetzte Membranen

Thermische Stabilität von 504-Typ Membranen via TGA

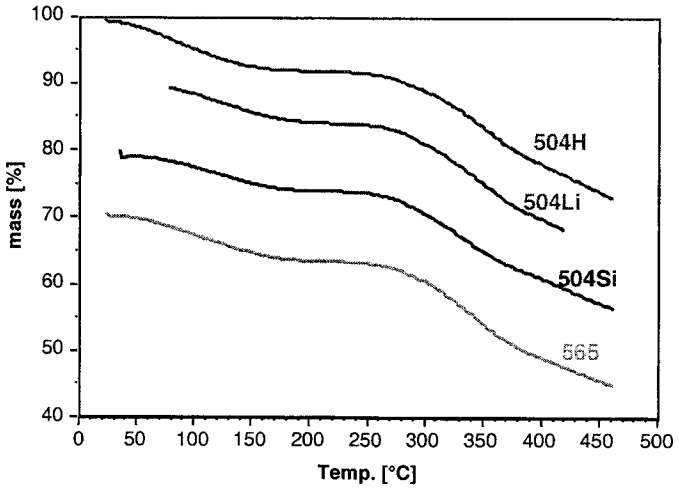

© Jochen Kerres 2002

Membraneigenschaften: Kovalent vernetzte Membranen

Thermische Stabilität von Sulfinat-vernetzten Membranen via TGA

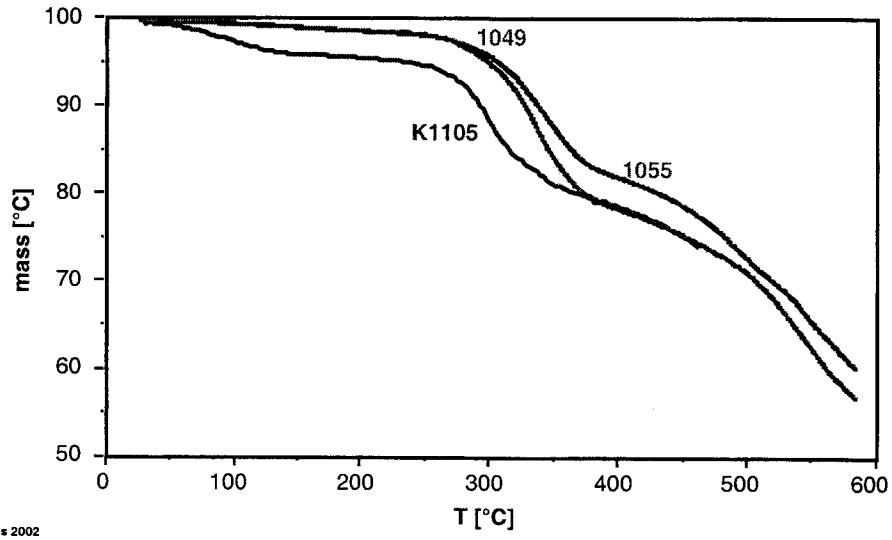

© Jochen Kerres 2002

DMFC-Anwendung von 504-Typ Membranen

I/U Polarisationskurven und MeOH-Permeabilität von 504-Membranen

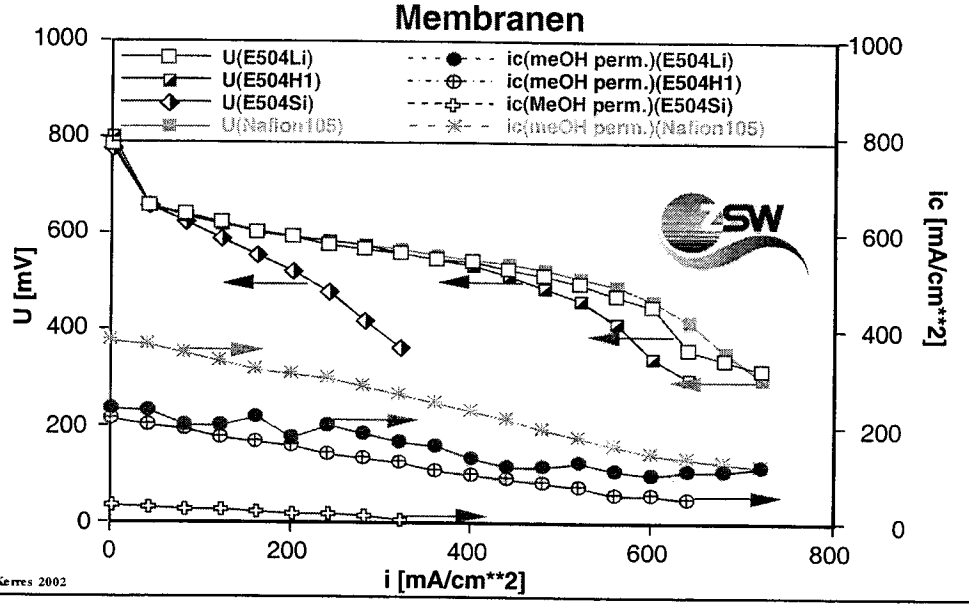

© Jochen Kerres 2002

DMFC-Anwendung unterschiedlich vernetzter Membranen

I/U Polarisationskurven

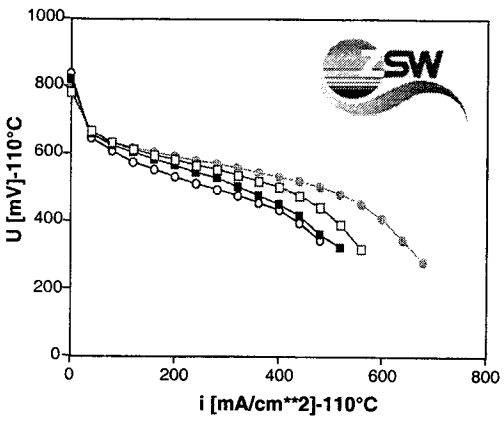

MeOH-Permeabilität

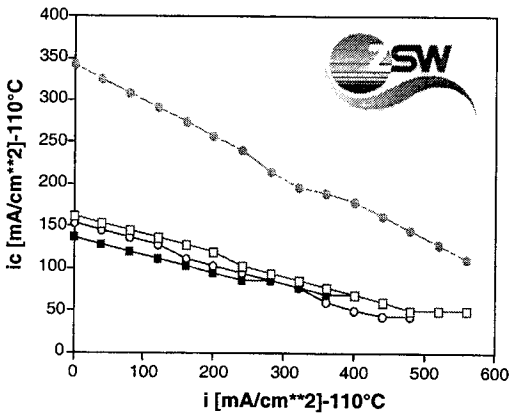

1029 (ionisch vernetzt) - 110°C
1028 (ionisch-kovalent vernetzt) - 110°C
1025 (kovalent vernetzt) - 110°C
Nafion - 110°C

DMFC-Bedingungen:

T_{Zelle}:	110°C	F_a:	1.5 l/min
c_{MeOH}:	0.8 mol/l	F_m:	4 l/min
dbp_a:	3 bar	Anode:	5.4 mg/cm² JM PtRu
dbp_m:	1.5 bar	Kathode:	6.4 mg/cm² JM Pt-black

DMFC: Verringerung Katalysatormenge

DMFC von 565 MEAs, T_{Zelle}=110/130°C

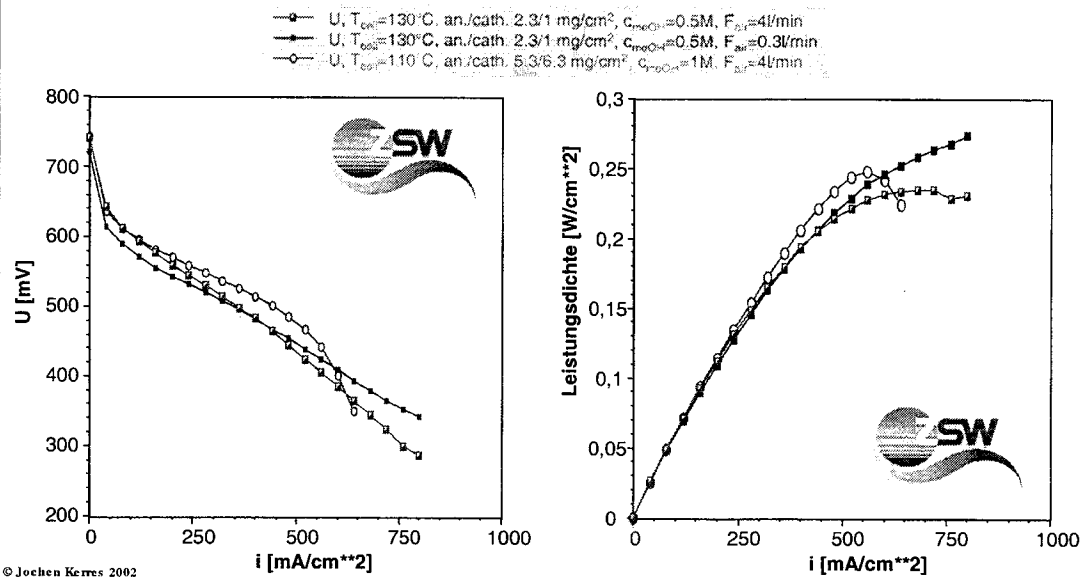

Zusammenfassung

- **Erfolgreiche Entwicklung stabiler Ionomerblendmembranen**
- **Membran-H^+-Leitfähigkeiten vergleichbar mit Nafion**
- **Membranmorphologie kann wunschgemäß eingestellt werden (homogen oder phasenseparіert)**
- **Die Membranen zeigen eine mit Nafion vergleichbare DMFC-Performance**
- **SiO_2-Zugabe vermindert die MeOH-Permeabilität stark, aber (bislang) auch die DMFC-Performance**

© Jochen Kerres 2002

Ausblick

- **Kovalent vernetzte Membranen:**
  - Entwicklung stabilerer Vernetzungsbrücken
- **ionisch vernetzte Membranen:**
  - Entwicklung polymerer Basen mit erhöhter Stabilität und Basizität
- **Komposit-Membranen:**
  - Einführung der anorganischen Partikel auch in kovalent vernetzte Membranen
  - Untersuchung verschiedener Typen von nanoseparierten Partikeln
  - Generierung der Nanopartikel in der Membran mittels bekannter Prozeduren

© Jochen Kerres 2002

Vielen Dank...

...an Dr. Jörissen und Dr. Gogel (ZSW Ulm), für die Herstellung der MEAs und für die Durchführung der DMFC-Tests

...und an meine Arbeitsgruppe!!

© Jochen Kerres 2002

Journal of New Materials for Electrochemical Systems 5, 97-107 (2002)
© J. New. Mat. Electrochem. Systems

Application of Different Types of Polyaryl-Blend-Membranes in DMFC

J. Kerres[a*], W. Zhang[a], L. Jörissen[b], V. Gogel[b]

[a] *Institut für Chemische Verfahrenstechnik (ICVT), Universität Stuttgart, Stuttgart, Germany*
[b] *Center for Solar Energy and Hydrogen Research (ZSW-BW), Ulm, Germany*

(Received June 6, 2001 ; received in revised form November 30, 2001)

Abstract: *In this comparative study, the preparation and characterization as well as the direct methanol fuel cell (DMFC) application of ionically, covalently, and covalent-ionically cross-linked polyaryl-blend membranes is described.*

The proton-conductive component of the blend membranes consists of sulfonated poly(etherketones) sPEK. Ionic cross-linked membranes were formed by mixing sPEK and two different basic PSU polymers, and covalently cross-linked membranes were prepared by mixing of sPEK with sulfinated PSU, where the covalent cross-links were formed by sulfinate-alkylation with α, ω-diiodobutane. Covalently and ionically cross-linked blend membranes were formed by mixing sPEK with sulfinated PSU and a basic PSU polymer, where the cross-linking took place by tertiary basic N and sulfinate alkylation with α, ω-diiodobutane.

The polyaryl-blend membranes showed thermal stabilities between 250 and 270°C. The covalently and the ionically cross-linked membranes show a homogeneous blend morphology, while the covalent-ionivally cross-linked membrane was microphase-separated. The differently cross-linked membranes showed similar proton-conductivity and ion-exchange capacity but different swelling behavior at T = 90°C: the swelling degree (SW) of the covalently cross-linked membrane was only 50% of the SW of the two other membranes. The DMFC performance of the differently cross-linked membranes was similar and comparable with that of Nafion 105, although the meOH permeability of the polyaryl-blend membranes was a factor 2 to 2.4 lower than that of Nafion 105. A better performance of the polyaryl-blend membranes was most probably prevented by a bad connection between recast Nafion-containing electrodes and the membranes.

Key words : polyaryl blend membrane, covalent and ionic cross-linking, swelling, FTIR, TEM, morphology, DMFC, meOH permeation

1. INTRODUCTION

The direct methanol fuel cell (DMFC) is a fuel cell type who is especially interesting for the application in automobile (cars, trucks, buses) or portable (cellphones, laptops) applications because of the simple fuel cell setup (easy storage of methanol, no reformer required). So far only a few membrane types have been used as the proton conductor in DMFC. Among them are the perfluorinated ionomer Nafion [1], polybenzimidazole / phosphoric acid blend membranes [2], Nafion membranes filled with inorganic particles like silicalite [3] or zirconium phosphate [4], and acid-base blend membranes developed in our lab [5]. The main disadvantages of the Nafion membrane types are their high price, and the disadvantage of unfilled Nafion is its high methanol permeability, leading to marked cathode potential reduction. It could be shown that acid-base blend membranes show a reduced methanol permeability, compared to Nafion [6], which makes them interesting candidates for DMFC [7]. The main disadvantage of acid-base blend membranes is their strong swelling at T > 70-90°C, depending on the base strength (the higher the basicity of the basic polymer, the higher the temperature at which extreme swelling starts). To avoid strong swelling at higher temperatures it is required to cross-link the ionomer membranes covalently. In our lab, two different types of covalently cross-linked ionomer membranes have been developed,

*To whom correspondence should be addressed: Fax: +497116412241; email : kerres@icvf.uni-stuttgart.de

at which the covalent cross-linking is accomplished by alkylation of pendent sulfinate groups by α, ω-dihalogenoalkanes, the first type being covalent cross-linked membranes prepared by crosslinking of the sulfinate groups of a polysulfone-(PSU)-sulfonate-sulfinate [8], the second being cross-linked blend membranes from mixtures of PSU-sulfinate and PSU-sulfonate, where only the sulfinate component of the blend membrane formed the covalent network, and the PSU-sulfonate component being entangled in this network [9]. The disadvantage of these membranes was their strong brittleness in dried state. To find out whether the strong brittleness of the aforementioned membrane types is caused by the backbone polymer(s) or by the cross-linking type, other combinations of sulfonated polymer and sulfinated PSU were prepared. Interestingly, it was found that covalently cross-linked blend membranes from sulfinated PSU with sulfonated poly(etheretherketone) (sPEEK) or sulfonated poly(etherketone) (sPEK) showed a markedly reduced dry-brittleness, compared to covalently cross-linked blend membranes from sulfinated PSU and sulfonated PSU. Therefore, we decided to prepare and characterize different series of sPEK/PSU-sulfinate and sPEEK/PSU-sulfinate blend membranes and to apply them to DMFC in order to find out whether these covalently cross-linked membranes show improved DMFC performance, due to their reduced swelling at higher temperatures, compared to ionically cross-linked acid-base blend membranes. Moreover, we prepared ternary ionomer blend membranes from sPEK, PSU-sulfinate, and different basic PSU polymers, containing both ionical and covalent cross-links, in order to compare the properties, especially the DMFC performance, of these membrane type with membranes only containing ionical or covalent cross-links. The basic PSU polymers were prepared by reaction of lithiated PSU with basic aromatic ketones, aldehydes, and carboxylic acid esters, as already described in a previous paper [10]. For this reaction type, as the basic group only tertiary basic N can be used, as for example a tertiary amino group NR_3 or a pyridyl group, because primary or secondary amino groups would react with the lithiated PSU under deprotonation so that no covalent bond could be formed between the organic base and the PSU. The cross-linking procedure leading to covalent and ionically cross-linked blend membranes is shown in the scheme Fig. 1. The cross-linking is accomplished by alkylation of both sulfinate and tertiary amino groups with α, ω-dihalogenoalkanes Hal-$(CH_2)_x$-Hal, so that three types of cross-linking bridges could be formed in the abovementioned ternary blend membranes:

$$PSU - N^+R_2 - (CH_2)_x - N^+R_2 - PSU$$
$$PSU - SO_2 - (CH_2)_x - SO_2 - PSU$$
$$PSU - SO_2 - (CH_2)_x - N^+R_2 - PSU$$

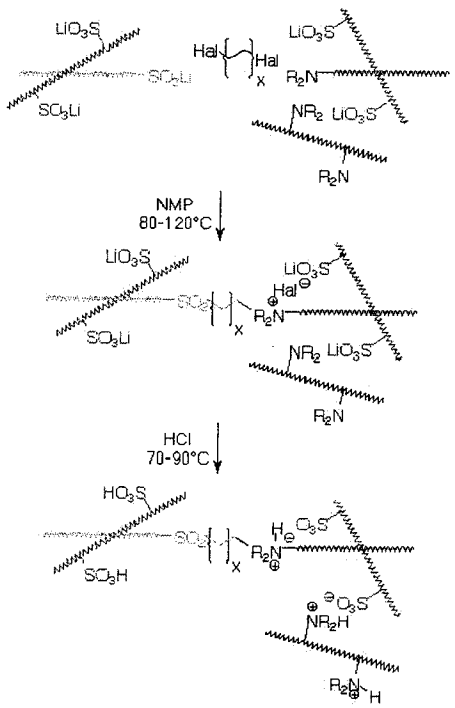

Figure 1: Schematical representation of a covalent-ionical cross-linking procedure by alkylation of sulfinate groups and tertiary amino groups via α, ω-dihalogenoalkanes

For the comparative study presented here the following polymers have been selected for membrane preparation:

i) as the acidic polymers, a water-soluble sulfonated PEEK (IEC=2,7 meq/g polymer, 1 SO_3H group per repeating unit, polymer 1 (Fig. 2)), and a water-insoluble sulfonated PEK (IEC=1.8 meq SO_3H/g Polymer, 0.4 SO_3H groups per repeating unit, polymer 2 (Fig. 2));

ii) as the sulfinated polymer, sulfinated PSU with 1 SO_2Li group per repeating unit,polymer 3 (Fig. 2);

iii) as the basic polymers, lithiated PSU being reacted with 4-Acetylpyridine (1.5 groups per repeating unit, polymer 4 (Fig. 2)), and lithiated PSU being reacted with 4,4'-Bis(diethylamino)benzophenone, 1 group per repeating unit, polymer 5 (Fig. 2).

The differently cross-linked ionomer blend membranes which were prepared from these polymers showed comparable ion-exchange capacities (IEC) in order to ensure comparability between them, especially in the DMFC application.

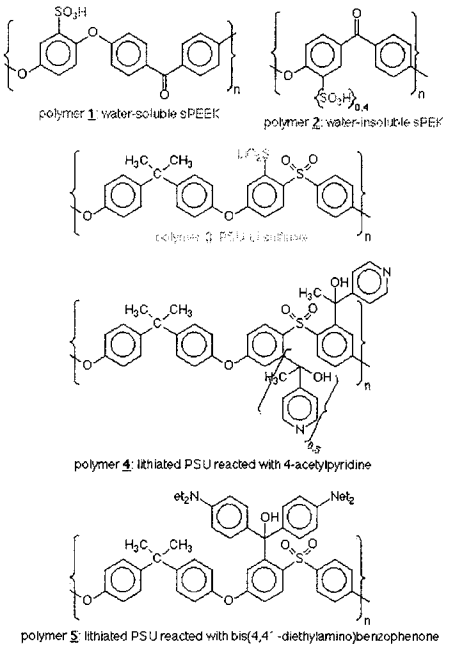

Figure 2: Polymers used for preparation of the blend membranes

2. EXPERIMENTAL

2.1 Preparation of Sulfonated PEEK 1

The sulfonated PEEK polymer was sulfonated by stirring for 4h in 96 wt% sulfuric acid at a temperature of 80°C like described in the literature [11]. After preparation, the polymer was precipitated in ice and filtered. Subsequently, the filter residue was filled into dialysis tubes and dialyzed till all excess sulfuric acid was removed. During the dialysis the polymer dissolved in the dialysis tube. After dialysis, the polymer solution was transferred to a ceramic bowl, and the water was removed at T=90°C. After drying, the polymer was fine-milled and dried to constant weight. The sulfonated PEEK had an ion-exchange capacity of 2.7 meq SO_3H/g polymer.

The sulfonated PEK (sPEK) having an ion-exchange capacity of 1.8 meq/g was kindly donated by Celanese Ventures GmbH.

2.2 Preparation of Sulfinated PSU 2

Sulfinated PSU was prepared as described in [12]. 44.2 g PSU P 1800 (0.1 mole, BP Amoco) were dissolved in 1400 mL anhydrous THF (Aldrich). The solution was cooled down under Argon to –65°C. Then the solution was titrated by dropwise addition of 2.5M n-buLi (Aldrich) to the solution with syringe via septum inlet. After the solution became slightly red, indicating beginning PSU deprotonation in position ortho to the sulfone bridge of the PSU repeating unit, 10 mL 10M n-buLi (0.1 mole, Aldrich) were added to the solution with syringe via septum inlet within 10 min. The solution became deep-red and viscous and was stirred for 30 min to complete ortho sulfone deprotonation. Subsequently, SO_2 was gassed into the solution via gas inlet. During 5 min, a white, thick PSU sulfinate precipitate was formed. The precipitate was filtered and carefully rinsed with methanol. Then the precipitate was dried at 50°C in a vacuum oven. The sulfinated PSU had a degree of substitution (DS) of 1 per repeating unit, as determined via ^{1}H-NMR.

2.3 Preparation of the Basic PSU Polymers 4 and 5

The common procedure for reaction of lithiated PSU with aromatic ketone bases is described in [13]. The preparation of the basic PSU polymer 5 is described in [13], and the preparation of the basic polymer 4 is described in the following:

Material:
22,1 g PSU Udel (0.05 mole)
1000 ml THF
10 ml 10 M n-BuLi (0.1 mole)
10 g 4-Acetylpyridine (0,166 mole)

Procedure:
PSU is dissolved in dry THF under Argon. The solution is cooled down to –60°C. Residual H_2O etc is titrated with 2.5 M n-BuLi till a red colour appears. Then the 10 M n-BuLi is dropped into the solution via syringe through a septum inlet. The BuLi is reacted for 1 h. Then the 4-acetylpyridine is slowly introduced into the reaction flask via syringe. Some yellow-colored precipitate is formed.The suspension is stirred for 4 h, while the reaction mixture is allowed to warming up to –20°C. Then the reaction is stopped by addition of a water/i-prOH mixture (2ml water/10 ml i-prOH). The mixture is allowed to warm to room temperature. The reaction mixture is then precipitated in 3 L isopropanol. The polymer is filtered. Subsequently, the polymer is again suspended and stirred in 1 L isopropanol. After 1 day of stirring, it is again filtered off and carefully washed with isopropanol until all residual 4-acetylpyridine monomer is removed. Then the polymer is filtered off. The polymer is dried in vacuum oven at 50°C under vacuum till weight constancy is reached. Then the yellow polymer is characterized: elemental analysis (N; C; H; S), and ^{1}H/^{13}C-NMR.

Characterization Results:
Yield: 27g (quantitative)
DS from ^{1}H-NMR: 1.5
Elemental analysis results (calculated for 1.5 4-acetylpyridine groups per PSU repeating unit):
C 68.7% (theo. 72.14%); H 5.16% (theo. 5.25%); N 3.2% (theo. 3.37%); S 6.14% (theo. 5.13%)

Table 1: Composition and characterization data of all membranes mentioned in the paper

membrane [No.]	type cross-linking	composition [g]	thickness [μm]	IEC_{calc} [meq SO_3H/g]	IEC_{found} [meq SO_3H/g]	swelling 25°C [%]	$R_{\alpha}^{H^+}$ 1a) Ω*cm^2]	$R_{sp}^{H^+}$ 1b) Ω*cm]
1025	covalently	4 PEK$(SO_3H)_{0.4}$ (67.3 wt%*) 1.8 PSU$(SO_2Li)_1$ (32.7 wt%*) cross-linker: 0.23 ml 1,4-diiodobutane	81	1.23	1.07	29.6	0.079	9.8
1030	covalently	2 PEEK$(SO_3H)_1$ (45.5 wt%*) 2.3 PSU$(SO_2Li)_1$ (54.5 wt%*) cross-linker: 0.3 ml 1,4-diiodobutane	89	1.23	1.14	28.1	0.084	9.4
550	covalently	2.86 PEEK$(SO_3H)_1$ (54.7 wt%*) 2.275 PSU$(SO_2Li)_1$ (45.3 wt%*) cross-linker: 0.2 ml 1,4-diiodobutane	61	1.5	1.1	49.6	0.141[2)]	23.12[2)]
504H	ionically	10 PEK$(SO_3H)_{0.4}$ (91.8 wt%*) 0.445 PBI[3)] (4.1 wt%*) 0.445 PSU-C(OH)(4-Diethylaminophenyl)$_2$ (4.1 wt%*)	71	1.11	1.12	28.3	0.168	23.7
1022	ionically	3 PEEK$(SO_3H)_{0.96}$ (77.1 wt%*) 0.445 PBI (11.4 wt%*) 0.445 PSU-C(OH)(4-Diethylaminophenyl)$_2$ (11.4 wt%*)	43	1.11	0.9	36.02	0.115	26.8
1029	ionically	7 PEK(SO3H)0.4 (86.8 wt%*) 1.06 PSU-[C(OH)-CH_3(4-Pyridyl)]$_{1.5}$ (13.2 wt%*)	86	1.23	1.35	43.6	0.084	9.74
1028	covalent-ionically	4 PEK$(SO_3H)_{0.4}$ (76 wt%*) 0.9 PSU$(SO_2Li)_1$ (11.4 wt%*) 0.363 PSU-[C(OH)-CH_3(4-Pyridyl)]$_{1.5}$ (12.6 wt%*) cross-linker: 0.17 ml 1,4-diiodobutane	114	1.17	1.24	38.5	0.115	10.07

1a) area H^+ resistance, measurement in 0.5N HCl
1b) specific H^+ resistance, measurement in 0.5N HCl
2) measurement in 0.5N H_2SO_4
3) polybenzimidazole, product of Celanese (Celazole)
* wt% of component in membrane

2.4 Membrane Preparation

At first from all polymers 15 wt% solutions in N-methylpyrrolidinone (NMP) were prepared (instead of polybenzimidazole PBI, from which a 8.9 wt% DMAc solution was prepared). Then the solutions were mixed in the referring mass relation (composition of the membranes see Table I). At the polymer solutions from which covalently cross-linked membranes were prepared, cross-linker 1,4-diiodobutane was added to the solution (amount of cross-linker see Table I). Then the solution was stirred for 10-20 min until it became homogeneous. Subsequently, the polymer solutions were degassed and filtered. Then they were spread onto a glassplate to a film of constant thickness, and the glassplate was transferred into a drying oven. The solvent was then evaporated at T=130°C and at reduced pressure (from 800 mbar in the beginning to 50 mbar after 2h). The membranes were dried a further hour under 50 mbar and 130°C, and then removed from the oven. After cooling down, they were transferred to a water bath to remove the membrane from the glassplate. Then the membranes were posttreated in the following manner: at first 48 h at 90°C in 7% HCl, and then 48h at 60°C in deionized water. Then the membranes were rinsed with deionized water till all excess acid was removed. The membranes were stored in closed plastic bags.

2.5 Membrane Characterization

2.5.1 FTIR Spectra

For recording of the FTIR spectra of the acidic and basic polymers, and of the acid-base blend membranes, a Biorad FTS 155 FTIR spectrometer was used. The FTIR spectra of the polymers (as KBr pills) were recorded in transmission mode. The FTIR spectra of the membranes were recorded in ATR (attuenated total reflection) mode. Resolution was 4 cm^{-1}.

2.5.2 Swelling Degree

For determination of the swelling degree (abreviation SW), the samples were equilibrated in water of the desired temperature (25-40-60-90°C) for 48 h. Then they were removed from the water container, quickly dry-wiped and immediately weighed. Subsequently, they were dried to weight constancy at 90°C and again weighed. Then the swelling degree was calculated as follows:

$$SW = \frac{m_{wet} - m_{dry}}{m_{dry}} \quad (1)$$

2.5.3 Ion-Exchange Capacity (IEC)

The IEC was determined via titration. The membranes in the H^+ form were immersed in conc. NaCl solution for 24h to liberate the H^+ ions. The H^+ ions were then titrated with 0.1N NaOH.

2.5.4 Specific Resistance

The specific resistance of the membranes was determined via impedance spectroscopy (EIS) using a method described in [7]. The samples were measured in the electrolyte 0.5N HCl at a temperature of 25°C with the IM6 model of Zahner elektrik.

2.5.5 Thermal Stability

The thermal stability of the membranes was determined via thermogravimetry in a Netzsch STA 449C Simultaneous Thermal Analyzer (STA). The heating rate was 20°C/min, and the measurement was performed in air atmosphere.

2.5.6 Electron-Microscopical Characterization

For a better contrast in electron microscopy, the SO_3H groups in the ionomer membranes have been exchanged with Pb^{2+} or Ag^+ ions by immersion in 1M $Pb(NO_3)_2$ solution or in 1M $AgNO_3$ solution, respectively. The samples for electron microscopy were prepared as described in [7].

2.6 Preparation of the Catalyst Ink [14]

Catalyst powder (1g) was dispersed in 10 ml demineralized water. Johnson Matthey Platinum black (fuel cell grade) was used for the cathode. The anode ink was made from unsupported Pt/Ru (50:50 at.%) from Johnson Matthey. Alcoholic Nafion solution (Ion Power) was added to a content of 15% in the dry mixture for the anode and to a content of 10% for the cathode. This mixture was stirred magnetically for at least 3 days at room temperature. The catalyst ink was kept under constant stirring. However, it should be used within 10-15 days in order to minimize morphology changes due to stirring.

2.7 MEA Preparation [14]

Wet membranes were fixed in an aluminum frame, allowed to dry and covered by a mask (5cm x 5cm). The catalyst ink was dispersed on the membranes by an air brush in multiple layers. In each layer approximately 1 mg/cm^2 of catalyst was deposited. The loading was determined by weighing the dried MEA. Membrane coating was carried out at a temperature of 120–130 °C . Nafion based MEAs were hot pressed at 130 °C at 100 bar for 2 minutes. The anode loading typically was 5 mg/cm^2 Pt/Ru, the cathode loading was approximately 6 mg/cm^2 Pt. Toray graphite paper (TGP 60) was used as a media diffusion layer. At the cathode side teflonized (25 wt% PTFE) TGP 60 was used.

2.8 Determination of Current Voltage Curves [14]

All measurements were carried out in a graphite cell housing using serpentine type flow fields of 1 mm depth and width. The distance between channels was 1 mm. Current-voltage curves were determined galvanostatically. Aqueous methanol solution (1 or 0.8 mole/l) was fed by mass flow controllers at a flow rate of 4 ml/min. The back anode pressure was 2,5 bar. Air was fed at a flow rate of 4 l/min at a back pressure of 4 bar. CO_2 evolution at the cathode was measured by a Fisher-Rosemound infrared analyzer as a measure for methanol crossover. No correction has been applied for CO_2 diffusion through the electrolyte membrane.

3. RESULTS AND DISCUSSION

3.1 Membrane Characterization Results

All membrane composition data and characterization results are summarized in Table I. Special attention in the following discussion will be put on the membranes 1025, 1029 and 1028 for whose the expected IEC (which can be calculated from the blend membrane composition) lies at 1.2 meq SO_3H/g membrane. 1025 is a covalently cross-linked membrane prepared from sPEK and PSU-sulfinate, 1029 is a ionically cross-linked membrane prepared from sPEK and the condensation product of lithiated PSU with 4-acetylpyridine, and 1028 a covalent-ionically cross-linked membrane prepared from sPEK and from a 1/1 equimolar mixture of sulfinated PSU and PSU modified with 4-acetylpyridine. From Table I results that these membranes have an IEC of around 1.1 to 1.35 meq/g, which is very close to the expected IEC values. Therefore these membranes can be regarded comparable to each other, which is further supported by the fact that their specific proton resistance values are lying very close together (Table I).

3.1.1 FTIR Spectra and Extraction Residuals of the Differently Cross-Linked Membranes

FTIR was used to check whether the sulfinate alkylation cross-linking procedure was complete. The sulfinate group shows a specific band in the region between 960 and 980 cm^{-1} [16]. From Fig. 3 no residual sulfinate vibration can be observed in the membranes containing sulfinate cross-links (1025, 1030, 1028). Therefore the cross-linking can be regarded complete. This conclusion is supported by the fact that after the extraction of those membranes containing covalent cross-links with 90°C hot dimethylacetamide (DMAc) residuals remained, corresponding to the covalently cross-linked weight portion of the

membranes. As an example, after extraction of the membrane 1028, an undissolved residue of 28.2% remained. From the 1028 membrane composition, a residue of 25.2% is calculated, if both the sulfinate and PSU-acetylpyridine blend component would form the covalent network. In Fig. 4, found and theoretically expected extraction residuals of a series of covalently cross-linked sPEK/PSU-SO_2Li blend membranes, including the 1025 type membrane, in dependence of the sPEK content of the blend membrane, are shown. It can be seen from Fig. 4 that there is a good fit between expected and found residuals, from which can be concluded that the covalent network has formed completely. As expected, no undissolved residuals remain when the ionically cross-linked membrane 1029 is treated with 90°C hot DMAc.

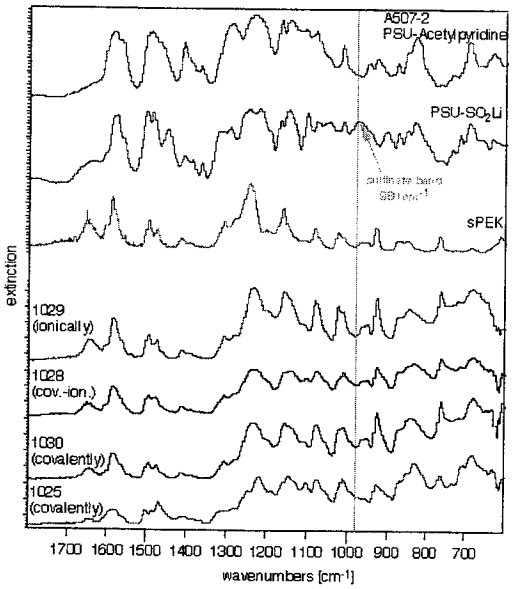

Figure 3: FTIR spectra of the polymers sPEK, PSU-SO_2Li, PSU-Acetylpyridine and of the membranes 1029, 1028, 1025, and 1030; recording mode: polymers KBr pill, membranes ATR (attuenated total reflection)

3.1.2 *TEM Micrographs of Differently Cross-linked Membranes*

Some of the ionomer membranes (1025, 1028, 1029, 504, 550) have been investigated by transmission electron microscopy in order to ascertain their microphase structure. In Fig. 5, the TEM micrograph of the ionically cross-linked acid-base blend membrane 1029 is shown in 6.600X-magnification (Fig. 5a) and in 52.000X-magnification (Fig. 5b). It can be seen that these membrane shows no microphase-separation, due to the acid-base interactions like hydrogen bridges and electrostatic forces. The tiny black dots in Fig. 5 are due to associates of silver-exchanged sulfonate groups of the acidic polymer.

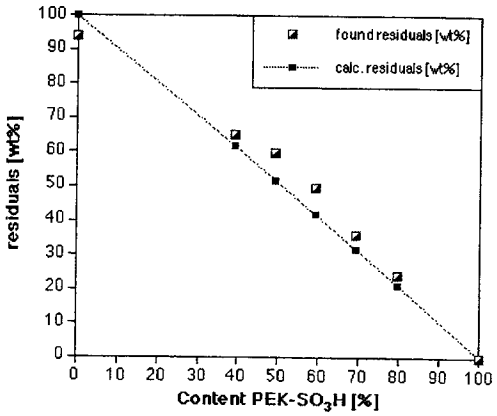

Figure 4: Residuals at a series of sPEK/PSU-SO_2Li covalently cross-linked blend membranes after extraction with 90°C hot DMAc

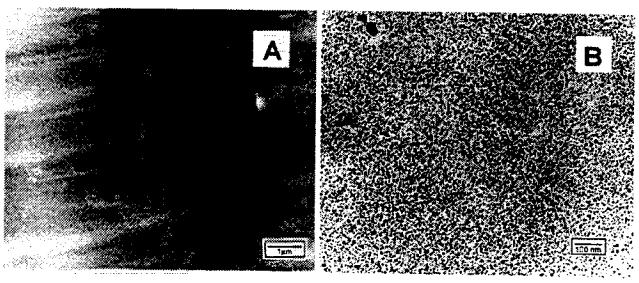

Figure 5: TEM micrographs of the Ag^+-exchanged ionically cross-linked acid-base blend membrane 1029 in 6.600X-magnification (a) and 52.000X magnification (b)

In Fig. 6, the TEM micrograph of the covalently cross-linked blend membrane 1025 is shown in 6.600X-magnification (Fig. 6a) and in 52.000X-magnification (Fig. 6b). It can be seen that these membrane also shows no microphase-separated morphology, which is due to the good miscibility between the sulfinated PSU and the PEK sulfopolymer. The black particles in the micrograph are highly probable due to gel and/or dust particles - the membranes were not prepared in dust-free environment. A very weak fine structure in nanometer size range is visible which can be regarded as aggregates of Pb^{2+}-exchanged sulfonate groups. The contrast of Pb^{2+} is however worse than that of Ag^+.

In Fig. 7, the TEM micrograph of the covalently and ionically cross-linked ternary blend membrane 1028 is shown in 6.600X-magnification (Fig. 7a), and in 52.000X-magnification (Fig. 7b). It can be clearly seen in Fig. 7a that these membrane shows a microphase-separated morphology with ovale-

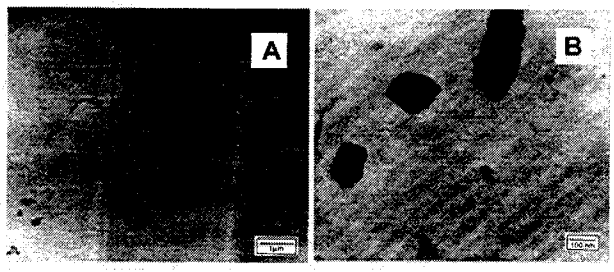

Figure 6: TEM micrographs of the Pb^{2+}-exchanged covalently cross-linked blend membrane 1025 in 6.600X-magnification (a) and 52.000X-magnification (b)

formed microphase particles in μm-size range, which is due to bad compatibility between sulfinated PSU and the PEK sulfopolymer/ PSU-acetylpyridine blend - when during preparation of the blend polymer solutions the solution of PSU-sulfinate is added to the -clear- mixture of PEK sulfopolymer and PSU-acetylpyridine, the solution immediately becomes cloudy. The reason for this imcompatibility between PSU-sulfinate one the one side and the blend of PEK sulfopolymer and PSU-acetylpyridine on the other side is not yet known. The fact that the dispersely distributed particles observable in Fig. 7a are brighter than the dark continuous microphase allows the conclusion that these particles contain cross-linked PSU-sulfinate, while the darker continuous microphase contains the Pb^{2+}-exchanged sPEK/PSU-acetylpyridine blend.

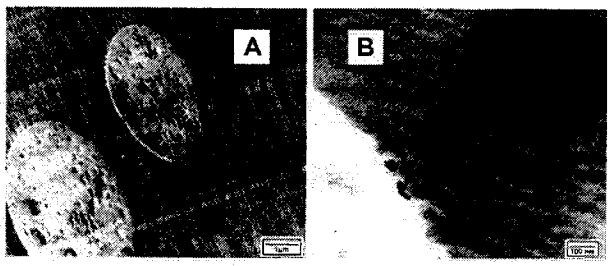

Figure 7: TEM micrographs of the Pb^{2+}-exchanged covalently and ionically cross-linked blend membrane 1028 in 6.600X-magnification (a),and 52.000X-magnification (b)

3.1.3 Swelling Degree in Dependence of Temperature (Comparison of Covalently, Ionically and Covalent-Ionically Cross-Linked Membranes Having Comparable IEC))

In Fig. 8, the swelling data of the membranes 1025 (covalently cross-linked), 1029 (ionically cross-linked) and 1028 (covalent-ionically cross-linked) are shown. It can be seen that the swelling degree (abbreviation SW) of the 1025 membrane is markedly lower at T=90°C than those of the other two membranes. The higher SW of the ionically cross-linked 1029, compared to the covalently cross-linked 1025, can be explained with the breakage of ionic cross-links in the T range from 70 to 90°C. The finding that the covalent-ionically cross-linked 1028 shows a markedly higher SW than 1025 at T=90°C is most probably due to the fact that this membrane shows, in contrast to the 1025, a microphase-separated morphology which can be read from the not complete transparency of this blend membrane type (1025 is completely transparent): the content of this blend membrane in covalently cross-linked PSU-sulfinate phase is 17.1 wt% from which can be concluded that this blend phase is most probably the disperse polymer blend phase: a covalently cross-linked polymer blend phase which is dispersely distributed within the polymer blend matrix can not effectively suppress swelling of the polymer blend, and this especially because SW is caused by the sPEK polymer blend component which has a share of 76 wt% of the mass of the blend membrane and therefore forms the continuous polymer blend phase.

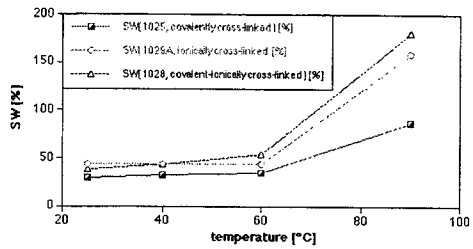

Figure 8: Swelling in dependence of T for the membranes 1025, 1028, 1029

3.1.4 Swelling Degree in Dependence of Temperature (Comparison of Two Covalently Cross-Linked Membranes Having Comparable IEC and Different Cross-Linking Density)

In Fig. 9, the SW of the two covalently cross-linked membranes having similar IEC: 1025 (IEC_{1025}=1.07 meq/g), which is containing water-insoluble sPEK (IEC=1.8 meq/g), and 1030 (IEC_{1030}=1.14 meq/g), which is containing water-soluble sPEEK (IEC=2.7 meq/g), in the dependence of T is shown. As expected, the 1030 membrane shows a markedly lower SW at T=90°C, due to the higher cross-linking density of 1030.

3.1.5 Thermal Stability of the Differently Cross-Linked Membranes

In Fig. 10, the TGA traces of the covalently cross-linked membrane 1025, the ionically cross-linked membrane 1029, and the covalent-ionically cross-linked membrane 1028 are shown. As can be seen, the thermal stability of all three membrane types is very similar, indicating that membrane degradation starts in the T range 250-270°C. The thermal stability of the other membranes presented in this study is similar.

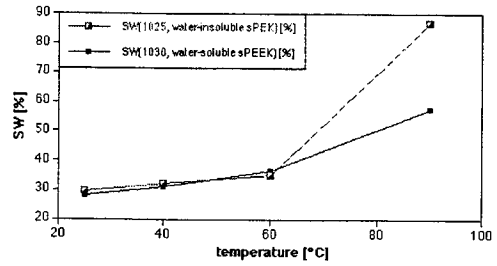

Figure 9: Swelling in dependence of T for the covalently cross-linked membranes 1025 and 1030

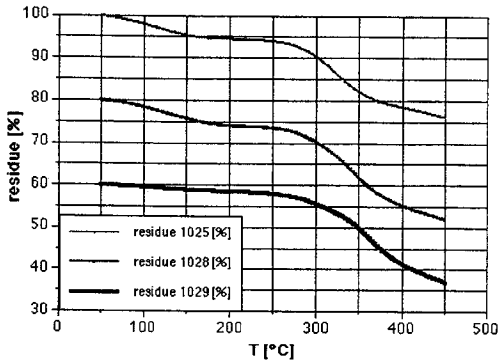

Figure 10: TGA traces of the membranes 1025, 1029, and 1028

3.2 DMFC Application Results

Two groups of membranes which show similar properties in terms of ion-exchange capacity (IEC) and proton conductivity (specific resistance) were tested in DMFC in terms of i/U polarization curves and meOH permeation and were compared with each other and with Nafion 105. The first membrane group was formed by the ternary, ionically cross-linked, blend membrane 504 and the covalently cross-linked blend membrane 550, and the second group of membranes consisted of the binary blend membranes 1029 (ionically cross-linked) and 1025 (covalently cross-linked), and of the ternary blend membrane 1028 (covalent-ionically cross-linked).

3.2.1 DMFC Application of 504 and 550

The i/U polarization curves and ic/i meOH permeation curves of MEAs made from the two membranes 504 and 550 are shown together with the respective curves of a Nafion 105 MEA in Fig. 11. It can be seen that the i/U polarization curves of all three membranes are very similar, proving that these membranes can be applied to DMFC instead of Nafion. The MeOH permeation of the two membranes is lower than the meOH permeation of Nafion 105. The worse DMFC performance of the 550 membrane, compared to the 504 membrane, is probably caused by its higher meOH permeability, because the proton conductivities of both polyaryl blend membranes are quite similar (Table I). In Fig. 12 the power density of the membranes 504, 550 and Nafion in dependence of the current density at a DMFC temperature of 110°C is displayed. It is obvious that the power density/i curves of 504 and Nafion MEAs are nearly congruent, reaching their peak power densities between 500 and 600 mA/cm^2 (550: 0.21 W/cm^2 at 500 mA/cm^2; 504: 0.24 W/cm^2 at 560 mA/cm^2; Nafion 105: 0.25 W/cm^2 at 560 mA/cm^2).

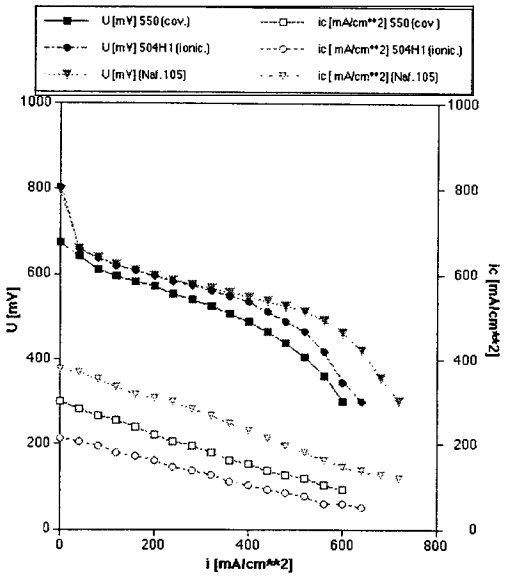

Figure 11: U/i polarization curves and meOH permeation curves (calculated from CO_2 determination at the cathode as ic in mA/cm^2) of MEAs made from the ionically cross-linked membrane 504, the covalently cross-linked membrane 550, and from Nafion 105, for comparison (DMFC conditions: T_{cell} =110°C, c_{meOH} =1 mol/l, dbp_a =3 bar, dp_m =1.5 bar, F_a=1.5 l/min, F_m =4 l/min, anode: 5.4 mg/cm^2 JM PtRu, cathode: 6.4 mg/cm^2 JM Pt-black)

From the fact that the meOH permeability of the 550 and 504 membrane is lower than that of Nafion 105 it is expected that the U/i polarization curves of the 504 and the 550 MEA should be superior to that of Nafion. This is, however, obviously not the case. The interface thin film electrode/polyaryl membrane is not optimal, as the cross-section of a 504 MEA (Fig. 13a) shows: after application in a DMFC, partial delamination of electrode and membrane has taken place, which is most probably caused by the fact that Nafion has been used as the binder in the thin film electrode - Nafion and polyaryl ionomers are not compatible with each other. As a contrast, the cross-section of a Nafion105 MEA (Fig. 13b) does not show any delamina-

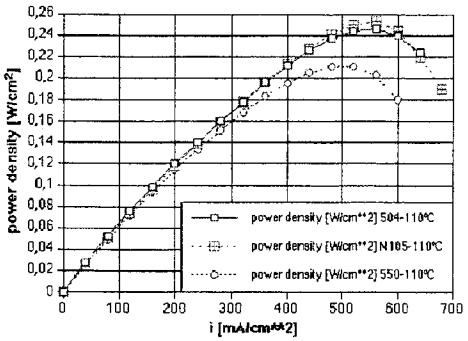

Figure 12: Power density vs current density of the 504, the 550, and the Nafion 105 MEA at DMFC, T=110°C; DMFC conditions see Fig. 11

tion between electrode and membrane after the use in a DMFC. At the preparation of MEAs from nonfluorinated ionomers it is therefore required to substitute the Nafion binder in the electrode ink by a nonfluorinated ionomer binder (for instance by a sulfonated poly(etherketone) or poly(ethersulfone)). The problem with these ionomers is however, that they are not soluble in the common electrode ink solvents like ethanol, glycerin and other alcohols. Therefore, electrode inks have to be developed in which the alcohols are substituted by solvents in which the polyaryl ionomers are soluble.

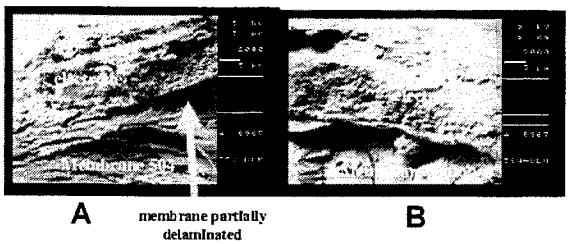

Figure 13: SEM cross-section of a 504 MEA (a) and a Nafion105 MEA (b) after use in a DMFC

3.2.2 DMFC Application of 1025, 1028, 1029

To investigate whether the cross-linking type of the ionomer blend membrane influences the DMFC performance, MEAs made from the three membranes 1029 (ionically cross-linked), 1025 (covalently cross-linked), and 1028 (covalent-ionically cross-linked) which contain the same proton-conductive ionomer sPEK, having comparable IEC, nearly the same proton conductivities and membrane thickness were investigated in DMFC at the same conditions, being compared to a Nafion 105 MEA. In Fig. 14, the U/i polarization curves of the MEAs at T=25°C are shown, in Fig. 15 the U/i polarization curves of the MEAs at T=70°C are displayed, in Fig. 16 the U/i polarization curves at 90°C, and in Fig. 17 the U/i polarization curves at T=110°C. It can be seen from the Figures 14 to 17 that the performance of all three membranes is nearly similar and comparable to that of a Nafion 105 MEA. From Fig. 18 follows that also the meOH permeation of all three polyaryl blend membranes at the respective DMFC temperature is comparable, lying at 110°C a factor of 2 to 2.4 below that of a Nafion 105 MEA. It is most probable that the binding of the thin layer electrode onto the membranes 1029, 1028, and 1025 is not optimal as it was found for the aforementioned 504 membrane. If the binding of the electrode to the membrane would be as good as for Nafion105, one could expect that the U/i polarization curves of the differently cross-linked polyaryl blend membranes should be superior over that of Nafion 105. Referring to the presented DMFC data it does not seem that one of the three membrane types (i. e. one of the cross-linking types) has advantages over the others in the DMFC application. Referring to the swelling data (Fig. 8), we conclude that it would be advantageous to apply the covalently cross-linked blend membrane (1025) to DMFC, due to their better dimensional stability at higher temperatures, compared to the blend membranes 1028 and 1029.

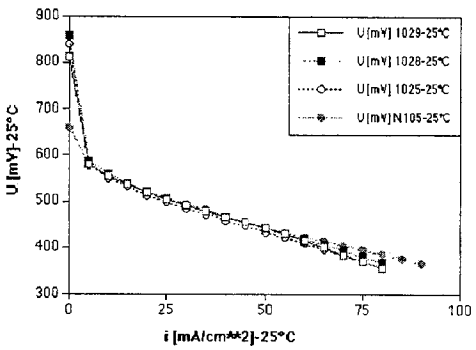

Figure 14: U/i polarization curves of MEAs made using the membranes 1029, 1028, and 1025, and, for comparison, of a Nafion105 MEA at T=25°C (DMFC conditions: cmeOH=0.8 mol/l, dbpa=3 bar, dpm=1.5 bar, Fa=1.5 l/min, Fm=4 l/min; catalyst loadings: 1029: anode A 5.3 mg/cm^2 JM PtRu, cathode C 6.3 mg/cm^2 JM Pt-black; 1028: A 5.4 mg/cm^2 JM PtRu, C 6.4 mg/cm^2 JM Pt-black; 1025: A 5.5 mg/cm^2 JM PtRu, C 6.4 mg/cm^2 JM Pt-black; Nafion 105: A 5.3 mg/cm^2 JM PtRu, C 6.4 mg/cm^2 JM Pt-black)

4. CONCLUSION

In this study, different polyaryl blend membranes having comparable membrane properties and different types of cross-linking, i.e. ionic, ionic-covalent, and covalent cross-linking, have been studied in terms of their behavior in direct methanol fuel cells

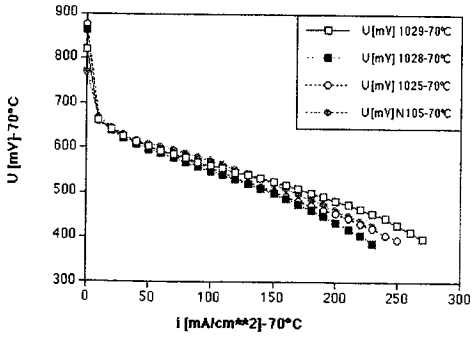

Figure 15: U/i polarization curves of MEAs made using the membranes 1029, 1028, and 1025, and, for comparison, of a Nafion 105 MEA at T=70°C (DMFC conditions see Fig. 14)

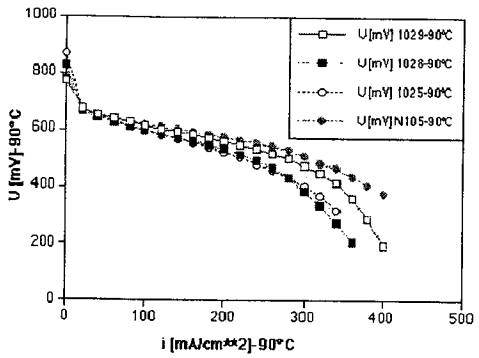

Figure 16: U/i polarization curves of MEAs made using the membranes 1029, 1028, and 1025, and, for comparison, of a Nafion 105 MEA at T=90°C (DMFC conditions see Fig. 14

(DMFC). The DMFC behavior of membrane-electrode assemblies (MEAs) containing these membranes was compared to the DMFC performance of Nafion 105 MEAs. The results showed that the performance of these membranes in DMFC was comparable to that of Nafion 105, even though the polyaryl blend type membranes show a lower meOH permeability than Nafion 105 and should therefore have a better DMFC performance than Nafion 105. It is believed that the main reason for not exhausting the potential of these membranes in the DMFC application is insufficient contact between membrane and thin film electrode in the MEA, as SEM micrographs of the polyaryl membrane MEAs suggest, showing partial delamination of electrodes and membrane.

To improve the DMFC performance of the polyaryl blend type ionomer membranes over that of Nafion membranes it is required to develop electrode inks containing nonfluorinated, preferently polyaryl, ionomers which lead to a better contact between electrodes and membrane. Moreover it is planned to develop organic-inorganic composite membranes based on the covalently and/or ionically cross-linked membrane systems developed in our lab within the last years in order to further improve the meOH retention and the water-holding ability especially at T>100°C.

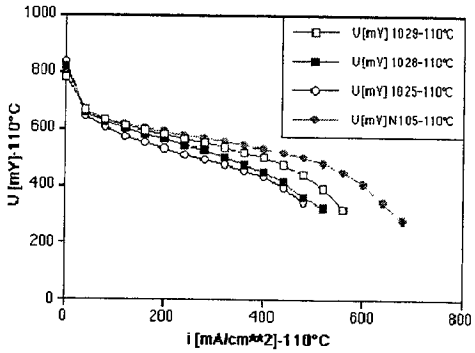

Figure 17: U/i polarization curves of MEAs made using the membranes 1029, 1028, and 1025, and, for comparison, of a Nafion105 MEA at T=110°C (DMFC conditions see Fig. 14)

5. ACKNOWLEDGMENTS

We gratefully acknowledge the financial support for this study given from:

- Deutsche Forschungsgemeinschaft, Schwerpunktprojekt (SPP) 32 1060 "Neue Schichtstrukturen für Brennstoffzellen", Project Ke 673-1/2
- VFI/BMBF/Industrial Consortium, Projekt "DFMC-Brennstoffzelle", FKZ 0326862

We gratefully acknowledge the generous donation of sulfonated Poly(etherketone) by the company "Celanese Ventures".

REFERENCES

[1] W. G. Grot, *Macromolecular Symposia*, 82, 161 (1994)

[2] J. S. Wainright, J.-T. Wang, D. Weng, R. F. Savinell, M. H. Litt, *J. Electrochem.Soc.*, 142, L121 (1995)

[3] A. S. Aricò, P. Creti, P. L. Antonucci, V. Antonucci, *Electrochem. Solid-State Lett.*, 1 (2), 66 (1998)

[4] C. Yang, S. Srinivasan, A. S. Aricò, P. Creti, V. Baglio, V. Antonucci, *Electrochem.Solid-State Lett.*, 4 (4), A31 (2001)

[5] J. Kerres, A. Ullrich, F. Meier, Th. Häring, *Solid State Ionics*, 125, 243 (1999)

[6] M. Walker, K.-M. Baumgärtner, M. Kaiser, J. Kerres, A. Ullrich, E. Räuchle, *J. Appl. Polym. Sci.*, 74, 67 (1999)

[7] J. Kerres, A. Ullrich, Th. Häring, W. Preidel, M. Baldauf, U. Gebhardt, *J. New Mat. Electrochem. Systems*, 3, 229 (2000)

[8] J. Kerres, W. Zhang, W. Cui, *J. Polym. Sci.: Part A: Polym. Chem.*, 36, 1441 (1998)

[9] J. Kerres, W. Cui, M. Junginger, *J. Memb. Sci.*, 139, 227 (1998)

[10] J. Kerres, A. Ullrich, *Sep. Purif. Techn.*, 22-23, 1 (2001)

[11] F. Helmer-Metzmann et al.: EP 0574 791 A2, Hoechst AG (1993)

[12] J. Kerres, W. Cui, S. Reichle, *J. Polym. Sci.: Part A: Polym. Chem.*, 34, 2421 (1996)

[13] J. Kerres, A. Ullrich, M. Hein, *J. Polym.Sci.: Polymer Chem.*, accepted

[14] L. Jörissen, V. Gogel, J. Kerres, J. Garche, *J. Power Sources*, accepted

[15] M.S. Wilson, US Patent 5211984 (1993)

[16] B. J. Lindberg, *Acta Chem. Scand.*, 21, 841 (1967)

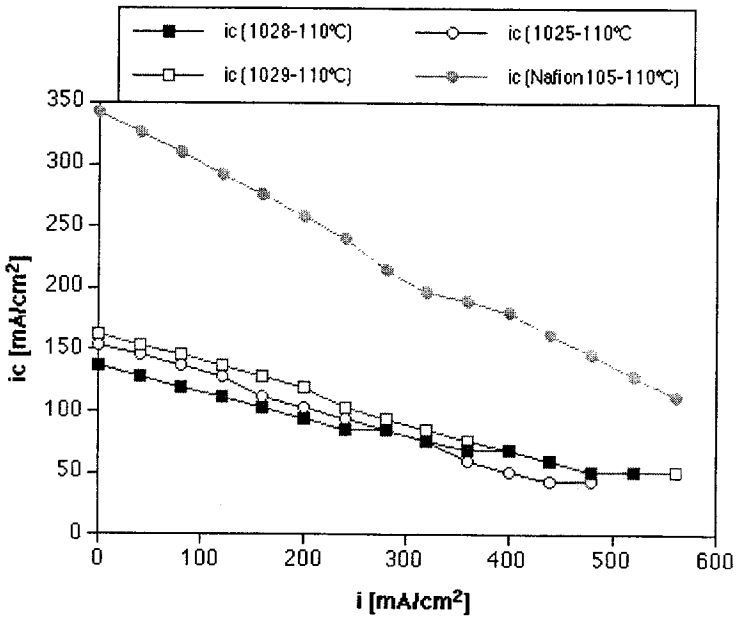

Fig. 18: MeOH permeation (ic vs. i) curves of MEAs made using the membranes 1029, 1028, and 1025 at T=110°C (DMFC conditions see Fig. 14); comparison: ic vs. i of a Nafion105 MEA at T=110°C

DAIMLERCHRYSLER Research & Technology

Überblick über Membrananforderungen aus Fahrzeugsicht - aktueller Stand der Technik

72. AGEF Seminar
Jülich, 4. Dezember 2002

Georg Frank
DaimlerChrysler AG

DAIMLERCHRYSLER Research & Technology

Inhalt

- Einführung
- Betrieb von Brennstoffzellenfahrzeugen
- Membrantypen
- Herausforderungen
- Zusammenfassung

DAIMLERCHRYSLER

Research & Technology

Einführung

- Brennstoffzellenfahrzeuge werden seit ca. 8 Jahren intensiv getestet
- Dramatische Verbesserungen bei Gewicht und Größe der Brennstoffzellensysteme erreicht
- Zunehmender Wettbewerb der Automobilunternehmen
- Zunehmende Industrialisierung
- Erhebliche Anstrengungen zur Kommerzialisierung der Technologie notwendig

DAIMLERCHRYSLER

Research & Technology

Brennstoffzellenfahrzeuge bei DaimlerChrysler

1994 NECAR I

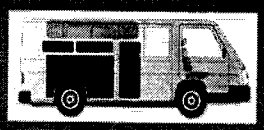

1996 NECAR II

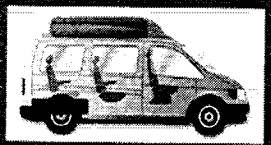

1997 NEBUS

1999 NECAR 4

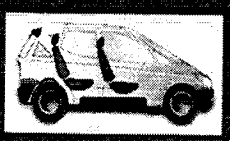

DAIMLERCHRYSLER

Research & Technology

NECAR 4

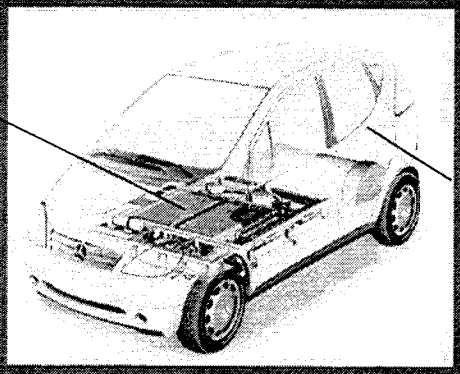

BZ-System:	**Leistung** (2 Stacks)	70 kW
	Leistungsdichte	5 kg/kW (200 W/kg)
Antrieb:	e-Motor	max. 55 kW
	Spitzengeschwindigkeit	145 km/h
	Reichweite	450 km
Gewicht:		1.750 kg

DAIMLERCHRYSLER

Research & Technology

NeCar IV Flüssig-H2 Brennstoffzellenfahrzeug

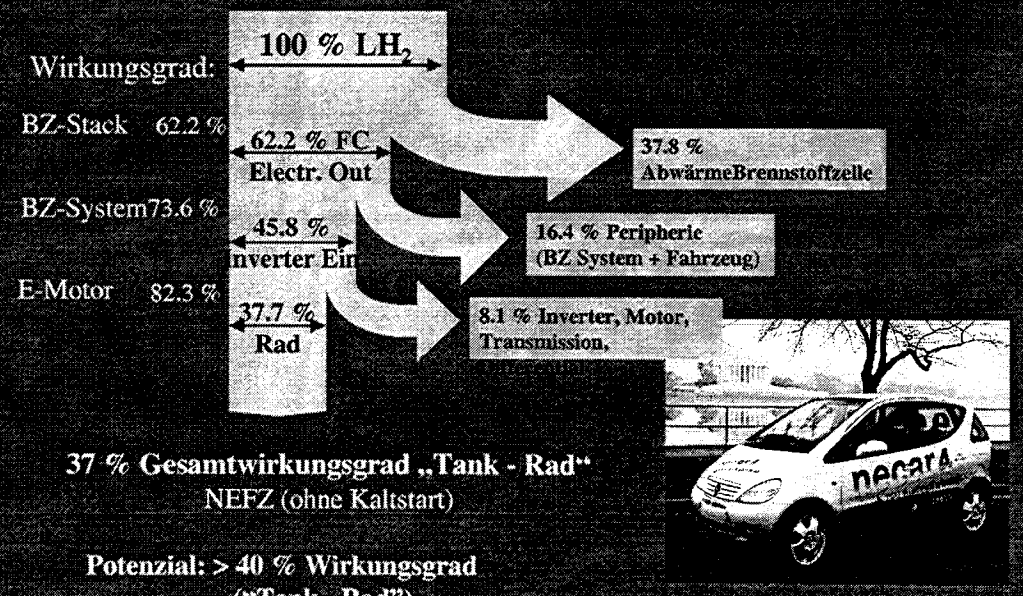

37 % Gesamtwirkungsgrad „Tank - Rad"
NEFZ (ohne Kaltstart)

Potenzial: > 40 % Wirkungsgrad
("Tank - Rad")

DAIMLERCHRYSLER

Research & Technology

Ansätze zur Systemvereinfachung und Effizienzsteigerung

- Niederdruck
- weniger Komponenten
- geringere parasitäre Einbußen
- geringere mechanische Belastung
- höhere Dynamik

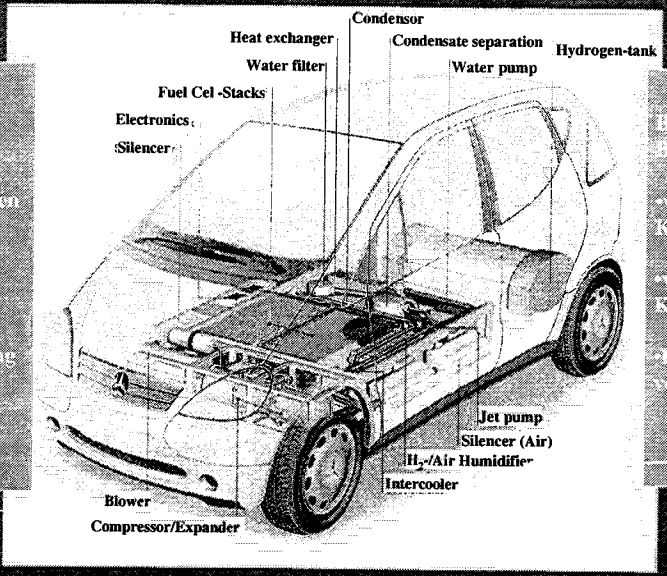

- Befeuchtungsfreier Betrieb
- weniger Komponenten
- vereinfachte Kühlung
- Frostsicher, vereinfachte Kaltstart

DAIMLERCHRYSLER

Research & Technology

Erkenntnisse aus den Demonstratoren

Vergleich Verbrennungsmotor Brennstoffzelle	Probleme der PEM-BZ	Aufgaben
Flächen- statt Volumen-prozess	Höhere Leistungsdichten zur Kosten-reduktion erwünscht Hohe Leistungsdichten erniedrigen den Wirkungsgrad	Neue Membran-Elektroden-Einheiten mit niedrigem Pt-Gehalt Sauerstoffanreicherung
Hohe Effizienz aber Wärme-abgabe bei niedrigen Temp-eraturen	Die Kühlung begrenzt die BZ leistung	Neue Kühlkonzepte Erhöhung der Zelltemperatur
Wassermanagement der Membran ungünstig	Eine externe Befeuchtung erhöht die Systemkomplexität	Neue Membranen
Hohe Leistungsdichten durch Kompression erreichbar	Erhöhung der Kosten und der parasitären Verluste	Effektivere Kompressoren Erhöhung der Leistungsdichte
Bessere Ausnutzung des Treibstoffes – aber H_2	Speicherung von H_2	Neue Speichersysteme

DAIMLERCHRYSLER Research & Technology

Die Bedeutung der Membran

Die Funktionalität heutiger Hochleistungsmembranen ist an ausreichende Wassermengen und deren Verteilung gebunden.

Die notwendige Wassermenge ist eine Funktion des *Materials*, der Dicke der Membran der Temperatur, der Überströmung und Befeuchtung.

Durch diese einfachen Zusammenhänge bestimmen die Membranen im allgemeinen die Betriebsbedingungen der Brennstoffzelle und damit die Systemkomplexität

DAIMLERCHRYSLER Research & Technology

Stammbau der Membranarten für die PEM

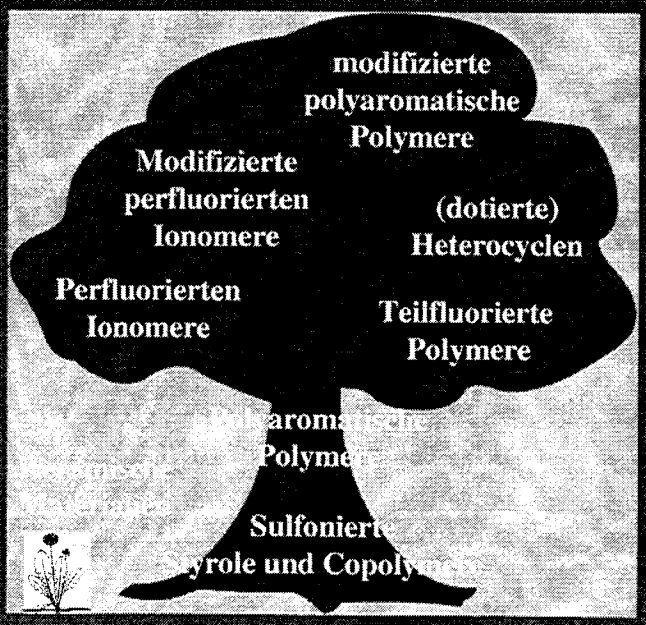

DAIMLERCHRYSLER Research & Technology

Überblick über heutige Membranen

Industriell herstellte Membranen für die automobile Anwendung:

Handelsname	Hersteller	Chemie	Dicke
Nafion®	DuPont	perfluoriert	25 -180 µm
Flemion®	Asahi Glass	perfluoriert	25 - 100 µm
Aciplex®	Asahi Chemicals	perfluoriert	25 - 100 µm
Hyflon	Solvay	perfluoriert	25 - 100 µm
Gore Select®	W.L. Gore	perfluoriert	10 - 40 µm
Celtec®	Celanese	polyaromatisch	?
?	FuMA-Tech	teilflouriert	20 - 100 µm
BAM® Ionomer	Ballard	teilfluoriert	20 - 50 µm

DAIMLERCHRYSLER Research & Technology

Ausgewählte Spezifikationen für Membranen der H_2-BZ

Eigenschaft	Zielwerte
Leitfähigkeit:	~ 140 mS/cm bei 60 % rel. Feuchte und 80 °C ~ 30 mS/cm bei - 30 °C
Betriebstemperatur:	-30 bis + 150 °C bei geringer/ohne Befeuchtung!
Lebensdauer:	> 5000 h Betriebsstunden über 10 Jahre
Gefrier- Tauzyklen:	> 2000
Dicke:	<< 50 µm
Quellverhalten:	< 20 % Fläche in Wasser bei 80 °C
H_2-Permeabilität:	<< 50 NL/(m²d bar) bei 23 °C, 50 % rel. Feuchte
Kosten:	< 20 •/m² bei Volumina größer 1 Mio m²/Jahr

DAIMLERCHRYSLER

Research & Technology

Heutiger Stand der Membranen

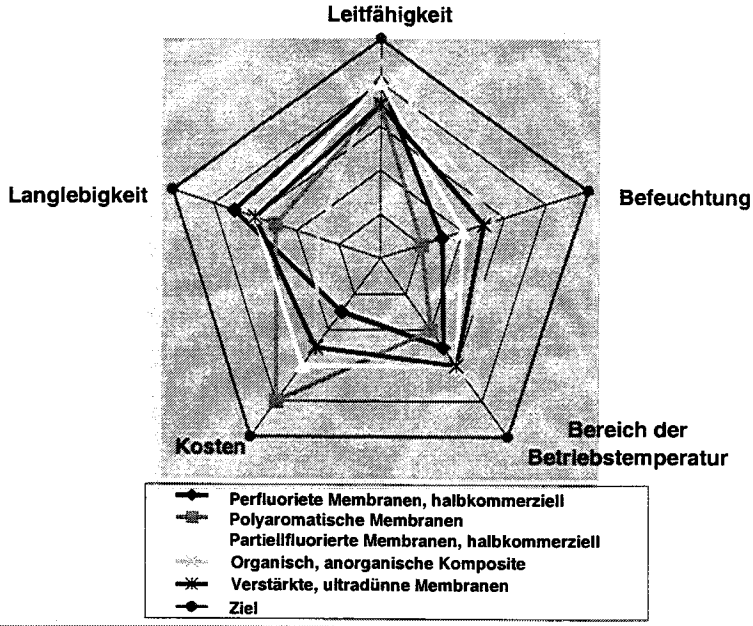

DAIMLERCHRYSLER

Research & Technology

Herausforderung Membran

- Membranen beeinflussen wesentliche Eigenschaften des BZ-Systems:
  - Design/Komplexität
  - Kosten
  - Leistung
- Verbesserungen folgender Membraneigenschaften notwendig:
  - höhere Leitfähigkeit bei geringen Wassergehalten
  - preiswerte Materialien
  - hohe Betriebstemperaturen unter Niederdruckbedingungen
  - Gefriertauglichkeit
  - Leitfähigkeit bei Temperaturen unter 0 °C
- Senkung der Platinbeladung wird durch gesteigerte Betriebstemperaturen vereinfacht

DAIMLERCHRYSLER

Research & Technology

Technologische Herausforderung bei der MEA

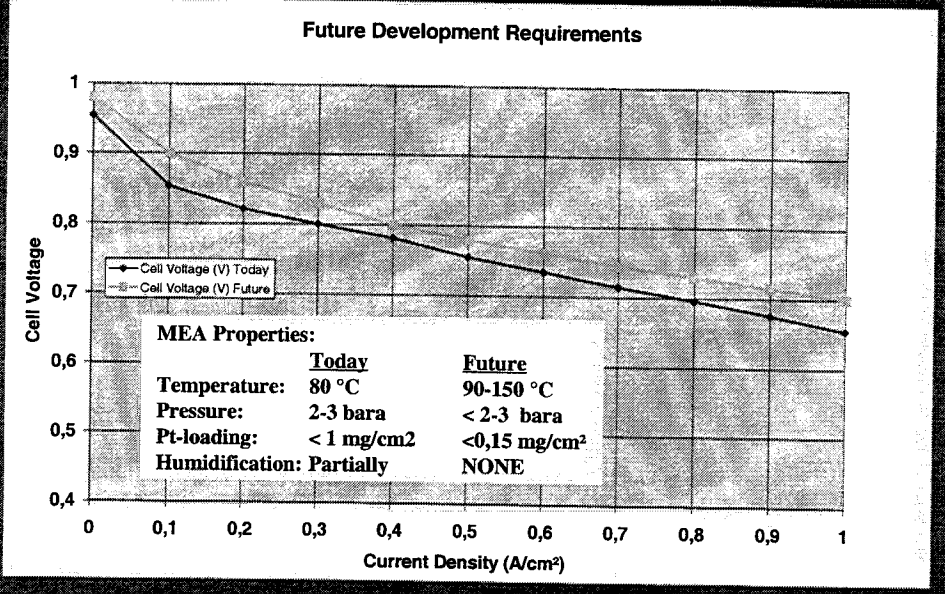

DAIMLERCHRYSLER

Research & Technology

Zusammenfassung

- Große Fortschritte bei BZ-Fahrzeugen
- Weitere Fortschritte nur mit Verbesserungen der Materialien:
  - **Membran**
  - Membran-Elektroden-Einheiten
- Eine weitere Kostenreduktion ist durch Hochtemperatur - Niederdruck-MEA zu erreichen
  - **Kritische Komponente: Membran**
- Ausgereifte Lösung ist noch nicht verfügbar!

Neue Protonenaustauschermembranen durch strahlungsinduziertes Pfropfen

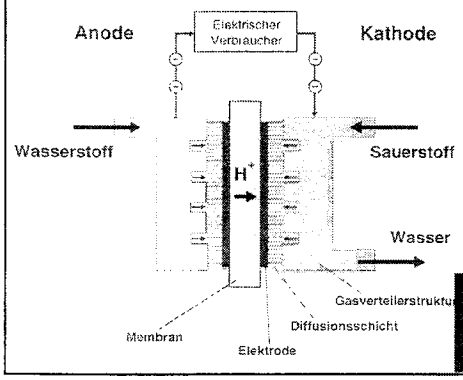

Gudrun Schmidt-Naake

Institut für Technische Chemie

TU Clausthal

http://www.itc.tu-clausthal.de/
Gudrun.Schmidt@itc.tu-clausthal.de

Anforderungen

PEM

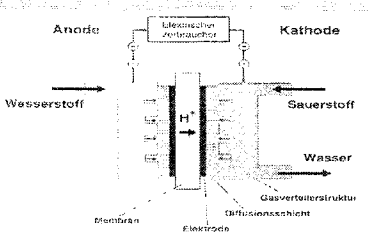

G. G. Scherer,
Ber. Bunsenges. Phys. Chem.
94 (1990) 1008-1014

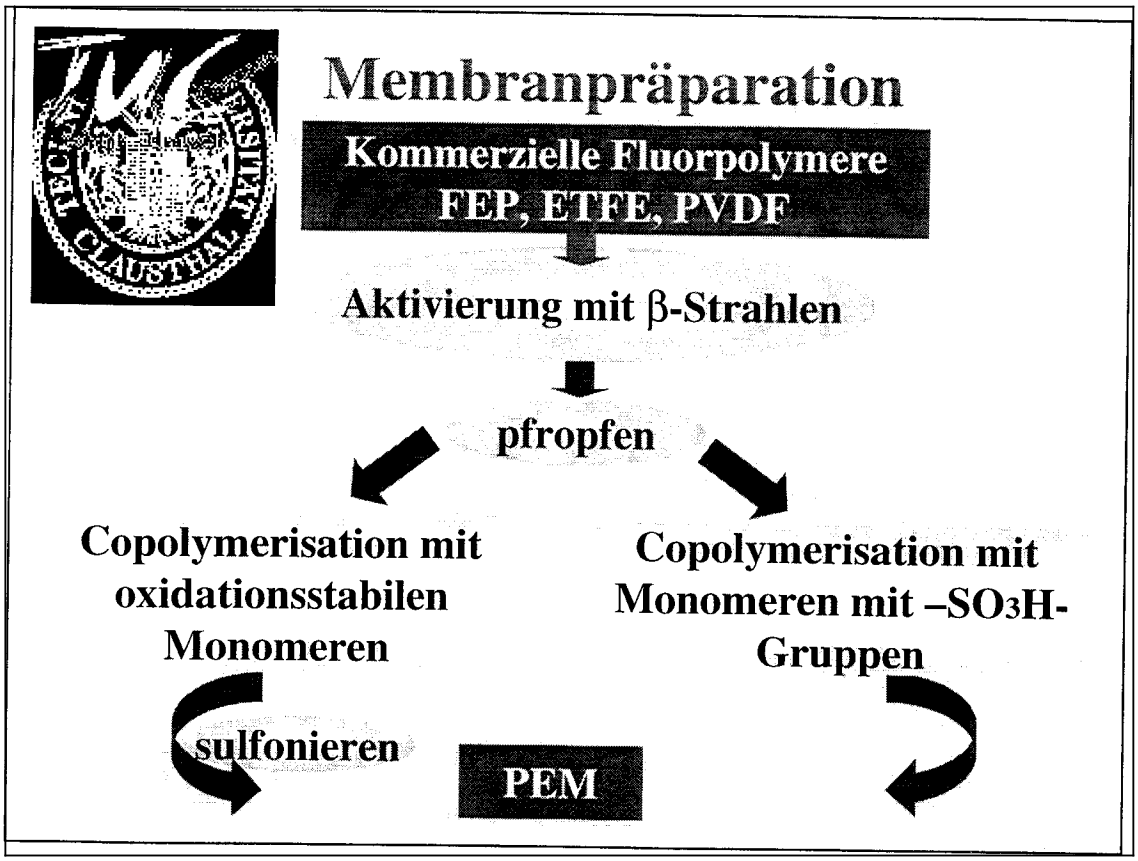
Membranpräparation
Kommerzielle Fluorpolymere
FEP, ETFE, PVDF
Aktivierung mit β-Strahlen
pfropfen
Copolymerisation mit oxidationsstabilen Monomeren
Copolymerisation mit Monomeren mit –SO3H-Gruppen
sulfonieren
PEM

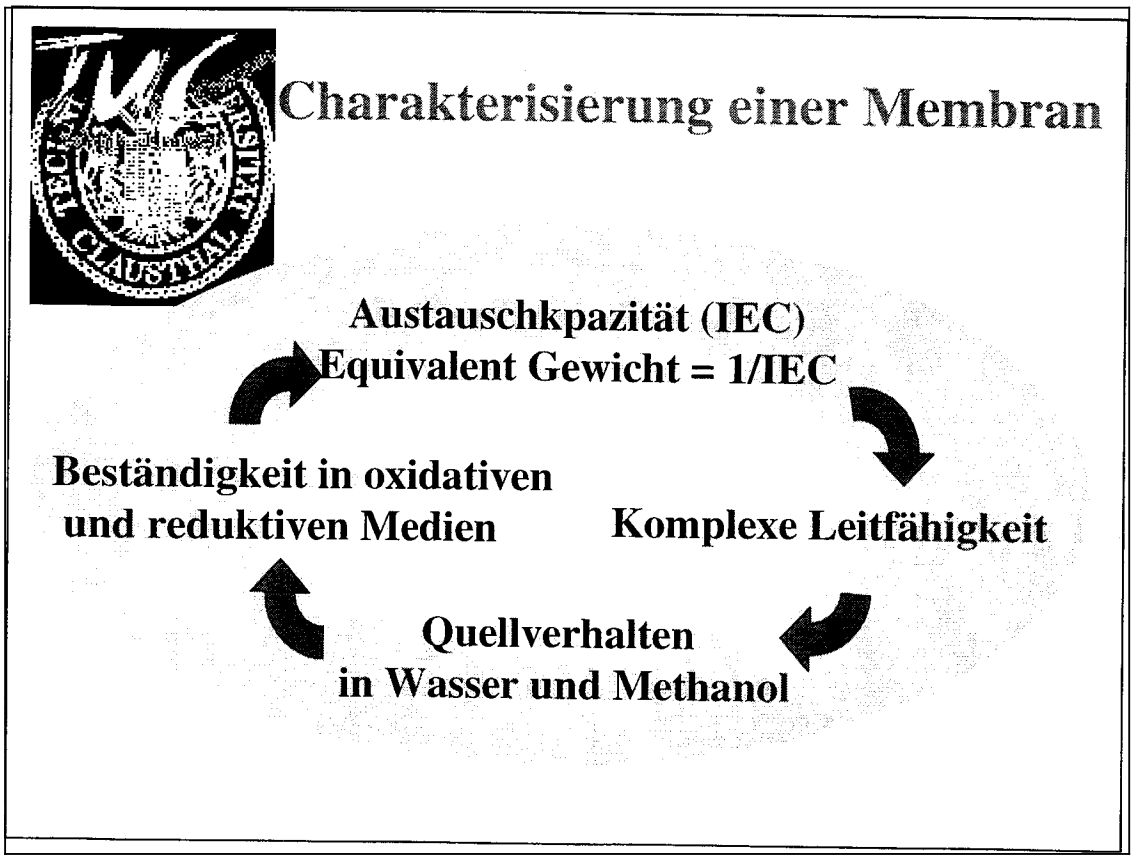
Charakterisierung einer Membran
Austauschkpazität (IEC)
Equivalent Gewicht = 1/IEC
Komplexe Leitfähigkeit
Quellverhalten
in Wasser und Methanol
Beständigkeit in oxidativen
und reduktiven Medien

Membran - Grundgerüste

Pfropfpolymer:
Styrol oder Styrol/Divinylbenzol

PE

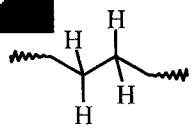

PTFE

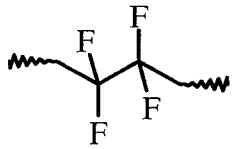

FEP

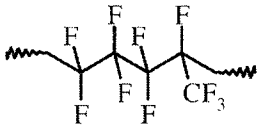

ETFE

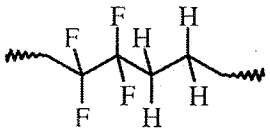

PFA:

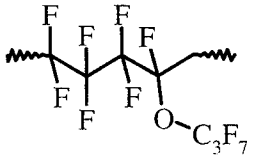

PVDF

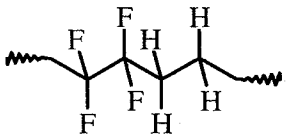

Styrolpfropfpolymere

O_2-Diffusion durch die Membran
? säurekatalysierte Wasserabspaltung
? Baeyer-Villiger Oxidation

Kettenbruch = Verringerung der SO_3H-Gruppen

⇨ Abbau

G. Hübner et al
J. Mater. Chem.
9(1999)409-418

Erhöhung der Oxydationsstabilität

Oxidationstendenz einer C-H-Bindung

Lösungsansätze:

- Reduktion der O_2- Diffusion
  - ? Vernetzer
- Reduktion Kettenbruch
  - ? stabilere Styrolcopolymere
  - ? Ersatz von Styrol

Wahl der Comonomere

Copolymere mit Styrolderivaten

sulfonierte Monomere

Styrolcopolymere

Grundgerüst-Pfropfbasis

gebildete Radikale ?

konservierte Radikale ?

ETFE

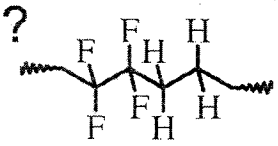

FEP

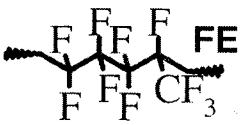

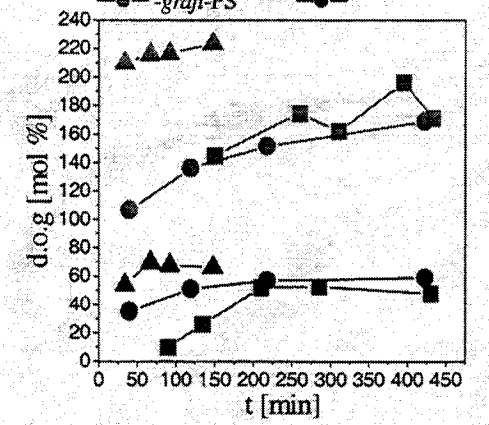

	Kristallinität [%]
ETFE	33
$ETFE_{50\ kGy}$	32
FEP	21
$FEP_{50\ kGy}$	16

Diffusionskontrolle

Pfropfen von S/AN und MS/AN

1. Sterischer Effekt

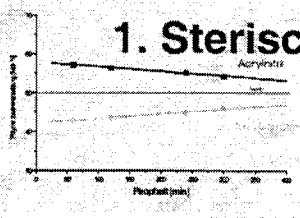

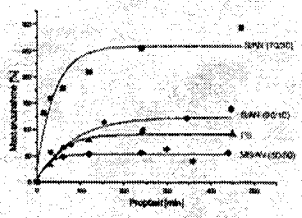

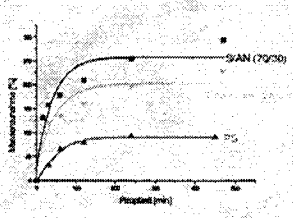

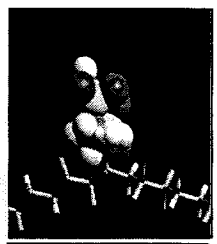

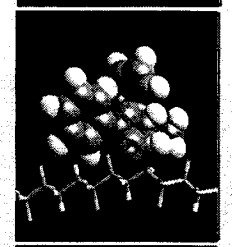

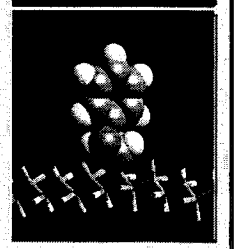

2. Reaktivitätseffekt

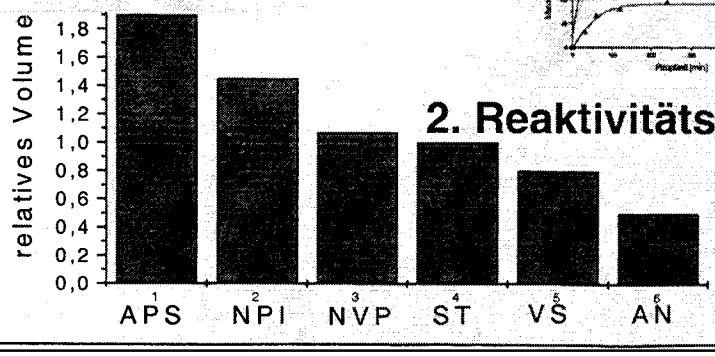

Relative Volumen der Monomere

Quellverhalten

Membranen ohne Vernetzer

Quellung = f (Temperatur)

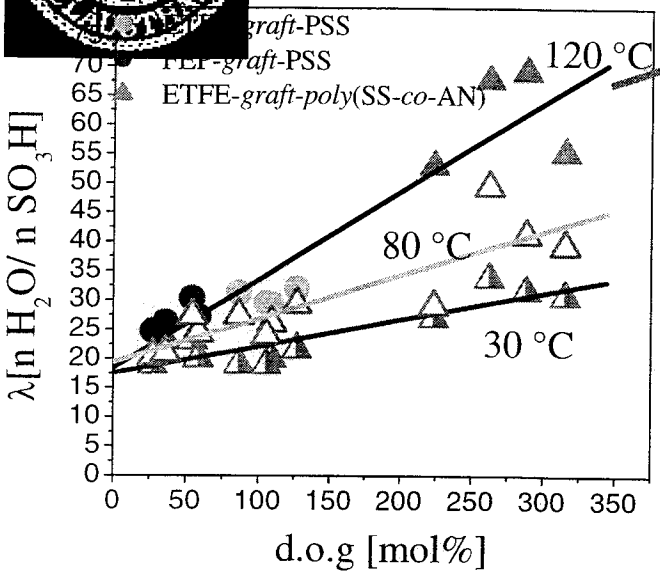

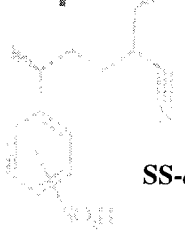

SS-*co*-AN

unabhängig vom:

Quellverhalten

Membranen ohne Vernetzer

Quellung = f (hydrophiler Anteil)

αMSS-*co*-AN

SS-*co*-AN

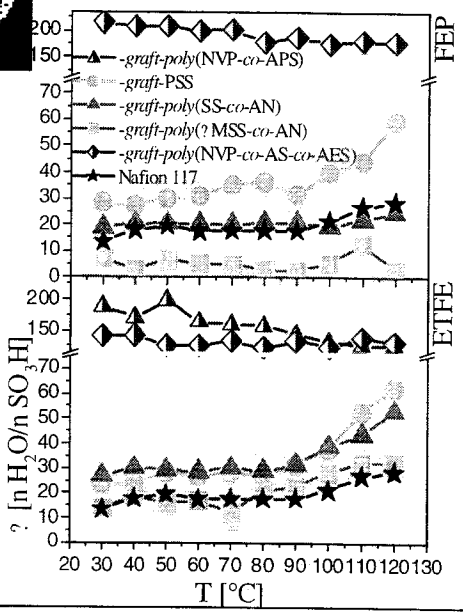

NVP-*co*-AES

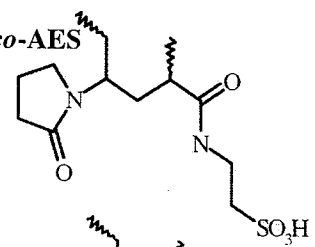

NVP-*co*-APS

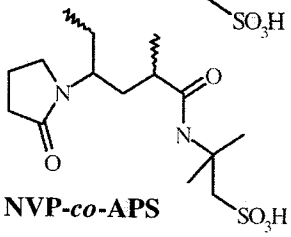

Einsatz von Vernetzern

? Separator-Eigenschaften

? chemische Stabilität

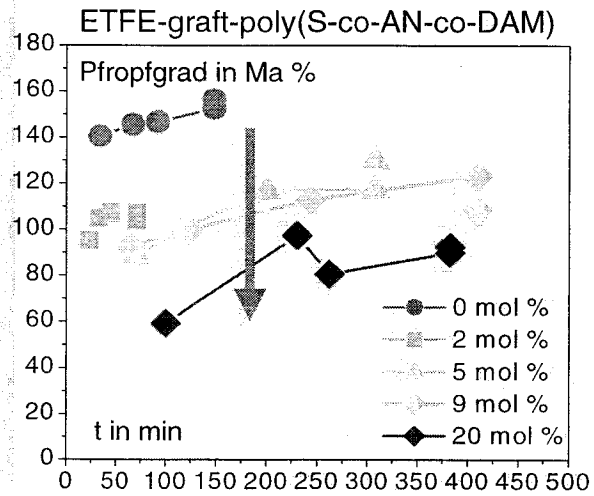

Behinderung der Pfropfreaktion ✓ Senkung der Pfropfgrade

Quellverhalten von SAN mit Vernetzern

Wasser

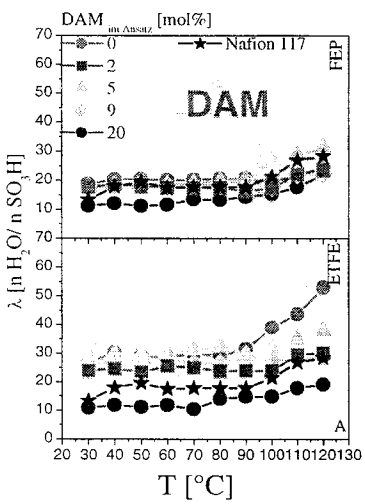

in Wasser/Methanol

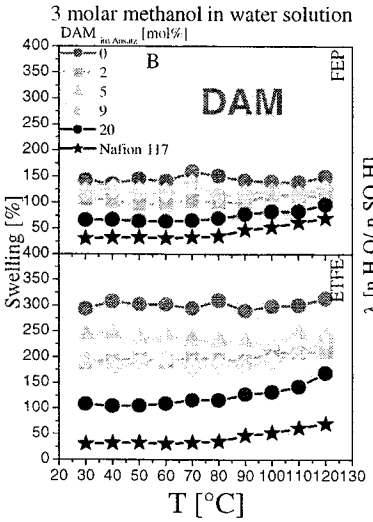

in Wasser

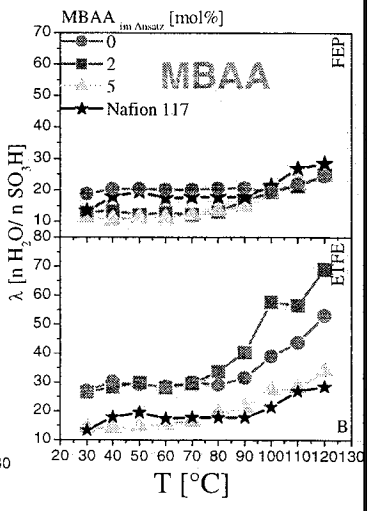

Austauschkapazität (IEC)

Einfluß des Pfropfpolymers

IEC = Nafion® 117

1) Nafion 117
2) poly(NVP-co-pSS)
3) poly(NVP-co-AES)
4) poly(NVP-co-APS)
5) poly(MSS-co-AN)
6) PSS
7) poly(SS-co-AN)

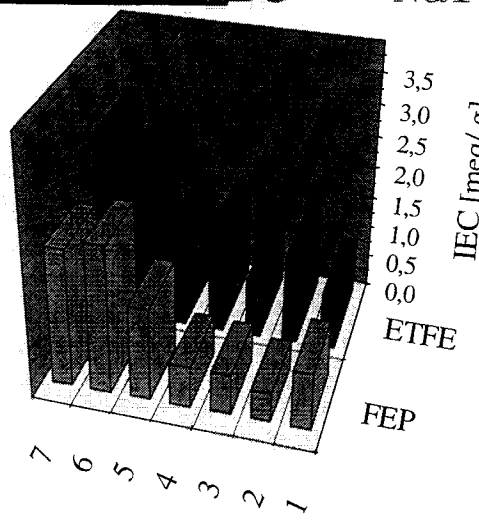

ETFE-*graft-poly*	σ [S/cm]	IEC [meq/g]
SS	0,11	3,05
SS-co-AN	0,34	3,67
NVP-co-APS	0,29	1,6

Oxidationsstabilität

Stabilitätssteigerung durch

(partieller) Ersatz von Styrol

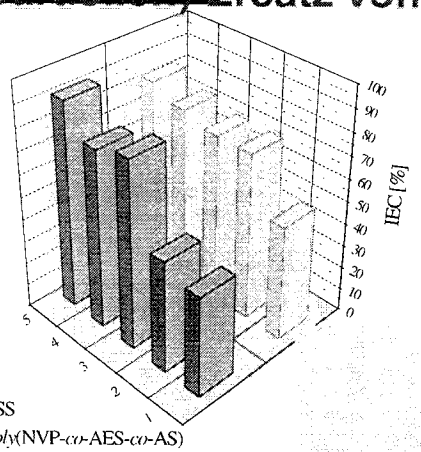

1) PSS
2) *poly*(NVP-*co*-AES-*co*-AS)
3) *poly*(NVP-*co*-APS)
4) *poly*(SS-*co*-AN)
5) *poly*(αMSS-*co*-AN)

Vernetzer

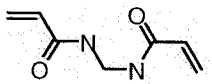

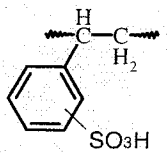

-*graft-poly*(SS-*co*-MBAA)
MBAA Anteil [%]
3) 2
4) 5
5) 8

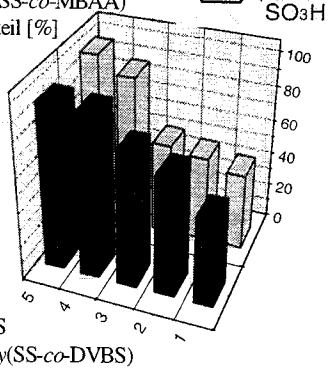

1) -*graft*-PSS
2) -*graft-poly*(SS-*co*-DVBS)

Leitfähigkeit bei 90 °C

= f (IEC, Wassergehalt,Temp.)

Stabilität

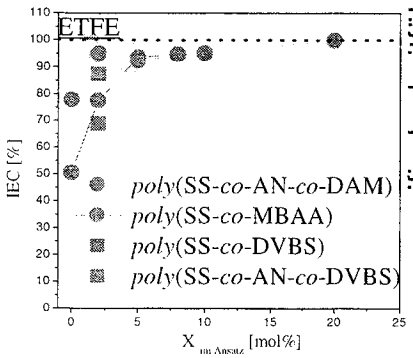

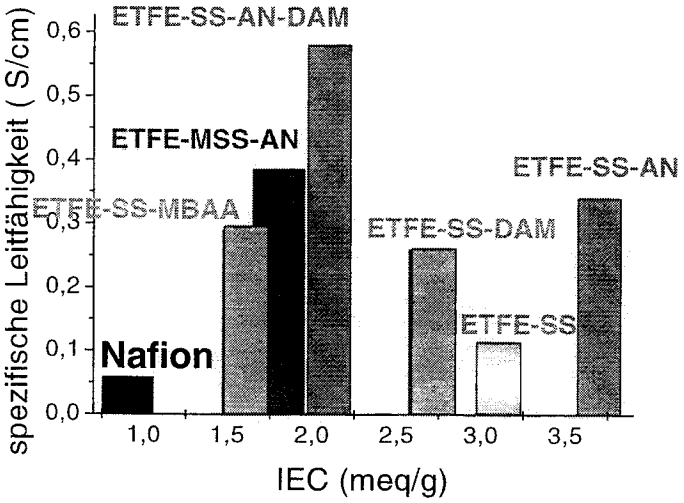

Spezifische Leitfähigkeit = f (IEC)

Pfropfpolymerisation mit GMA

Austausch-Kapazität ⇑

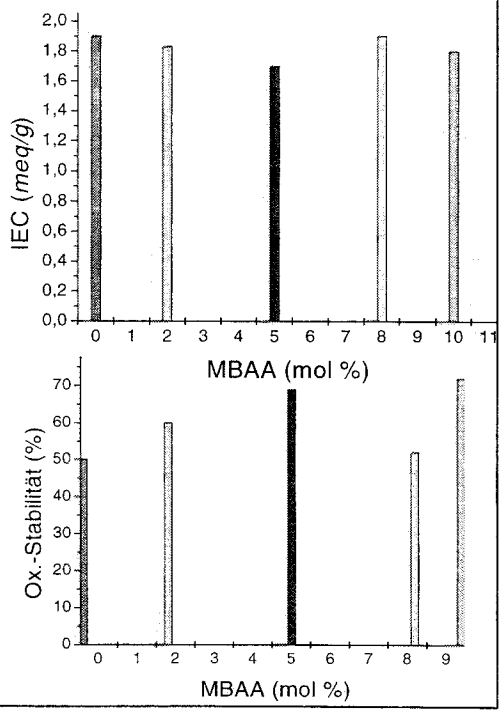

ETFE-*graft*-PGMA-*co*-MBAA

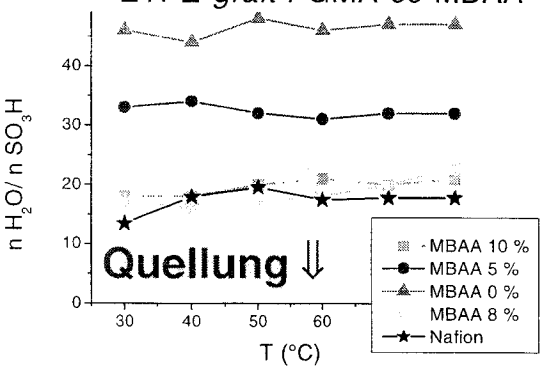

Quellung ⇓

Oxydationsstabilität noch zu niedrig

Pfropfpolymerisation mit HEMA

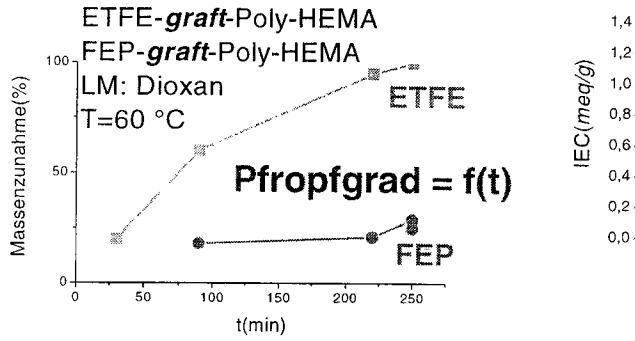

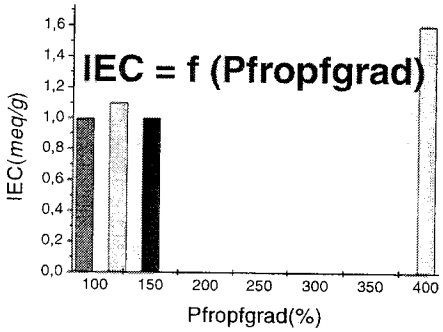

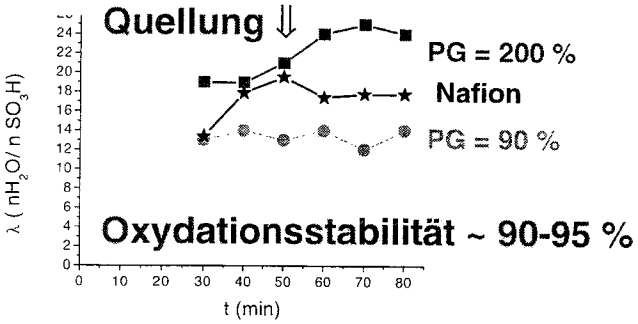

Oxydationsstabilität ~ 90-95 %

HEMA-co-GMA

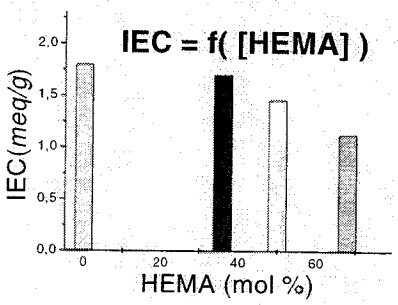

Zusammenfassung

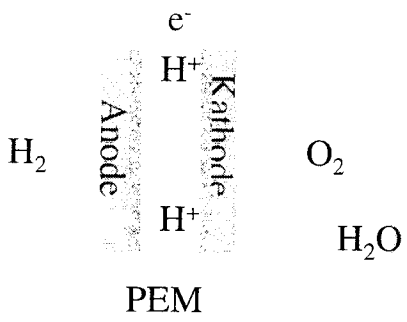

Eigene Publikationen:

1. W. Becker, M . Bothe, G. Schmidt-Naake
   Grafting of Poly(styrene-co-acrylonitrile) into pre-irradiated FEP and ETFE Films;
   Angew. Makromol. Chem. 273 (1999) 57
2. W. Becker, G. Schmidt-Naake
   Eigenschaften polymerer Protonenaustauschmembranen aus strahlungsinduzierter Pfropfpolymerisation;
   Chem. Ing. Techn. 72 (2000) 1541
3. G. Schmidt-Naake
   Kunststoffmodifizierung; TU Contact 9 (2001) 34
4. W. Becker, G. Schmidt-Naake
   Properties of Polymer Exchange Membranes from Irradation Introduced Graft Polymerization;
   Chem.Eng.Technol. 24 (2001) 1128
5. W. Becker, G. Schmidt-Naake
   Protonenaustauschmembranen durch strahlungsinduziertes Pfropfen von Styrol auf FEP und ETFE:
   Einfluss des Vernetzers N, N,-Methylen-*bis*-acrylamid
   Chem. Ing. Techn. 73 (2001) 1042
6. W. Becker, G. Schmidt-Naake
   Proton Exchange Membranes by Irradiation Induced Grafting of Styrene onto FEP and ETFE: Influence of the Crosslinker N,N-Methylene-bis-acrylamide
   Chem. Eng.Technol. 25 (2002) 373
7. W. Becker, Entwicklung von Protonenaustauschermembranen mit erhöhter Oxydationsbeständigkeit;
   Dissertation, TU Clausthal, 2002

Priv.-Doz. Dr.-Ing. Jakob Jörissen
Universität Dortmund
Fachbereich Chemietechnik
Technische Chemie A (Chemische Prozessentwicklung, Leitung: Prof. Dr. Arno Behr)
44221 Dortmund

Anionen-Austauschermembranen als Polymer-Ionenleiter

- **Direct Methanol Fuel Cell (DMFC)**
  - **konventionell: mit Kationen-Austauschermembran als H^+-Ionenleiter**
  - **Problem: Methanol-„Schlupf" zur Kathode**
    - **Beispiele für Methoden zu seiner Vermeidung**
- **Transportmechanismen in Ionenaustauscher-Membranen**
  - **Diffusion**
  - **Migration**
  - **Konvektion: elektro-osmotischer Strom (EOS)**
    - **Messergebnisse für die Methanol-Oxidation**
- **Alternative Polymer-Ionenleiter: Anionen-Austauschermembranen (AAM)**
  - **der EOS ist der Diffusion entgegengerichtet und kann sie somit zurückdrängen**
  - **Erfahrungen mit AAM für organische Anionen**
  - **AAM als OH^--Ionenleiter**
    - **Messergebnisse**
    - **Stabilitätsprobleme der verfügbaren Membranen**
    - **mögliche verbesserte Membranmaterialien**
  - **AAM als CO_3^{2-} / HCO_3^--Ionenleiter**
    - **Besonderheiten beim Transport mehrfach geladener Anionen**

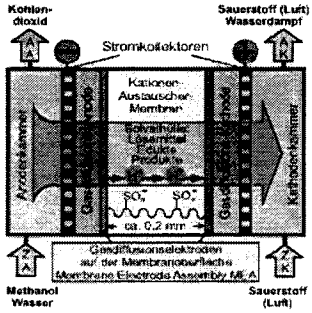

Direct Methanol Fuel Cell (DMFC) mit Kationen-Austauschermembran als H^+-Ionenleiter

Bei vollständiger Oxidation des Methanols zu Kohlendioxid

Reaktionen an der Membran-Elektroden-Grenzschicht

Anode:

$$CH_3OH + H_2O \rightarrow CO_2 + 6\,H^+ + 6\,e^-$$

H^+-Ionen wandern durch die Membran

Kathode:

$$3/2\,O_2 + 6\,H^+ + 6\,e^- \rightarrow 3\,H_2O$$

Transport in Ionenaustauscher-Membranen:
erweiterte Nernst-Planck-Bewegungsgleichung

$$n_i = -D_i \frac{dc_i}{dx} - c_i D_i \frac{z_i F}{R T} \frac{d\varphi}{dx} + c_i v$$

Diffusion — Migration — Konvektion

Anode

stark vergrößerter Ausschnitt nicht maßstabsgerecht

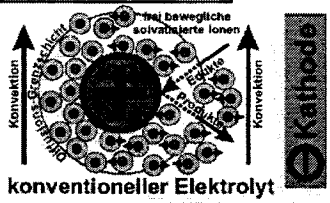

konventioneller Elektrolyt

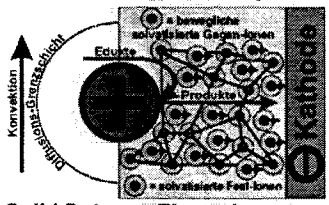

Solid Polymer Electrolyte

In einem konventionellen Elektrolyten sind sowohl Anionen als auch Kationen beweglich, so dass deren Solvathüllen keinen effektiven Stofftransport bewirken. Innerhalb der laminaren Diffusionsgrenzschicht unmittelbar an der Elektrodenoberfläche erfolgt der Stofftransport nur durch Diffusion.
In der Ionenaustauscher-Membran als Solid Polymer Electrolyte ist nur eine Ionenart beweglich, so dass deren Solvathüllen den elektro-osmotischen Strom hervorrufen, der einen konvektiven Stoffaustausch bis unmittelbar an die Elektrodenoberfläche bewirkt.

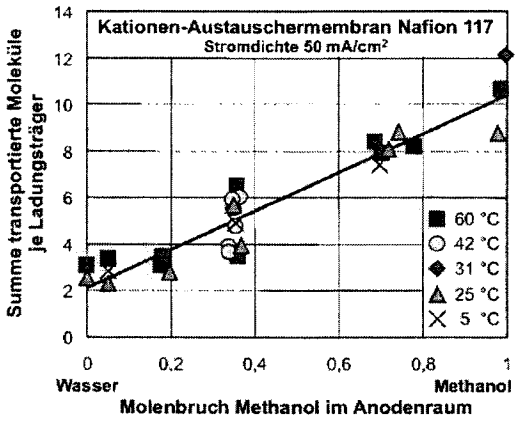

Der elektro-osmotische Strom nimmt offenbar unselektiv alle Stoffe in den Konzentrationen, die in der Reaktionszone an der Membranoberfläche vorliegen, mit.

Bei flüssigen Phasen gleicher Konzentration auf beiden Seiten ist ein Effekt der Temperatur nicht erkennbar.

Der elektro-osmotische Strom hängt sehr stark ab von der Zusammensetzung der Flüssigkeit und vom Zustand der Membran.

Bei Nafion nimmt er proportional zur Flächenvergrößerung infolge einer verstärkten Quellung zu.

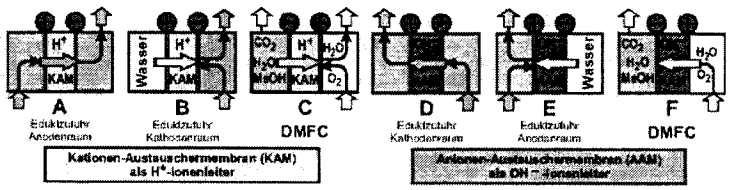

Betriebsvarianten elektrochemischer Zellen mit Ionenaustauscher-Membranen als Festelektrolyte

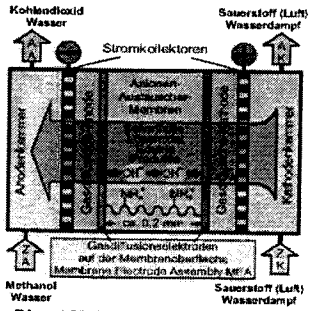

Direct Methanol Fuel Cell (DMFC) mit Anionen-Austauschermembran als OH^--Ionenleiter

Bei vollständiger Oxidation des Methanols zu Kohlendioxid

Reaktionen an der Membran-Elektroden-Grenzschicht

Kathode:

$3/2\ O_2 + 3\ H_2O + 6\ e$

$\downarrow$

$6\ OH^-$

OH^--Ionen wandern durch die Membran

Anode:

$CH_3OH + 6\ OH^-$

$\downarrow$

$CO_2 + 5\ H_2O + 6\ e$

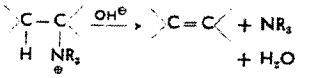

HOFMANN-Abbau quaternärer Ammoniumsalze

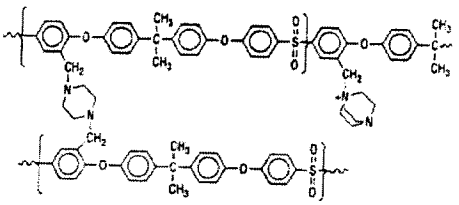

Alkaline resistant anion-exchange layer polymer
Dabco: Diaminobicyclooctane

Versuche erfolgten in SPE-Elektrolysezellen mit 21 cm² aktiver Fläche in den Varianten E, A und B im kontinuierlichen Betrieb mit Wasserstoff entwickelnden Kathoden (Pt-Ir-Netz 90:10 oder Graphitfilz). Es ist zu erwarten, dass sich die Membranen in diesen Zellen so verhalten wie in den entsprechenden DMFC-Varianten F oder C, die sich nur durch den Einsatz von Sauerstoff-Diffusionskathoden unterscheiden.

Variante	Anode	Kathode	°C	A/m²	Methanol-Konzentration [Gew-%] Anolyt Zulauf	Anolyt Ablauf	Katholyt Zulauf	Katholyt Ablauf	Methanol-Transport [g/(h·m²)]
Anionen-Austauschermembran Neosepta AHA (Elektrodialyse-Membran Tokuyama Corp.)									
E	(Pt/Ir)	(Graphit)	50	–	10	5,4	0	2,1	53,1
E	Pt/Ir	Pt/Ir	50	200	10	6,1	0	0,7	17,5
E	Pt/Ir	Pt/Ir	50	400	10	2,6	0	0,8	14,1
E	Pt/Ir	Graphit	50	400	10	2,0	0	0,5	14,6
E	Pt/Ir	Graphit	65	400	10	2,1	0	0,6	12,0
E	Pt/Ir	Graphit	50	600	10	1,7	0	0,3	4,9
Kationen-Austauschermembran Nafion 117 (DuPont)									
A	(Pt/Ir)	(Graphit)	50	–	10	5,7	0	2,1	51,5
A	Pt/Ir	Graphit	50	400	10	–	0	2,7	100,1
B	Pt/Ir	Graphit	50	400	0	0,4	10	2,7	40,5

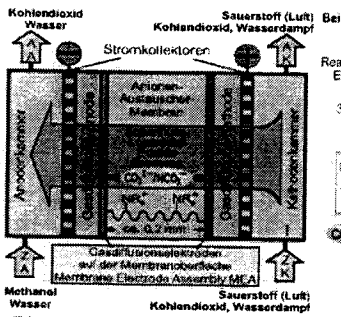

Direct Methanol Fuel Cell (DMFC) mit Anionen-Austauschermembran als CO_3^{2-}/HCO_3^--Ionenleiter

Bei vollständiger Oxidation des Methanols zu Kohlendioxid

Reaktionen an der Membran-Elektroden-Grenzschicht

Kathode:

$3/2\ O_2 + 3\ CO_2 + 6\ e^-$

$\downarrow$

$3\ CO_3^{2-}$

$CO_3^{2-} + CO_2 + H_2O$

$\downarrow$

$2\ HCO_3^-$

CO_3^{2-}/HCO_3^--Ionen wandern durch die Membran

Anode:

$CH_3OH +$

$(3-n)\ CO_3^{2-} + 2n\ HCO_3^-$

$\downarrow$

$(4+n)\ CO_2 + (2+n)\ H_2O + 6\ e^-$

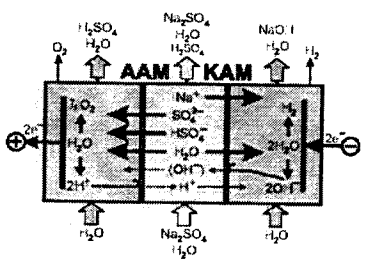

Dreikammerzelle für die Elektrolyse von Natriumsulfat zum Recycling von Natronlauge und Schwefelsäure

Ion Transport Model for Anion Exchange Membranes for the case of Sodium Sulfate Electrolysis

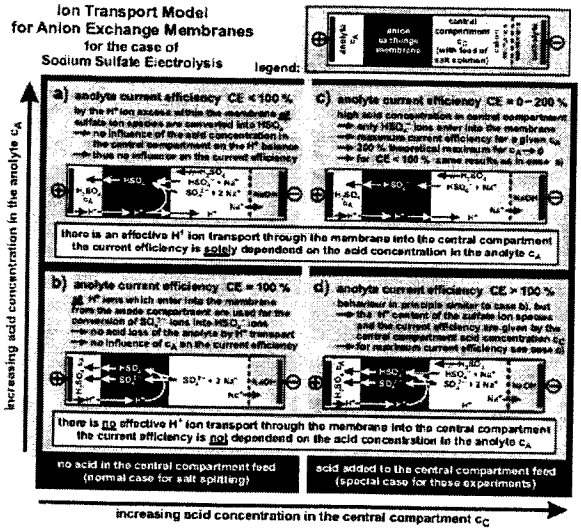

Herstellungsstrategien und Eigenschaftsspektrum bei anorganisch-organischen perfluorierten Hybridmembranen für die DMFC

M. Willert-Porada, F. Bauer
LS für Werkstoffverarbeitung
Fakultät für Angewandte Naturwissenschaften
Universität Bayreuth

- **Entwicklungsziele bei anorganisch-organischen Hybridmembranen**
- **Beispiele für verschiedene Stoffsysteme**
- **Perfluorierte anorganisch-organische Hybridmembranen**
- **Einfluß der Zusammensetzung auf die Eigenschaften**
- **Ausblick: 3D-Strukturen**

Universität Bayreuth
Lehrstuhl für Werkstoffverarbeitung
Prof. Dr. M. Willert-Porada
11/02

Entwicklungsziel von Ionomer-Membranen für DMFC, Direct Methanol Fuel Cell

- **Hohe Protonen-Leitfähigkeit**
- **Funktionsfähigkeit T>100°C in wässrigen Säuren**
- **Geringe Quellung**
- **Geringe Methanol-Permeation**
- **Hohe Gasdichtigkeit bei geringer Dicke der Membran**

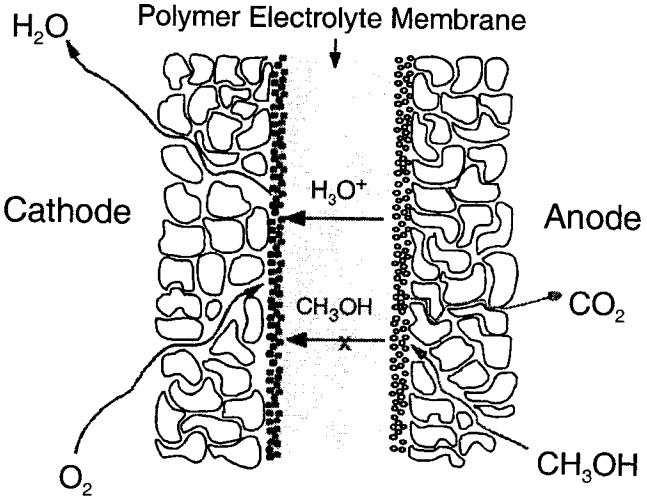

Lösungsansatz für DMFC-Membranen durch anorganisch-organische Hybridmembranen

- **Verringerung der Quellung und Methanol-Permeation durch Verstärkung des Polymers mit anorganischen Einlagerungen**

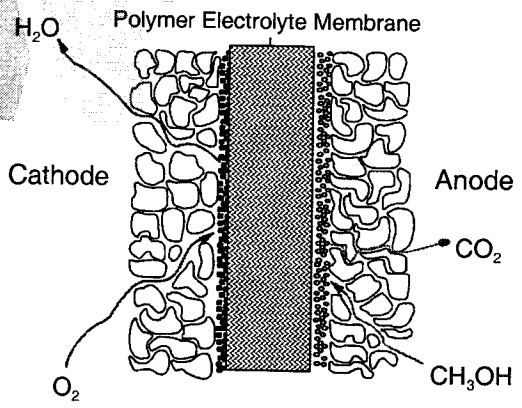

- **Hohe Protonen-Leitfähigkeit durch Synergie unterschiedlicher H^+-Leitfähigkeits-Pfade, z.B. nicht nur entlang der Sulfonsäuregruppen sondern auch an der "sauren" Oberfläche der anorganischen Einlagerungen**
- **Funktionsfähigkeit bei T>100°C in Säuren durch Wasser-Rückhaltevermögen anorganischer Einlagerungen**

Beispiele für verschiedene Stoffsysteme

I. Foliengiessen ausgehend von Polymer-Precursor Lösungen, gefolgt von der Hydrolyse des Prekursors und ggf. Umesterung.

Organische Matrix

- **Sulfonierte Polyetherketone, SPEK und Poly(ether-etherketone), SPEEK**

S.P. Nunes, B. Ruffmann, E. Rikowski, S. Vetter, K. Richau, J. of Memebrane Science, 203,215-225 (2002)

Anorganische Komponente

- **SiO_2, TiO_2, ZrO_2 , $Zr(HPO_4)_2$**

S.P. Nunes, B. Ruffmann, E. Rikowski, S. Vetter, K. Richau, J. of Memebrane Science, 203,215-225 (2002)

Beispiele für verschiedene Stoffsysteme

II. Filmziehen ausgehend von Polymer-Säure-Gelen, gefolgt von Trocknung und Vernetzung

Organische Matrix

- **Sulfonierte Polysulfone, SPSF**

P. Genova-Dimitrova, B. Baradie, D. Foscallo, C. Poinsignon, J.Y. Sanchez, J. of Membrane Science, 185, 59-71 (2001)

Anorganische Komponente

- **Phosphoantimon-Säure, $H_nSb_nP_2O_{(3n+5)} \cdot x\ H_2O$, n=1,3**

P. Genova-Dimitrova, B. Baradie, D. Foscallo, C. Poinsignon, J.Y. Sanchez, J. of Membrane Science, 185, 59-71 (2001)

Beispiele für verschiedene Stoffsysteme

III. Anorganisch-organische Molekülverbindungen, z.B. organisch substituierte Phosphonatester der Titansäure

Titanphosphat-Sulfenylphosphonat,
$Ti(HPO_4)_{1,00}(O_3PC_6H_4SO_3H)_{0,85}(OH)_{0,30}{\cdot}n\ H_2O$

G. Alberti, U. Constantino, M. Casciola, S. Ferroni, L. Massinelli, P. Staiti, Solid State Ionics, 145, 249-255 (2001)

Anorganisch-organische Hybridmembranen auf der Basis von Nafion-Membranen

Basierend auf der Mikrostruktur von Nafion können anorganische Einlagerungen entweder in das vorhandene hydrophile Mizellen-Netzwerk der wasserreichen Sulfonsäure-Phase oder in die hydrophoben $(-CF_2)_n$- Bereiche eingebaut werden.

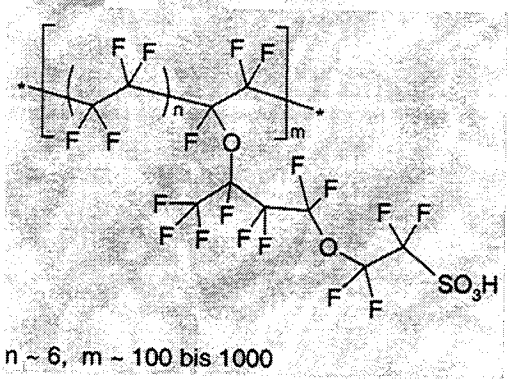

n ~ 6, m ~ 100 bis 1000

Hydrophobe Bereiche

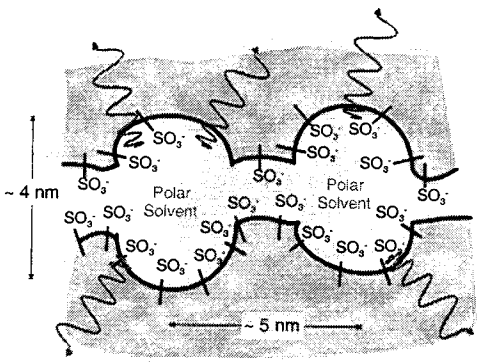

$\lambda_{H_2O} = 22\ (n(H_2O) / n(-SO_3H))$

Hydrophile Bereiche

Modellvorstellung zu anorganisch-organischen Hybrid-Membranen am Beispiel Nafion + Oxide

Anorganischen Einlagerungen können als perkolierte Netzwerke in den hydrophoben CF_2-reichen Zonen des Ionomers entstehen, wenn eine Inversion der Mizellen als Folge extremer Prekursor-Quellung der hydrophilen Bereiche erfolgt.
Erwünscht, da eine Verringerung der Transportkapazität für CH_3OH erwartet wird, ohne Verringerung der H_3O^+ -Leitfähigkeit.

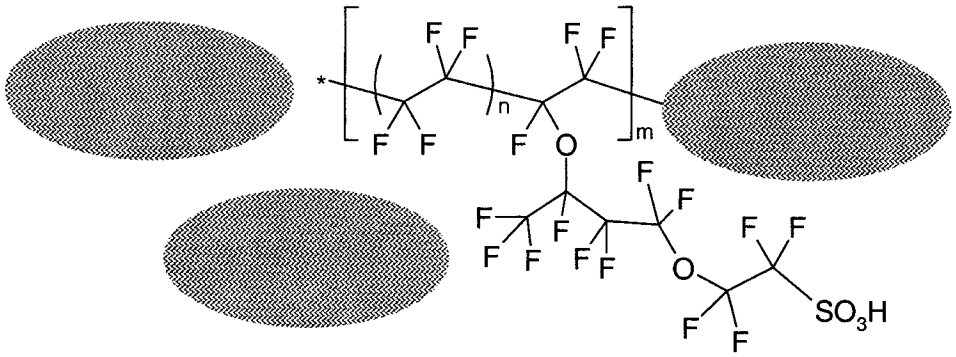

n ~ 6, m ~ 100 bis 1000

Modellvorstellung zu anorganisch-organischen Hybrid-Membranen am Beispiel Nafion + Zirkonylphophonat

•Hohe Protonen-Leitfähigkeit durch Synergie unterschiedlicher H^+-Leitfähigkeits-Pfade, z.B. entlang der Sulfonsäuregruppen und an der "sauren" Oberfläche der anorganischen Einlagerungen

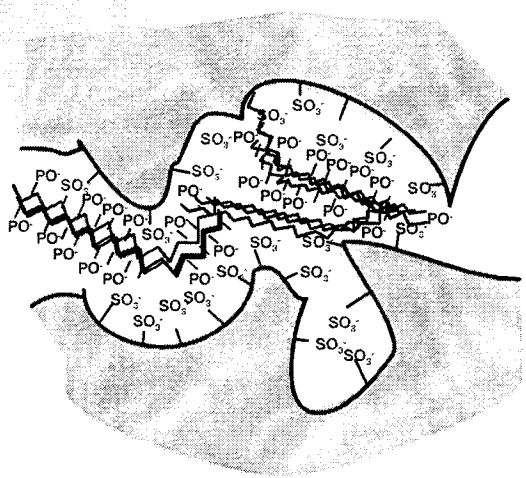

•Verringerung der Quellung und Methanol-Permeation durch Verstärkung des Polymers mit anorganischen Einlagerungen

•Funktionsfähigkeit bei T>100°C in wässrigen Säuren durch Wasser-Rückhaltevermögen anorganischer Einlagerungen

Perfluorierte anorganisch-organische Hybridmembranen

I. Foliengiessen ausgehend von Polymer-Precursor Suspensionen oder Lösungen, gefolgt von der Hydrolyse des Prekursors

Organische Matrix	Anorganische Komponente
• Nafion-Suspension • Nafion-Vorstufe	• SiO_2, TiO_2, ZrO_2

II. Infiltration von Nafion-Folien mit Metaloxychlorid-Lösungen, gefolgt von der Hydrolyse bzw. einer Umesterung des Chlorides

Organische Matrix	Anorganische Komponente
• Nafion-Folie	• SiO_2, TiO_2, ZrO_2 , $Zr(HPO_4)_2$

Perfluorierte anorganisch-organische Hybridmembranen

III. Infiltration und Co-Infiltration von Nafion-Folien mit Metalalkoholaten, gefolgt von der Hydrolyse oder Pyrolyse der Alkoholate, anschließend Umsetzung der Oxide zu Phosphonaten

Organische Matrix	Anorganische Komponente
• Nafion-Folie	• SiO_2, TiO_2, ZrO_2 , $Zr(HPO_4)_2$

Mit Hilfe der Metallalkoholat-Infiltration sind sehr hohe Beladungen möglich und somit sowohl eine Einlagerung in das Mizellen-Netzwerk als auch eine Mizellen-Inversion.

Herstellung anorganisch-organischer Nafion-Membranen

Die hydrophilen Mizellen dienen als "Mikroreaktoren" für die Infiltration mit Oxid-Prekursoren, wie beispielsweise Ti- und Zr-Metallalkoholaten. Die Nafion-Prekursor-Komplexe werden durch Hydrolyse, Pyrolyse und nachfolgende Phosphorylierung zu den anorganischen Einlagerungen umgesetzt.

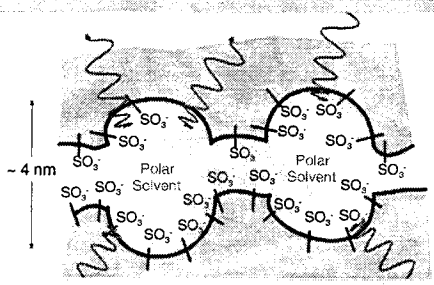

Mikrowellen, Wärme und/oder Solvens

Infiltration & Komplexbildung

$$\text{Nafion}^{®} + Ti(O\text{-}nC_4H_9)_4 \xrightarrow{\text{2 h, n-}C_4H_9OH} [\text{Nafion}^{®}]^+ [Ti(OR)_4SO_3H]^-$$

Hydrolyse

$$Ti(O-nC_4H_9)_4 + H_2O \rightarrow Ti(O-nC_4H_9)_3 + C_4H_9OH$$
$$C_4H_9OH \leftrightarrow H_2O + C_4H_8$$

Pydrolyse

$$Ti(O-nC_4H_9)_4 \xrightarrow{\Delta T} Ti(O-nC_4H_9)_2O + (C_4H_9)_2O$$
$$Ti(O-nC_4H_9)_4 \xrightarrow{\Delta T} Ti(O-nC_4H_9)_2O + C_4H_9OH + C_4H_8$$

Herstellung anorganisch-organischer Nafion-Membranen durch Pyrolyse Infiltrierter Prekursoren mittels Mikrowellenerwärmung

β -Relaxation der ionomeren Region, 53%rh, Nafion ^{117}, λ = 4

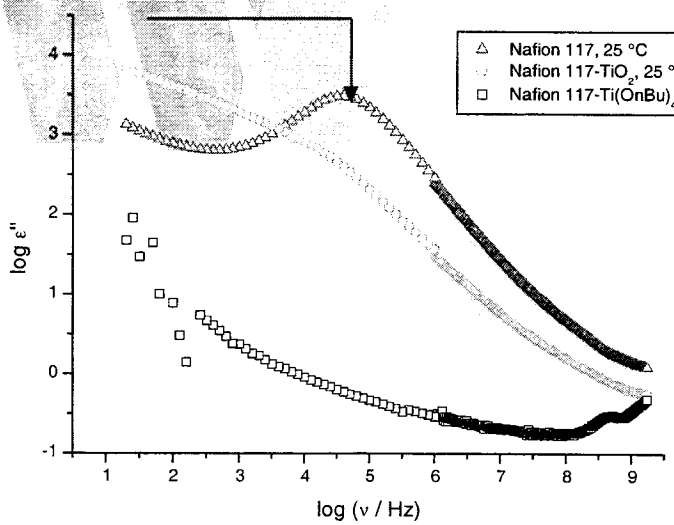

- **λ-Wert bestimmt die dielektrischen Verluste**
- **Titan-alkoholate bilden Komplexe mit Nafion**
- **An der Komplexbildung sind die Ionomer-Seitenketten beteiligt**

Einfluß des Feuchtegehaltes und der Temperatur auf die dielektrischen Eigenschaften von Nafion ^{117} und von Hybridmembranen

Herstellung anorganisch-organischer Nafion-Membranen durch Pyrolyse mittels Mikrowellenerwärmung

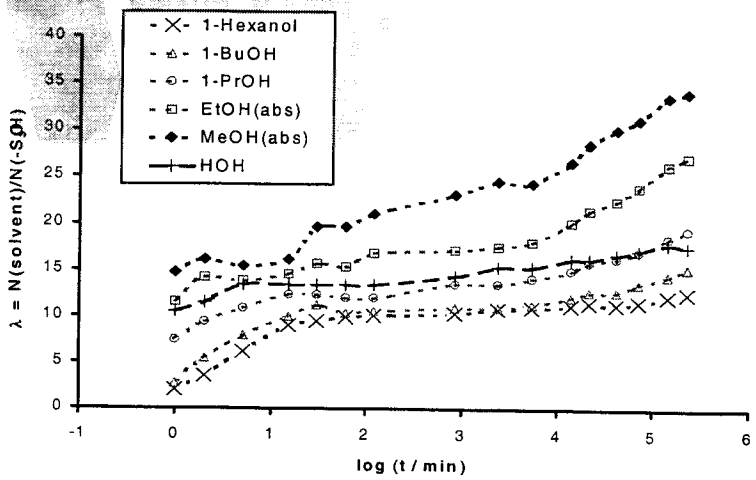

Quellfähigkeit von Nafion^{117} in unterschiedlichen Lösungsmitteln

- Die Quellfähigkeit nimmt mit steigender Kettenlänge des Alkohols ab
- Titan-alkoholat-BuOH-Lösungen können zur gezielten Einstellung der dielektrischen Verluste und des Anteils anorganischer Einlagerung genutzt werden

Herstellung anorganisch-organischer Nafion-Membranen durch Pyrolyse infiltrierter Prekursoren mittels Mikrowellenerwärmung

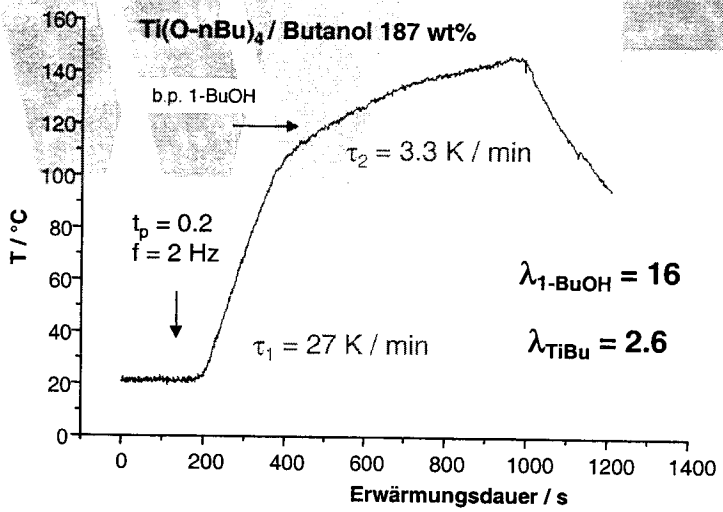

Mikrowellen-Erwärmungsverhalten von $Ti(O\text{-}nBu)_4$/BuOH-infiltrierten Nafion ^{117}-Membranen

- Durch Mikrowellen-Pulserwärmung gelingt es, bei geringer thermischer Belastung der Nafion-Membran das Alkoholat zu pyrolysieren

Eigenschaften anorganisch-organischer Nafion-Membranen

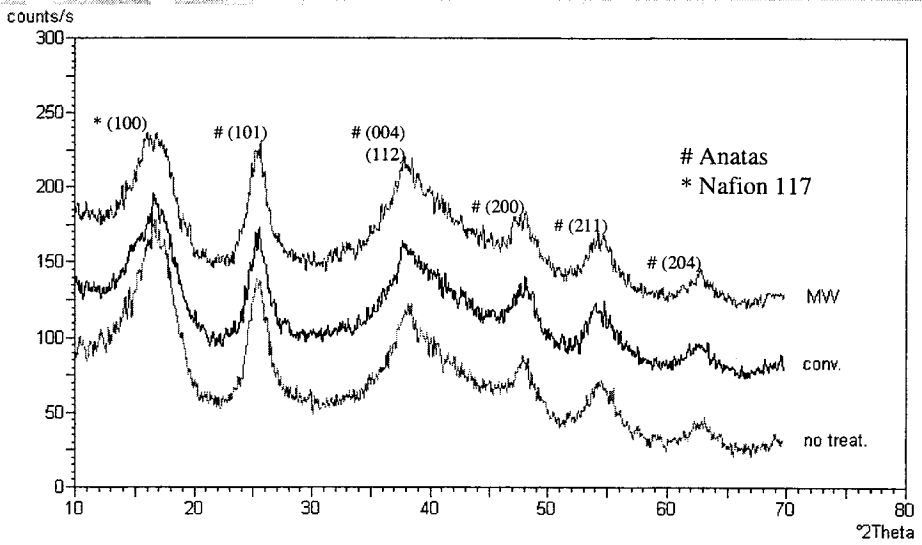

XRD: Hybridmembranen aus der Hydrolyse von $Ti(O\text{-}nBu)_4$ in Nafion ^{117} --> Anatas

Eigenschaften anorganisch-organischer Nafion-Membranen

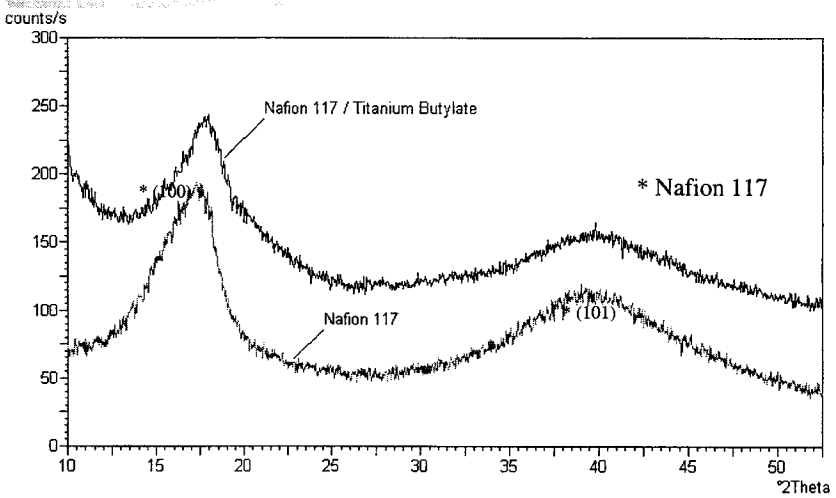

XRD: Hybridmembranen aus der Pyrolyse von $Ti(O\text{-}nBu)_4$ in Nafion ^{117} --> keine kristalline TiO_2-Phase

Eigenschaften anorganisch-organischer Nafion-Membranen

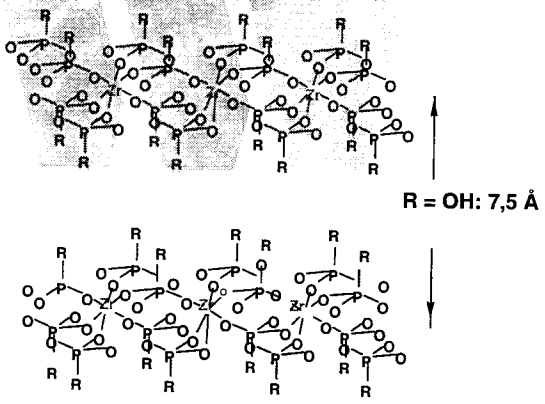

R = OH: 7,5 Å

R = OH, Alkyl- Arylsulfonate und Phosphonate

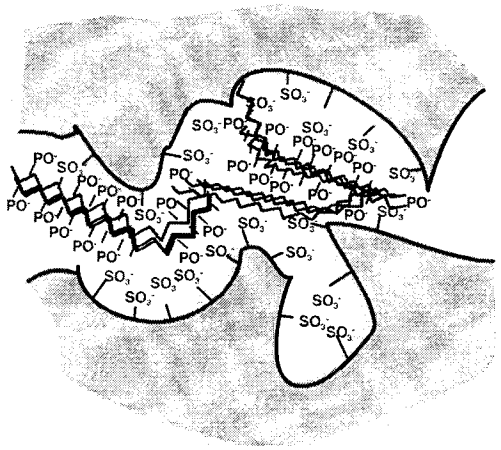

XRD: die Ausbildung des Schichtengitters hängt von der Größe der $Zr(HPO_4)_2$ -Bereiche ab!

Eigenschaften anorganisch-organischer Nafion-Membranen

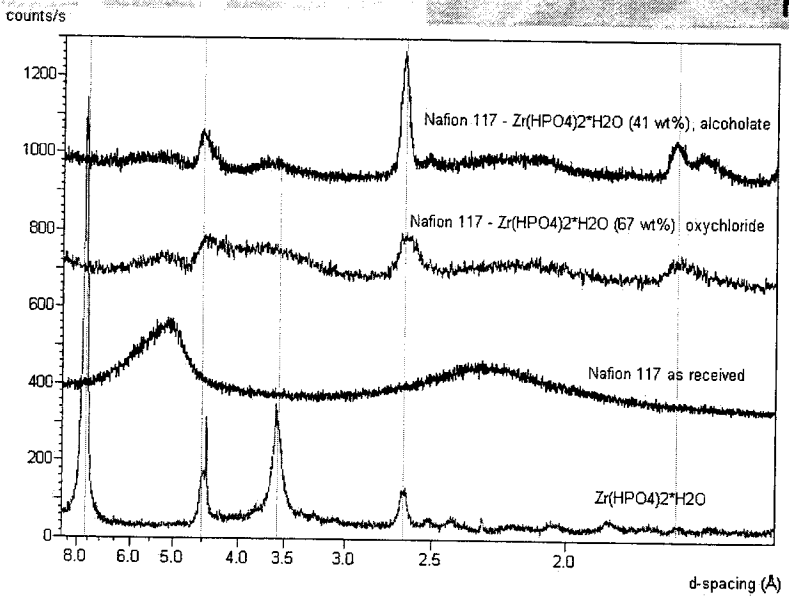

XRD: $Zr(HPO_4)_2$ Nafion^{117} - Hybridmembranen --> Exfoliated $Zr(HPO_4)_2$ Reflexe der Schichtsruktur fehlen! Keine kristalline ZrO_2-Restphase

XRD von $Zr(HPO_4)_2$ Nafion^{117} -Hybridmembranen aus organischer (Alkoholat) und anorganischer ($ZrOCl_2$) Route

Thermische Eigenschaften anorganisch-organischer Nafion-Membranen

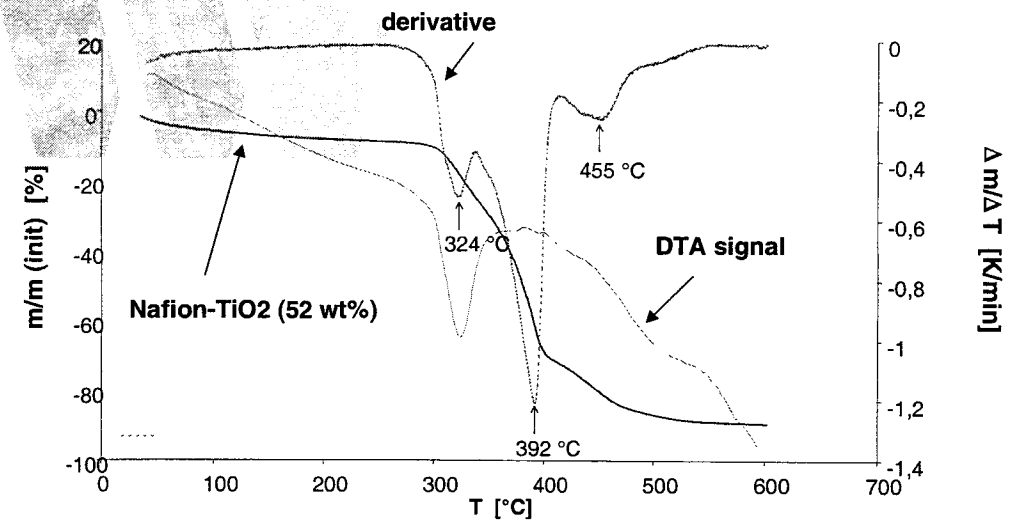

DTA-Untersuchung an Nafion^{117}-TiO_2 in Ar

Mechanische Eigenschaften anorganisch-organischer Nafion-Membranen

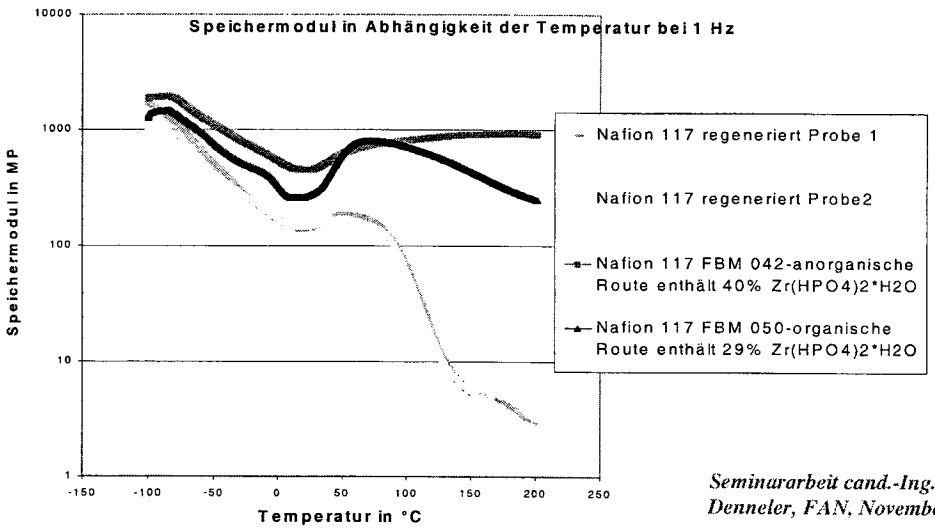

Seminararbeit cand.-Ing. Stefan Denneler, FAN, November 2002

Mechanische Impedanzspektroskopie (DMA): durch die anorganischen Einlagerungen verringert sich die Beweglichkeit des Nafion-Polymers erheblich

Mikrostruktur anorganisch-organischer Nafion-Membranen

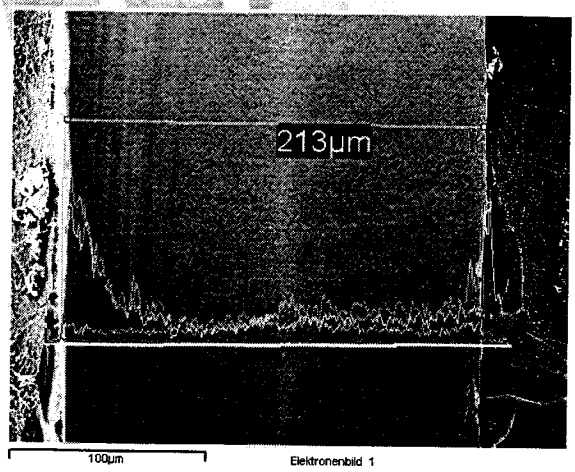

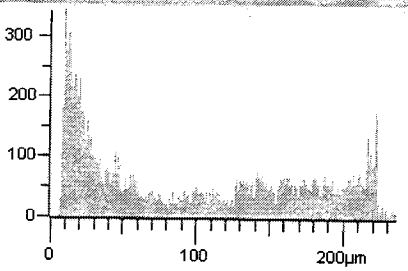

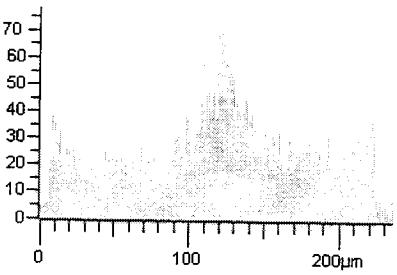

Cryo-REM-EDX: Querschnitt einer Hybridmembran
Hydrolyse von Ti-Butylat in Nafion

Eigenschaften anorganisch-organischer Nafion-Membranen

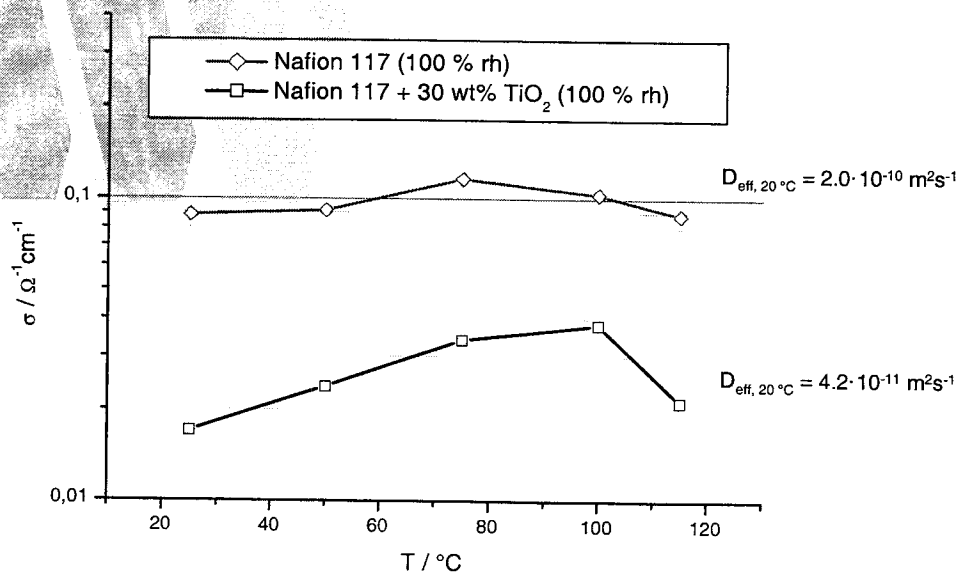

Elektrische Leitfähigkeit von Nafion 117 vs. TiO_2-Hybridmembran

Eigenschaften anorganisch-organischer Nafion-Membranen

Nafion 117 + 30 wt% TiO_2

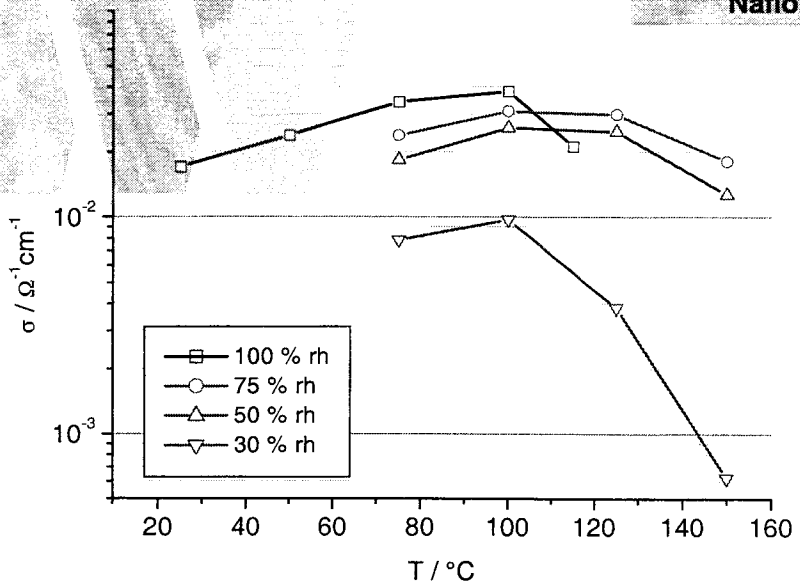

Elektrische Leitfähigkeit als Funktion der Befeuchtung

Eigenschaften anorganisch-organischer Nafion-Membranen

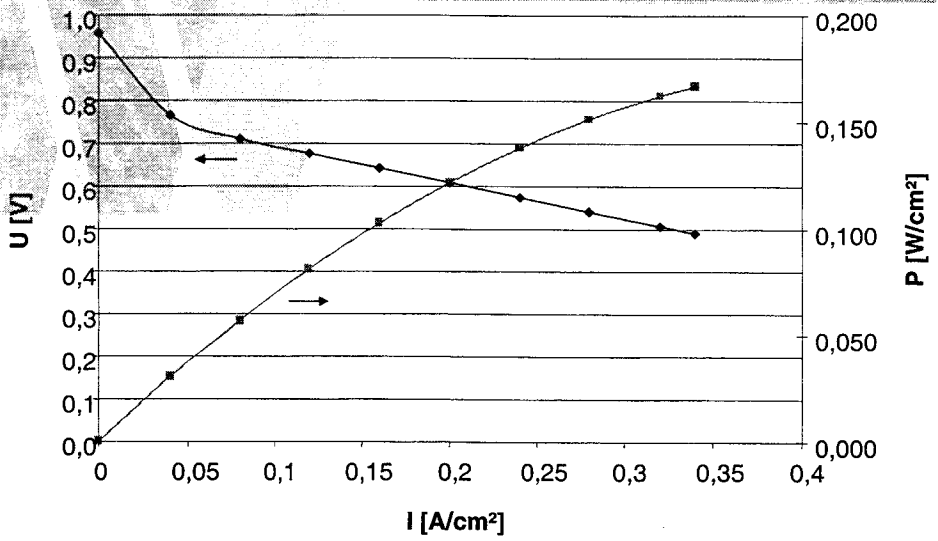

MEA-Messung, Einzel-Zelle H_2/Luft 84°C wasserdampfgesättigt)
Hybridmembran Nafion^{117} mit 10Gew% ZrO, 90 °C

Eigenschaften anorganisch-organischer Nafion-Membranen

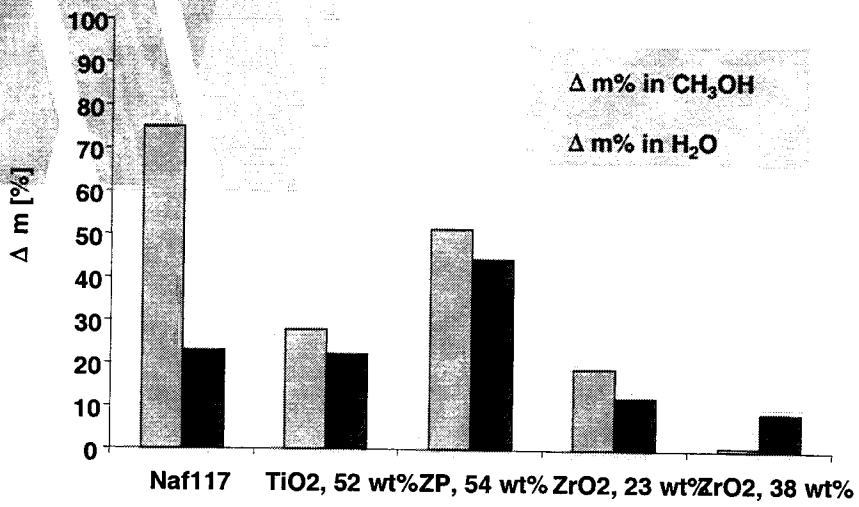

Quellverhalten und Gewichtzunahme unterschiedlich anorganisch dotierter Nafion-Membranen, 7 Tage, 25 °C

Ausblick anorganisch-organische Hybridmembranen aus Nafion-Basis

Die erforderliche Eigenschaftskombination kann mit einer Sorte Hybridmembran bisher nicht gewährleistet werden. Ein geringes Methanol-Aufnahmevermögen ist in der Regel gekoppelt an eine zu starke Abnahme der Ionenleitfähigkeit.

Die thermische Stabilität und die mechanischen Eigenschaften können mit ausreichender Genauigkeit eingestellt werden.

Zukünftig sollten daher 3D-Membranstrukturen erprobt werden, bei denen eine teilweise räumliche Trennung der Funktionen erfolgen könnte, so dass der Membranverbund die geforderten Eigenschaftskombinationen liefert.

Ausblick: 3D-strukturierte anorganisch-organische Nafion-Membranen

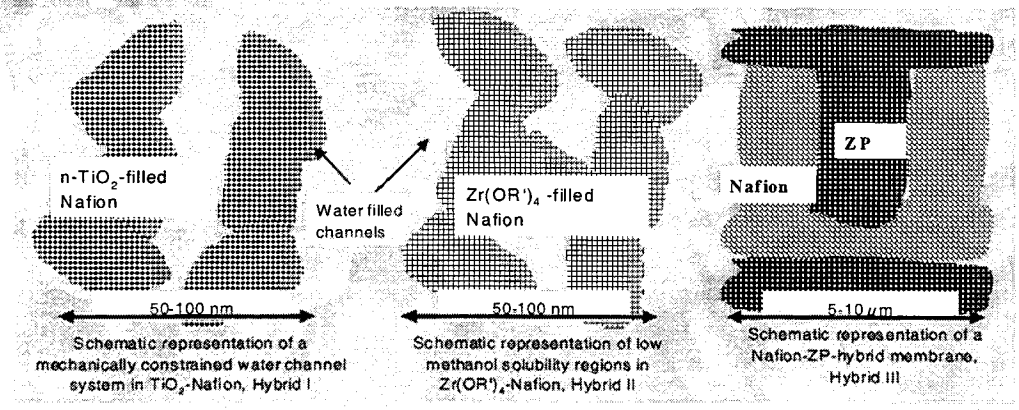

Schematic representation of a mechanically constrained water channel system in TiO_2-Nafion, Hybrid I

Schematic representation of low methanol solubility regions in $Zr(OR')_4$-Nafion, Hybrid II

Schematic representation of a Nafion-ZP-hybrid membrane, Hybrid III

Molekulare Aspekte des Proton-Transports in Polymer-Elektrolyt-Membranen

Michael Eikerling, TU München

72. AGEF-Seminar

Forschungszentrum Jülich, 4. Dez. 2002

Materials Science Division,
Los Alamos National Laboratory, MST 11

Tom Zawodzinski (Case Western)

Stephen Paddison (Motorola)

Lawrence Pratt, LANL, T12

Proton-Transport in PEM

Überblick – Aspekte der PEM-Funktion

Säure-Hydratation und -Dissoziation

Proton-Transport in einem Monohydrat-FK

Überblick – Aspekte der Funktion von PEM

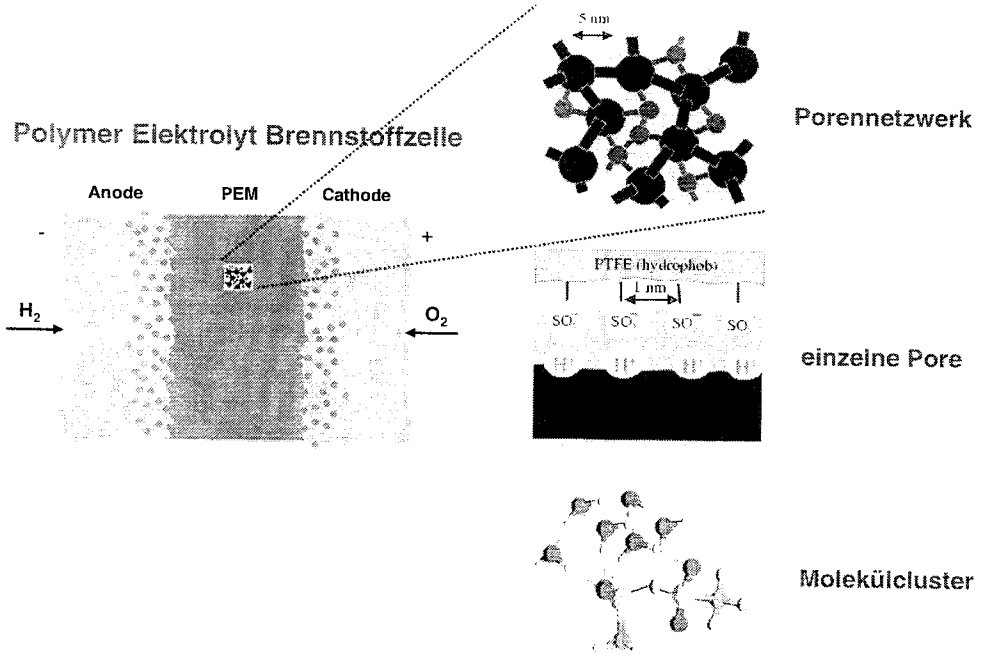

Relevante Prozesse – Geeignete Modellsysteme

Hydratation und Dissoziation (mobile Protonen/fixierte Anionen)	Säure/Wasser-Molekülcluster, DFT
Konzentration und Verteilung hydratisierter Protonen in Pore (Einfluss der Anionen)	Poisson-Boltzmann-Gl., Statistische Mechanik, MD
Proton-Mobilität in unterschiedlichen Umgebungen (wässrig/nichtwässrig)	Proton-Transfer in Wasser, Pore, Monohydrat-FK, Theorie, MD, AIMD
Pfade des Proton- und Wasser-Transports, Phasenseparation, Anschwellverhalten	Netzwerkmodelle, Perkolationstheorie, Evolution des Porenraums

Leistungscharakteristik in Brennstoffzelle

Proton-Transport in einer Pore

Porenvolumen (bulk)

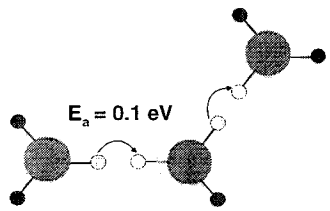

hohe Mobilität – niedrige Konzentration

Strukturdiffusion („Grotthuss", „Relais")

$(H_5O_4^+ \leftrightarrow H_5O_2^+)$-Fluktuationen

H^+-Transfer entlang H-Brückenbindung

Rotation

Porenoberfläche

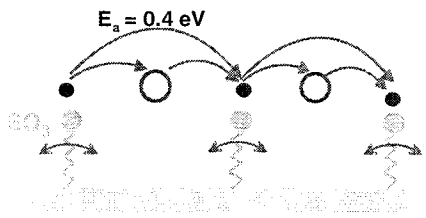

hohe Konzentration – geringe Mobilität

Mechanismus?

Einfluss der Anionen

Flexibilität der Seitenketten

Polarisation, Grenzflächen

Oberfläche – Bulk: **nützliches Konzept in Transportmodellen**

Protonen-Leitfähigkeit in Nafion und anderen PEM

Abhängigkeit der Leitfähigkeit vom Wassergehalt

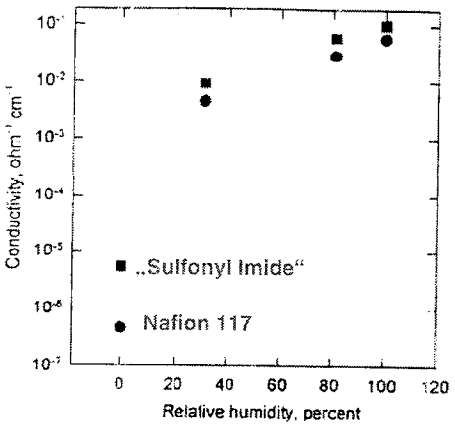

J. J. Sumner et al.,
J. Electrochem. Soc. **145**, 1, 107, 1998.

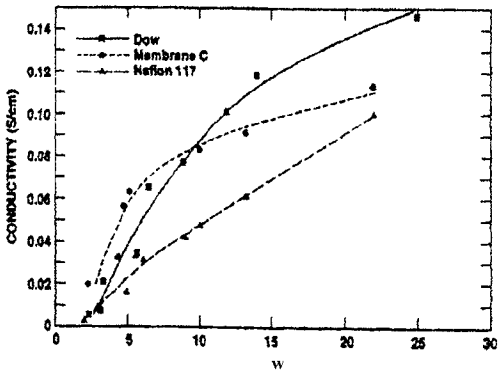

S. Gottesfeld and T.A. Zawodzinski Jr.,
In Adv. Electrochem. Sci. Eng., Vol. 5,
Eds. R.C. Alkire et al., VCH, Weinheim, 195, 1997.

Molekulare Struktur (kleine w) & Wasserverteilung (große w)

Struktur von Nafion und „Sulfonyl-Imide-Ionomer"

$$\begin{array}{l} -(CF_2CF)-(CF_2CF_2)_n- \\ \quad\quad | \\ \quad O(CF_2CFO)_xCF_2CF_2-Y \\ \quad\quad\quad | \\ \quad\quad\quad CF_3 \end{array}$$

Nafion® 117: $Y = -SO_3H$ **(n = 6.6)**

„Sulfonyl Imide": $Y = -SO_2NHSO_2CF_3$ **(n = 5.1)**

„Bis(trifluoromethanesulfonyl) Imide": $(CF_3SO_2)_2NH$

- **eine der stärksten Säuren**
- **zwei unabhängige Seiten für strukturelle Modifikation**
- **exzellente thermische Stabilität**

J. J. Sumner et al.,
J. Electrochem. Soc. **145**, 1, 107, 1998.

Modellierung molekularer Eigenschaften

Verständnis – auf molekularer Ebene – der Hydratation und Dissoziation funktioneller Monomer-Einheiten für „Sulfonyl-Imide-Ionomer"

$CF_3SO_2 - NH - R\ (H_2O)_n$, $R = CF_3SO_2, CH_3SO_2$, $n = 1 - 6$

M. Eikerling, S.J. Paddison, and T.A. Zawodzinski Jr.,
J. New Mat. Electrochem. Sys. 5, 1, 2002.

Methode: Standard *ab-initio* Molekülorbital-Berechnungen (GAUSSIAN 98)

(6-31G(d,p) split valence basis set, HF and B3LYP)

M. J. Frisch et al., Gaussian 98 (Rev. A.1), Gaussian Inc., Pittsburgh, PA, 1998

Hydratation und Dissoziation der Imide

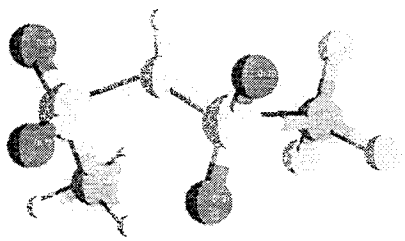

Optimierte Geometrien + Energien (B3LYP)

Struktur des hydratisierten Hydronium-Ions

Dissoziationsenergie: $\Delta E_d = E_{diss} - E_{undiss}$

Bindungsenergie:

$$\Delta E_b = E\left[\mathrm{Imide}(H_2O)_n\right] - E\left[H_2O\right] - E\left[\mathrm{Imide}(H_2O)_{n-1}\right]$$

Veränderung der freien Energie: ΔG^0

Vergleich mit „Triflic Acid" ($CF_3SO_3H\ (H_20)_n$)

(S. J. Paddison et al., Fluid Phase Equilibria 150 –151, 235,1998)

Dissoziation des perfluorierten Imids

$(CF_3SO_2)_2NH$

nicht-dissoziiert **dissoziiert**

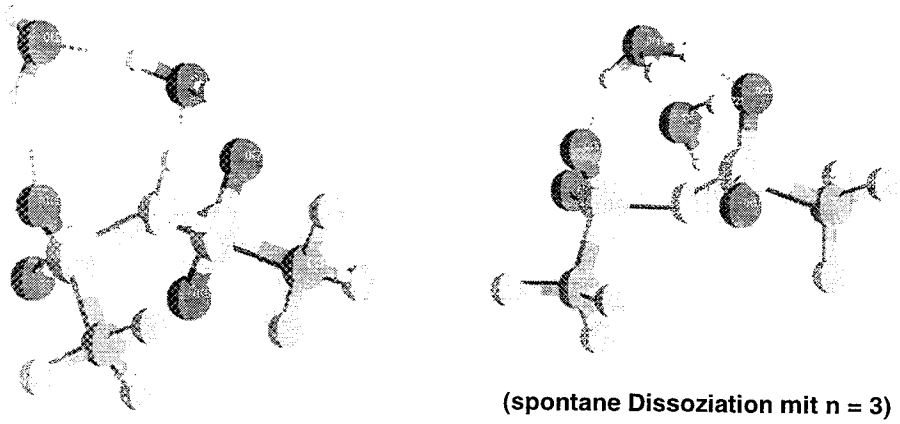

(spontane Dissoziation mit n = 3)

Dissoziierter Zustand ist energetisch günstiger mit 2 H_2O!

ΔE_d = - 0.7 kcal/mol

Dissoziation des teilweise fluorierten Imids

CF_3SO_2-NH-CH_3SO_2

nicht-dissoziiert **dissoziiert**

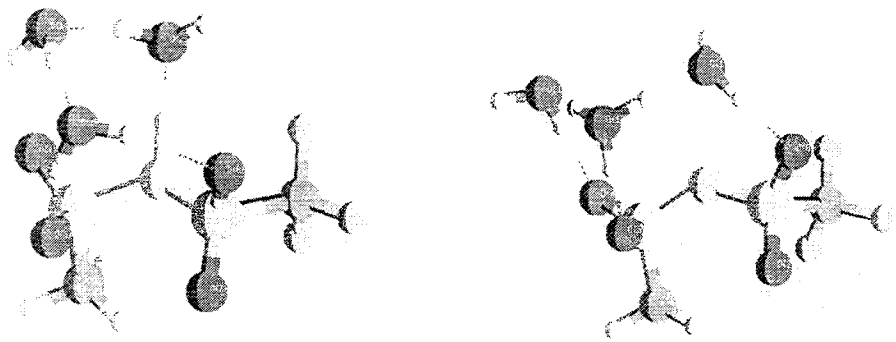

(spontane Dissoziation mit n = 6)

Dissoziierter Zustand ist energetisch günstiger mit 3 H_2O!

ΔE_d = - 1.4 kcal/mol

Cluster mit 4 Wassermolekülen

perfluoriert

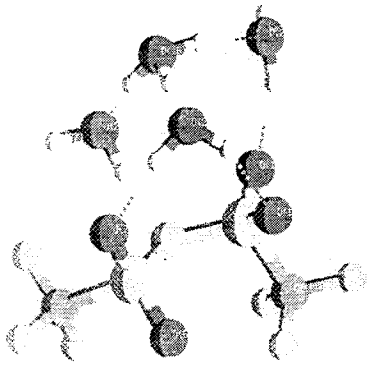

3.84 Å (O – N Abstand)

teilweise fluoriert

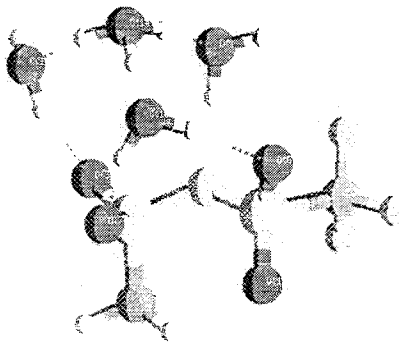

3.90 Å (O – N Abstand)

H_3O^+ bildet Eigen-Ion ($H_9O_4^+$) mit umgebenden Wassermolekülen

Delokalisierung der positiven Ladung (75% auf H_3O^+)

Vergleich verschiedener Säuregruppen

Imid (perfluoriert)

Dissoziation
mit n = 2

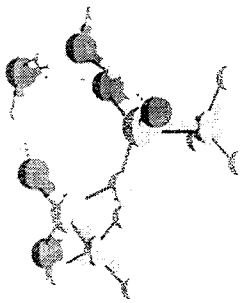

Ladungsseparation
mit n = 4

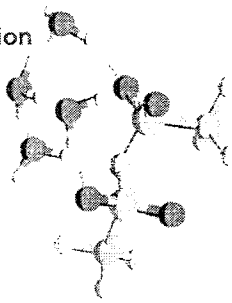

„Triflic acid"

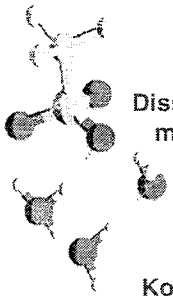

Dissoziation
mit n = 3

Kontaktionenpaar
für n < 6

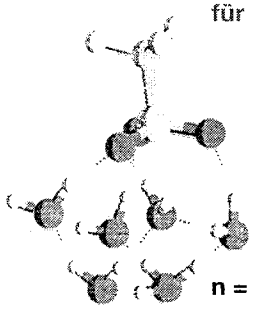

n = 6

Ladungsverteilung und -separation

Ladung auf Imiden/konj. Basen

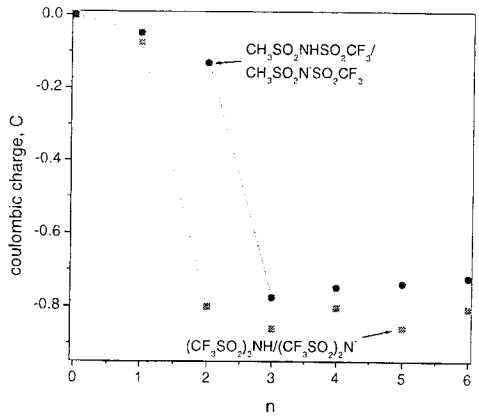

N – O-Abstand (konj. Base – H_3O^+)

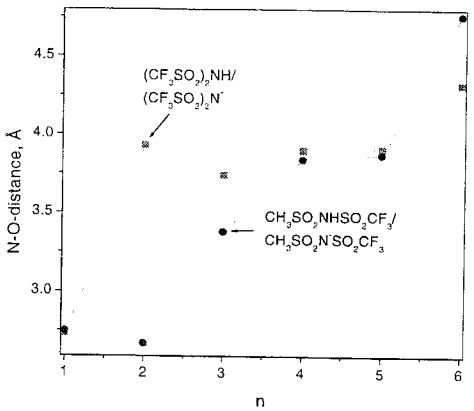

Wichtige Resultate

Imide besitzen stärkere Tendenz zur Dissoziation,
Dissoziation führt unmittelbar zu ladungsseparierter Konfiguration

H_3O^+ bildet Eigen-Ion ($H_9O_4^+$) für n > 3, Stabilisierung durch vielfache H-Brückenbindungen

Maximale Distanz des H_3O^+ zum Anion:
effektive Abschirmung **durch dazwischenliegende Wassermoleküle**

Delokalisierung **der negativen Ladung auf Anion (Effekt der Sauerstoffatome) stabilisiert die dissozierte Struktur**

Ionomer-Leitfähigkeit bei niedrigem Wassergehalt:
größere Mobilität **der Protonen für Sulfonyl-Imide-Ionomer im Vergleich zu Nafion**

Proton-Transport in „Triflic Acid" Monohydrat-FK

Mechanismus des PT in Wasser ist intensiv untersucht worden (*ab initio* MD): konzertierte Dynamik ("Grotthuss", structure diffusion)

Effekt der Anionengruppen in PEM ist ausgesprochen wichtig - sie liefern die Protonen und begünstigen/behindern deren Mobilität

Es ist unmöglich die konzertierte Dynamik des PT in PEM mit *ab initio* Methoden zu untersuchen

Perspektive der *initio* MD-Untersuchungen am TAM-Kristall: Identifizierung relevanter Übergangsstrukturen für PT in PEM

Experimentelle Charakterisierung ist möglich

„Triflic Acid" Monohydrat-Kristall

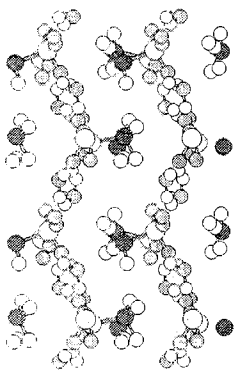

Algorithmus

A Ab initio MD
1. Quench
2. Thermalisierung (300 K), 4 ps (Δt = 1 fs)
3. mikrokan. Trajektorie, 10 ps (Δt = 0.2 fs)
4. Extract 5 uncorrelated conformations during final 2 ps in (3)

B Für die 5 Konformationen in (A.4):
1. Quench
2. Thermalisierung (300 K), 4 ps (Δt = 1 fs)
3. mikrokan. Trajektorie, 4 ps (Δt = 0.2 fs)

C Proton aus Einheitszelle entfernen (Defekt erzeugen)
Wiederholung der Schritte 1 - 3 in **B**

D Put the defect proton back (to acid site)
Wiederholung der Schritte 1 - 3 in **B**

M. Eikerling, S.J. Paddison, L.R. Pratt, and T.A. Zawodzinski, Chem. Phys. Lett., accepted.

‚Ab initio‘ Molekulardynamik

Universität Wien (G. Kresse)

DFT/GGA, plane wave basis, ultra-soft pseudo potential,
periodic boundary conditions, exchange correlation - PW91

Mammoth Linux Cluster,
Motorola, Los Alamos

Kristallstruktur ohne Defekt (A,B)

monoklinische Einheitszelle (4 x $CF_3SO_3^-$ H_3O^+)
(5.963 Å, 9.975 Å, 9.708 Å, b = 98.661º at 298 K)

Schmelzpunkt: 35° C, σ = 0.96281 Sm^{-1} (309.15 K)

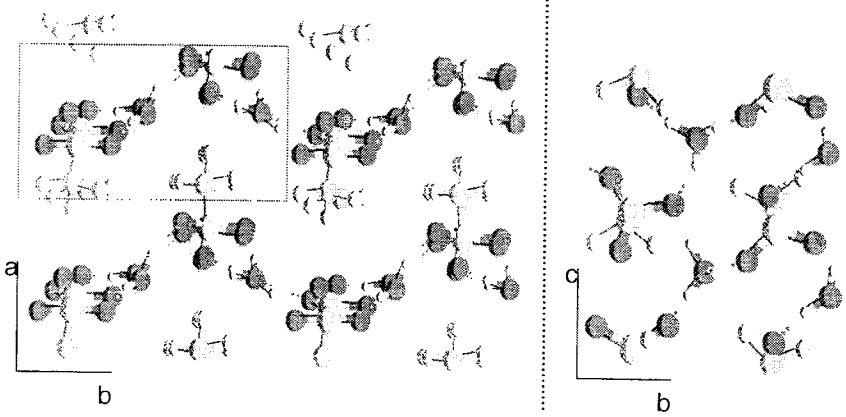

Stabil! Kurzzeitiger (~ fs) Transfer eines Protons entlang H-Brücke

Erzeugung des Proton-Defekts

Bildung eines Zundel-Ions

(3 mal beobachtet während 20 ps MD)

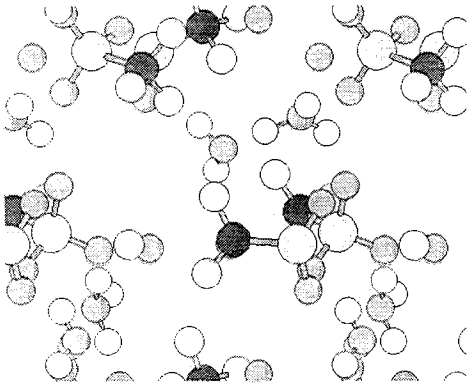

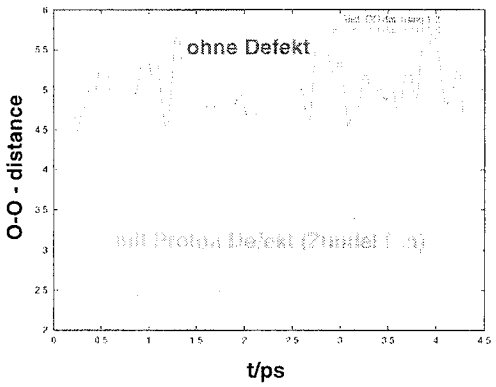

Zundel-Ion: Stabil, reduzierte Fluktuationen
(O-O – Abstand und O-H – Abstände),
delokalisiertes Proton

Defekt-Zustand – Delokalisierte Protonen (D)

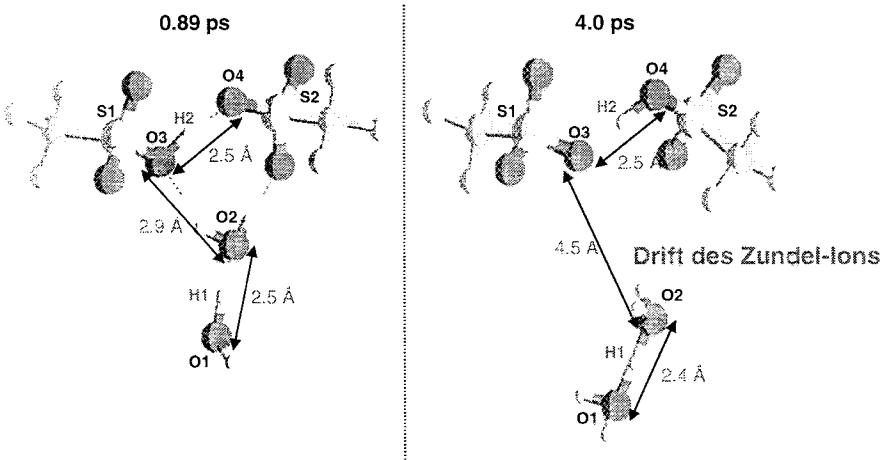

Delokalisierte Protonen: $H_5O_2^+$ (Zundel-Ion) **und** O3•••H2•••O4-Komplex

Korrelierte Dynamik im Defekt-Zustand

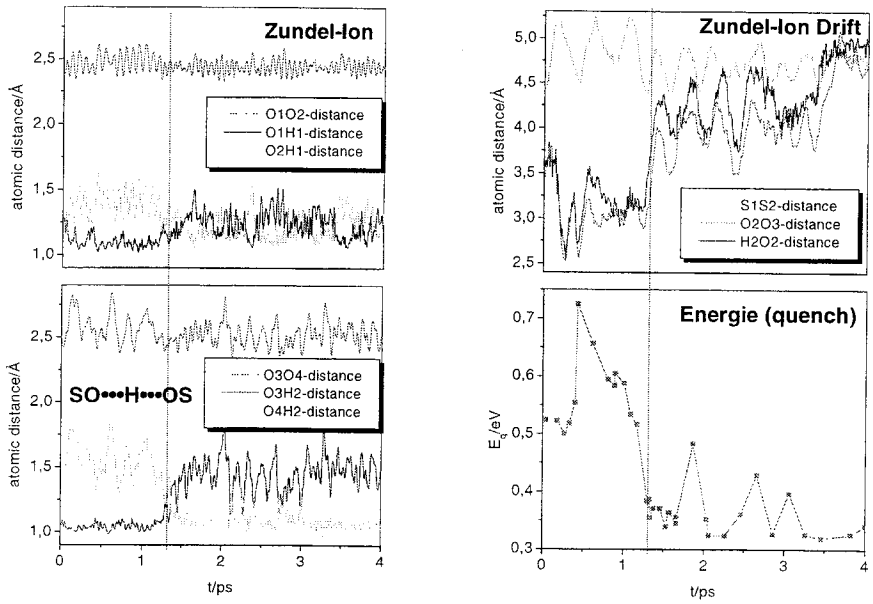

Energieschema

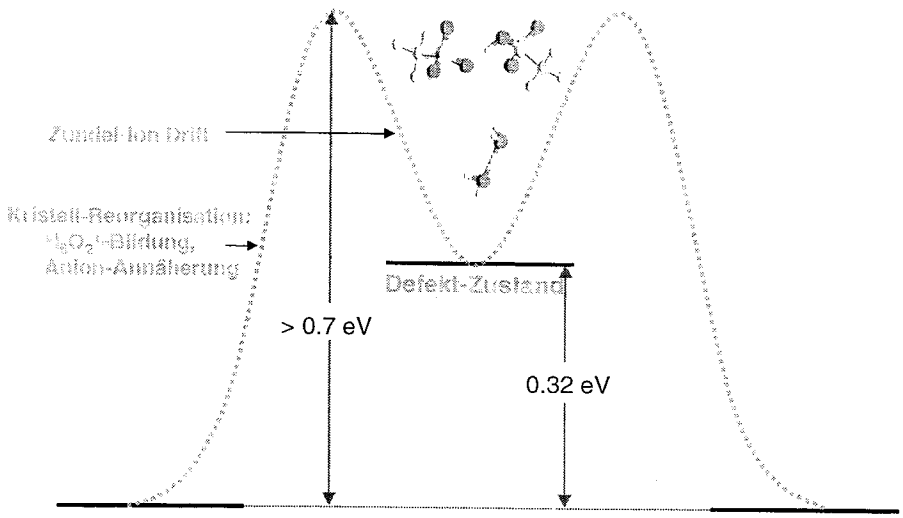

(Aktivierungsenergie von Nafion bei kleinem w: 0.3 – 0.4 eV, in TAM: ~ 0.3 eV)

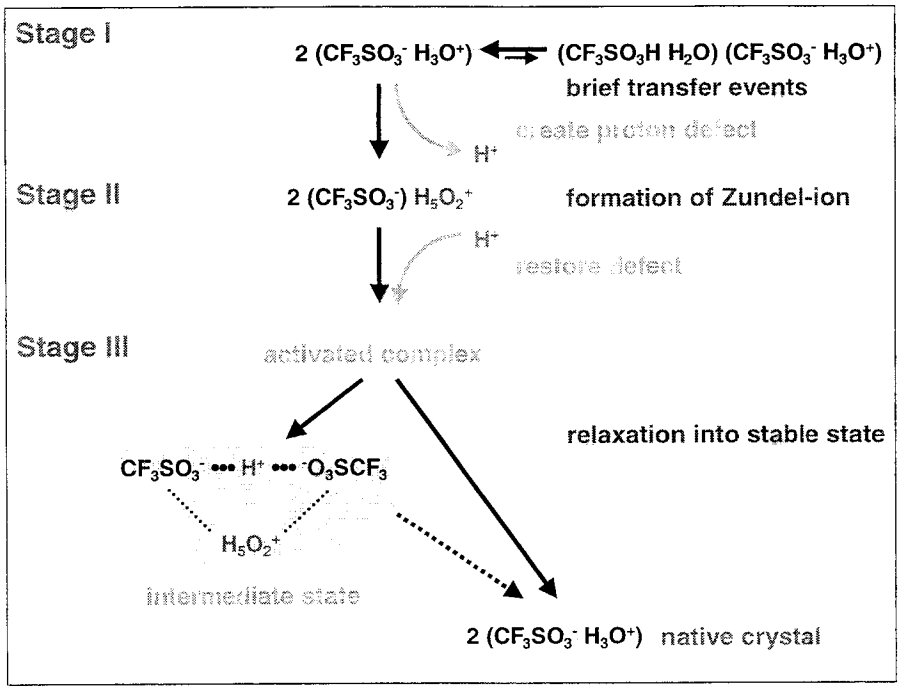

Protonen-Mobilität in Monohydrat-Kristall

PT erfordert Übergang zwischen einem stabilen Zustand mit lokalisierten Protonen und einem Defekt-Zustand mit zwei delokalisierten Protonen

Die zwei Proton-Komplexe stabilisieren den Defekt-Zustand (metastabil)

Beträchtliche Reorganisation der Kristallstruktur (stark korreliert):
Bildung eines Zundel-Ions, (SO – OS)-Annäherung, Rotation der SO_3-Gruppe

Drift des Zundel-Ions stabilisiert/destabilisiert den Defekt-Zustand und vermittelt effektiven Proton-Transport – als Relais-Gruppe zwischen

(1) Hydronium Ionen

(2) SO_3^--Anionen

Annäherung zwischen $H_5O_2^+$ und SO•••H•••OS destabilisiert Defekt-Zustand

Eigenschaften anorganisch-organischer Nafion-Membranen

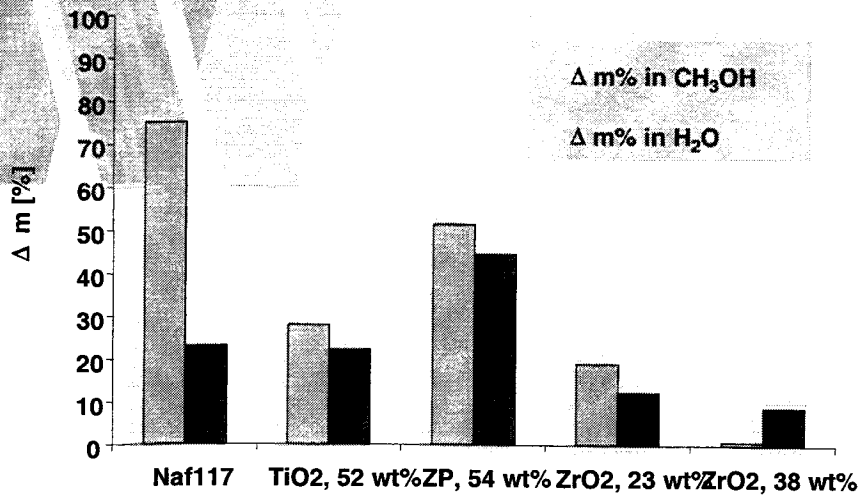

Quellverhalten und Gewichtzunahme unterschiedlich anorganisch dotierter Nafion-Membranen, 7 Tage, 25 °C

Ausblick anorganisch-organische Hybridmembranen aus Nafion-Basis

Die erforderliche Eigenschaftskombination kann mit einer Sorte Hybridmembran bisher nicht gewährleistet werden. Ein geringes Methanol-Aufnahmevermögen ist in der Regel gekoppelt an eine zu starke Abnahme der Ionenleitfähigkeit.

Die thermische Stabilität und die mechanischen Eigenschaften können mit ausreichender Genauigkeit eingestellt werden.

Zukünftig sollten daher 3D-Membranstrukturen erprobt werden, bei denen eine teilweise räumliche Trennung der Funktionen erfolgen könnte, so dass der Membranverbund die geforderten Eigenschaftskombinationen liefert.

Ausblick: 3D-strukturierte anorganisch-organische Nafion-Membranen

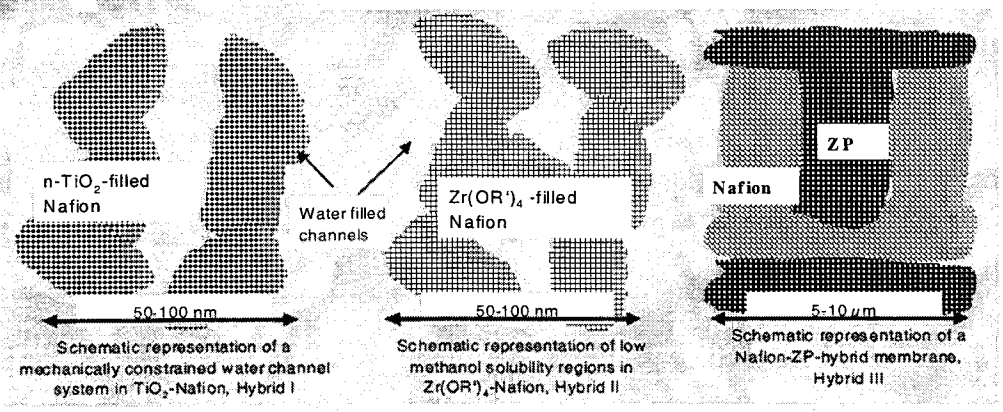

Schematic representation of a mechanically constrained water channel system in TiO_2-Nafion, Hybrid I

Schematic representation of low methanol solubility regions in $Zr(OR')_4$-Nafion, Hybrid II

Schematic representation of a Nafion-ZP-hybrid membrane, Hybrid III

Stofftransportprozesse in PEMs für die DMFC: Modellierung auf Basis des vollständigen Maxwell-Stefan Ansatzes

Thorsten Schultz[1] und Kai Sundmacher[1,2]

[1] Max-Planck-Institut für Dynamik komplexer technischer Systeme
Sandtorstraße 1, 39106 Magdeburg, Germany

[2] Lehrstuhl Systemverfahrenstechnik, Otto-von-Guericke-Universität
Universitätsplatz 2, 39106 Magdeburg, Germany

Outline

1 Different Approaches
2 Model based on Maxwell-Stefan Approach
3 Parametric Sensitivities
4 Experimental Results
5 Conclusions

Mass Transport Approaches for Polymer Electrolyte Membranes (PEM) I

Anode: $CH_3OH(l) + H_2O(l) \xrightarrow{PtRu} CO_2(g) + 6\,H^+ + 6\,e^-$

Cathode: $3/2\,O_2(g) + 6\,H^+ + 6\,e^- \xrightarrow{Pt} 3\,H_2O(l)$

Overall: $CH_3OH(l) + 3/2\,O_2(g) \longrightarrow CO_2(g) + 2\,H_2O(l)$

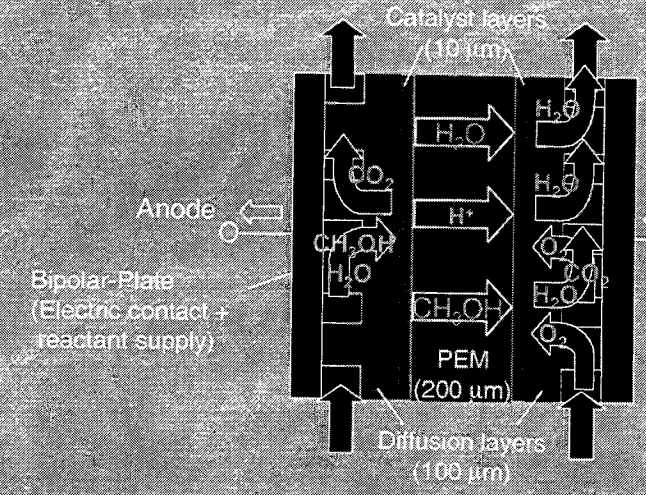

$T = 70 - 90\ ^\circ C$

$p = 0.1 - 0.3$ MPa

Mass Transport Approaches for Polymer Electrolyte Membranes (PEM) II

Structure of NAFION under DMFC conditions (similar for many other sulfonated polymers)

H_2O and CH_3OH supplied

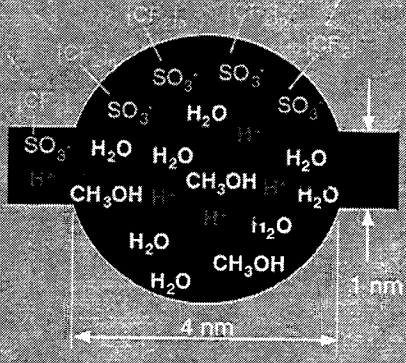

H_2O produced, CH_3OH consumed

H^+ transport forced by electric field

H_2O and CH_3OH transport driven by diffusion, migration and pressure-driven flow

Transport mechanisms:

Mechanism	*Driving force*	*Directly influences*	*Indirectly influences*
Diffusion	Activity gradients	H^+, H_2O, CH_3OH	H^+, H_2O, CH_3OH
Migration	El. Potential gradient	H^+	H_2O, CH_3OH
Pressure-driven flow	Pressure gradient	H^+, H_2O, CH_3OH	H^+, H_2O, CH_3OH

Mass Transport Approaches for Polymer Electrolyte Membranes (PEM) III

MODEL	Advantages	Disadvantages
Fick	simple very few parameters	no convection only highly diluted systems diff. coeff. dep. on mixture composition
Nernst-Planck + Schlögl	all driving forces accounted for few parameters	only highly diluted systems all coeff. dep. on operating conditions
	all driving forces accounted for applicable to non-ideal systems diff. coeff. only weakly dependent on mixture composition	many parameters few data for parameters available
Momentum Balance	all driving forces accounted for flow field in pores accounted for realistic influence of pore size	2-dimensional simulation necessary continuum approach not valid in nanopores ! real pore geometry unknown
Molecular Dynamics	all driving forces accounted for params. indep. of operating conditions	large-scale simulation difficult formulation of species interactions not suitable for bigger system models

Outline

1 Different Approaches
2 Model based on Maxwell-Stefan Approach
3 Parametric Sensitivities
4 Experimental Results
5 Conclusions

Maxwell-Stefan Approach: Formulation

Dusty-fluid formulation of Maxwell-Stefan equations[1]:

$$\underbrace{\frac{c_i}{RT}\nabla_{T,p}\mu_i}_{\text{Chemical potential gradient}} - \underbrace{\frac{c_i}{RT}V_i\nabla p - \alpha_i' c_i \frac{B_0}{\eta D_{iM}}\nabla p}_{\text{Pressure gradient}} - \underbrace{c_i z_i \frac{F}{RT}\nabla\phi}_{\text{Electric potential gradient}} = \sum_{j\neq i}\frac{x_i N_j - x_j N_i}{D_{ij}^{\varepsilon}} + \frac{N_i}{D_{iM}^{\varepsilon}}$$

Our model: one-dimensional (coordinate z)
differences approach gradients
3 mobile species ($i = H^+, H_2O, CH_3OH$)

$$\gamma_i \frac{c_i}{c_T}\frac{\Delta(\gamma_i x_i)}{\Delta z} - \frac{c_i}{RT}V_i\frac{\Delta p}{\Delta z} - \alpha_i' c_i \frac{B_0}{\eta D_{iM}}\frac{\Delta p}{\Delta z} - c_i z_i \frac{F}{RT}\frac{\Delta\phi}{\Delta z} = \sum_{j\neq i}\frac{x_i N_j - x_j N_i}{D_{ij}^{\varepsilon}} + \frac{N_i}{D_{iM}^{\varepsilon}}$$

=> 3 linear equations with the unknowns: $N_{H_2O}, N_{CH_3OH}, \Delta\phi$

Faraday's law: $N_{H^+} = \frac{i_{cell}}{F}$ Concentrations: $c_i = c_{total}\, x_i, c_{total} \neq const.!$

In total ≥ 17 Parameters !

[1] Krishna, R.; Wesselingh, J.A. Chem. Eng. Sci. 52 No.6 (1997) 861-911

Maxwell-Stefan Approach: Parameters I

Membrane parameters:

Porosity/Void fraction: $\varepsilon \approx 0.4$ for well humidified NAFION [1]

Tortuosity: $\tau \approx \varepsilon^{-1.5}$ simplest, most often used form [1,2]

Permeability: $B_0 = \frac{d_{pores}^2}{32}$ Poiseuille flow for cylindrical pores [2]

Viscous selectivity factors: $\alpha_i' = \alpha_i + \sum_j \frac{D_{jM}^{\varepsilon}}{D_{ij}^{\varepsilon}}(\alpha_i - \alpha_j)$ acc. to [2]

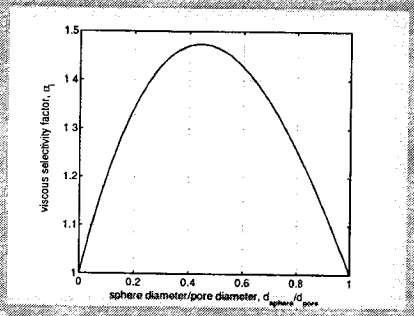

with [2]: $\alpha_i = f\left(\frac{d_i}{d_{pore}}\right)$

diameters from molar volumes: $d_i = \sqrt[3]{\frac{6\, V_i}{\pi\, N_A}}$

Problem: $V_{H^+} = ?$

First guess: $V_{H^+} = 3 \cdot V_{H_2O}$ solvate water !

[1] Wesselingh, J.A.; Vonk, P.; Kraaijeveld, G. Chem. Eng. J. 57 (1995) 75-89
Krishna, R.; Wesselingh, J.A. Chem. Eng. Sci. 52 No.6 (1997) 861-911

Maxwell-Stefan Approach: Parameters II

Estimation of Binary Diffusion Coefficients:

$$D_{ij}^{\varepsilon}(T) = D_{ij}^{\varepsilon}(T_0)\lambda_{H_2O}\exp\left[\frac{E_{ij}^{A}}{R}\left(\frac{1}{T}-\frac{1}{T_0}\right)\right] \quad \lambda_{H_2O} = \frac{x_{H_2O}}{x_{H_2O}+x_{M}}$$

for pairs: H^+ / H_2O [3], H^+ / M [3], H_2O / M [3], H^+ / CH_3OH, CH_3OH / M

$$D_{ij}^{\varepsilon} = \frac{\gamma}{\tau^2} D_{ij} \approx \varepsilon^{1.5} D_{ij}$$

for pair: CH_3OH/H_2O [4]

+ symmetry condition: $D_{ij}^{\varepsilon} = D_{ji}^{\varepsilon}$

[3] Wöhr, M. et al., Int. J. Hydrogen Energy 23 No.3 (1998) 213-218
[4] Wesselingh, J.A., Krishna, R., Mass transfer in multicomponent mixtures (2000) Delft University Press

Mass Transport Processes in PEMs for the DMFC: Model Formulation based on the complete Maxwell-Stefan Approach

Outline

1 Different Approaches
2 Model based on Maxwell-Stefan Approach
- Parametric Sensitivities
4 Experimental Results
5 Conclusions

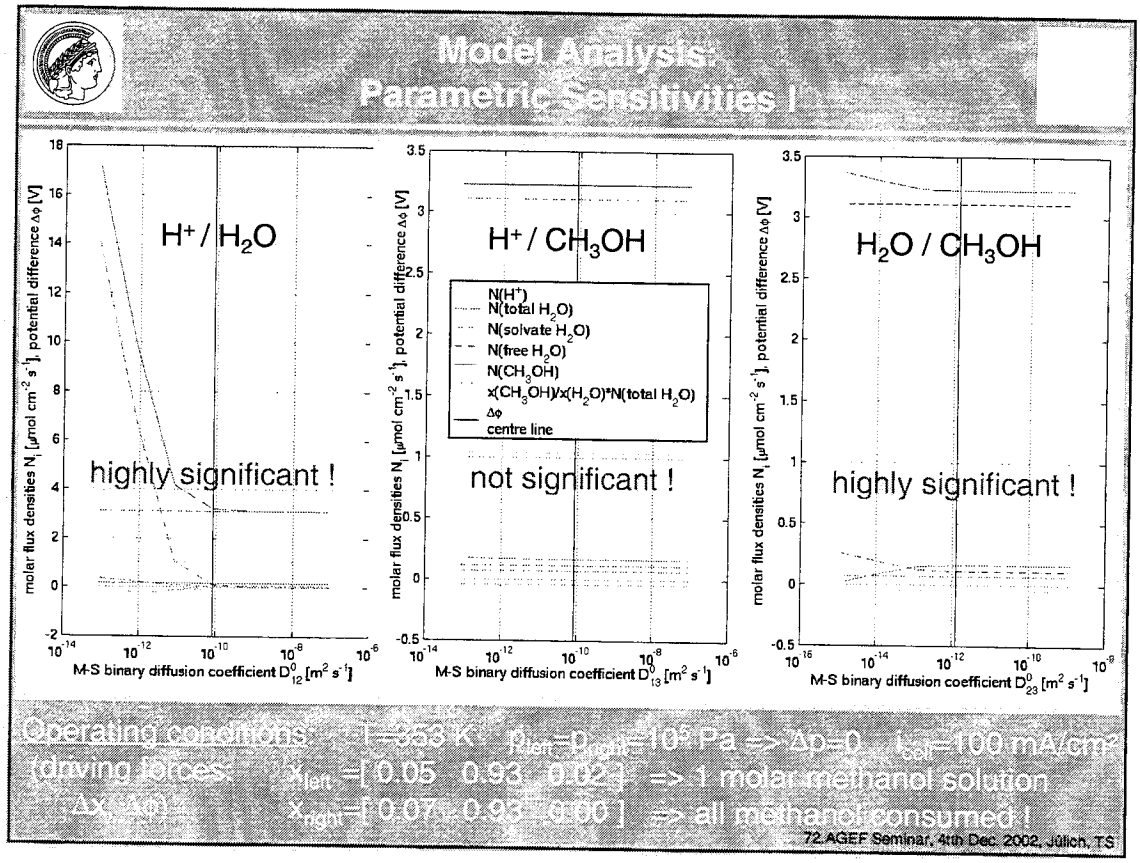
Model Analysis:
Parametric Sensitivities I
H+ / H2O
highly significant !
H+ / CH3OH
not significant !
H2O / CH3OH
highly significant !
N(H+)
N(total H2O)
N(solvate H2O)
N(free H2O)
N(CH3OH)
x(CH3OH)/x(H2O)*N(total H2O)
Δφ
centre line
molar flux densities Ni [μmol cm-2 s-1], potential difference Δφ [V]
M-S binary diffusion coefficient D0 12 [m2 s-1]
M-S binary diffusion coefficient D0 13 [m2 s-1]
M-S binary diffusion coefficient D0 23 [m2 s-1]
Operating conditions: T=363 K pleft=pright=10^5 Pa => Δp=0 icell=100 mA/cm²
(driving forces: Δxi, Δφ) xleft=[0.05 0.93 0.02] => 1 molar methanol solution
xright=[0.07 0.93 0.00] => all methanol consumed !
72.AGEF Seminar, 4th Dec. 2002, Jülich, TS

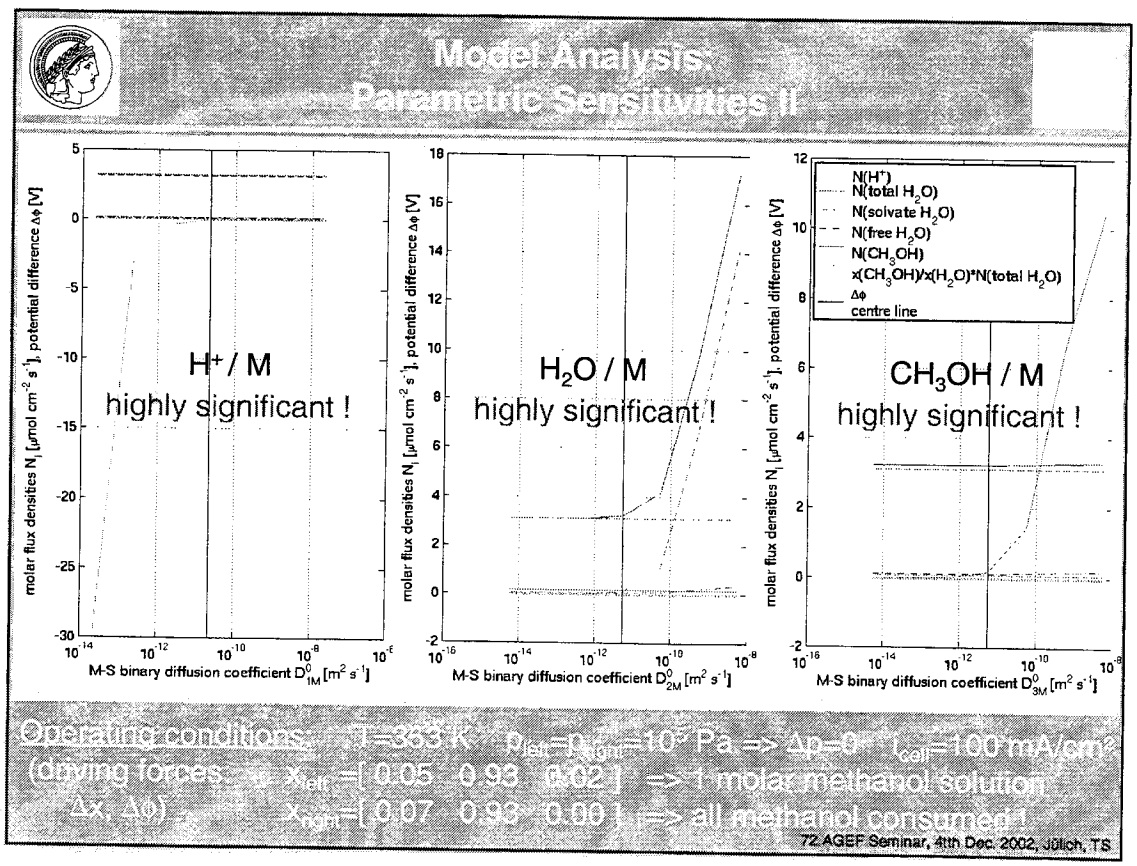
Model Analysis:
Parametric Sensitivities II
H+ / M
highly significant !
H2O / M
highly significant !
CH3OH / M
highly significant !
N(H+)
N(total H2O)
N(solvate H2O)
N(free H2O)
N(CH3OH)
x(CH3OH)/x(H2O)*N(total H2O)
Δφ
centre line
molar flux densities Ni [μmol cm-2 s-1], potential difference Δφ [V]
M-S binary diffusion coefficient D0 1M [m2 s-1]
M-S binary diffusion coefficient D0 2M [m2 s-1]
M-S binary diffusion coefficient D0 3M [m2 s-1]
Operating conditions: T=363 K pleft=pright=10^5 Pa => Δp=0 icell=100 mA/cm²
(driving forces: Δxi, Δφ) xleft=[0.05 0.93 0.02] => 1 molar methanol solution
xright=[0.07 0.93 0.00] => all methanol consumed !
72.AGEF Seminar, 4th Dec. 2002, Jülich, TS

Model Analysis: Parametric Sensitivities III

operating conditions			sensitivity w.r.t. binary diffusion coefficient					
$i_{cell}\neq 0$	$\Delta x\neq 0$	$\Delta p\neq 0$	H_2 – H_2O	H_2 – CH_3OH	H_2O – CH_3OH	H_2 – M	H_2O – M	CH_3OH – M
X			++	++	o	++	++	+
X	X		++	o	++	++	++	++
X	X	X	++	o	++	++	++	++

all 6 coefficients are significant !

Outline

1 Different Approaches
2 Model based on Maxwell-Stefan Approach
3 Parametric Sensitivities
4 Experimental Results
5 Conclusions

Experimental Results: Water and Methanol Fluxes through a DMFC I

DMFC Miniplant: Online mass balancing to observe fluxes through the fuel cell

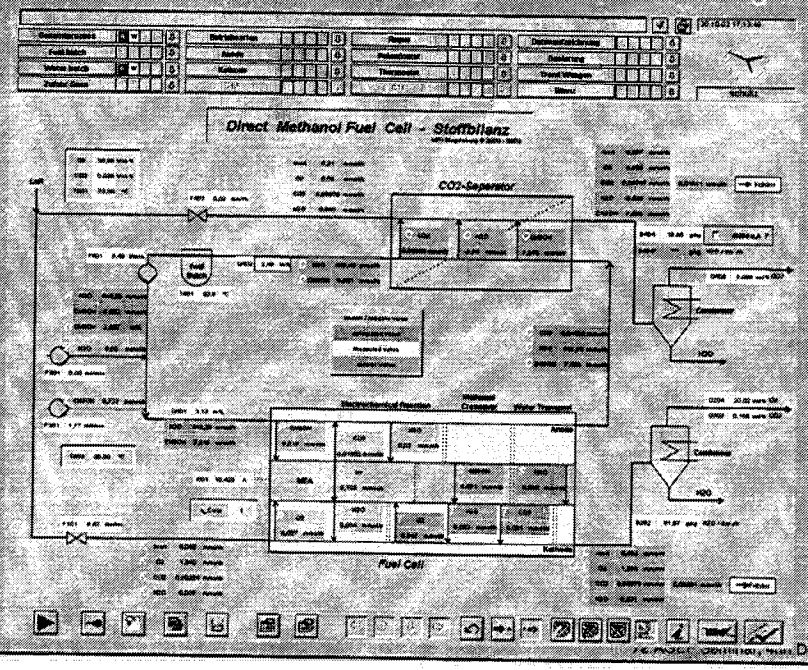

Dec. 2002, Jülich, TS

Experimental Results: Water and Methanol Fluxes through a DMFC II

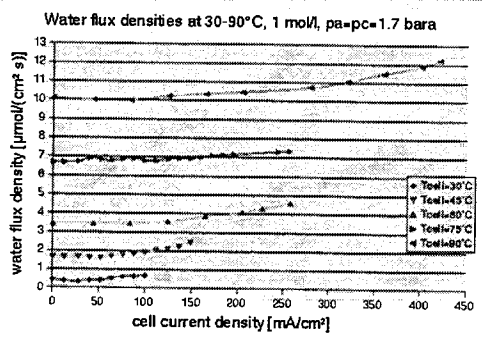

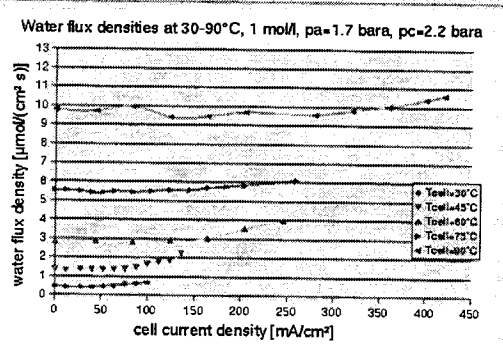

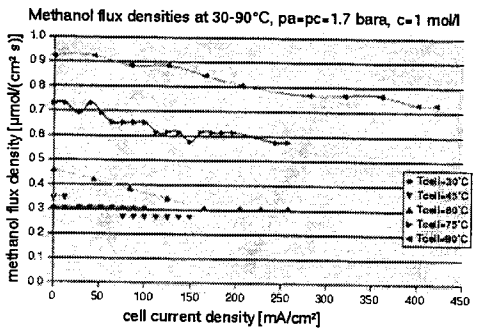

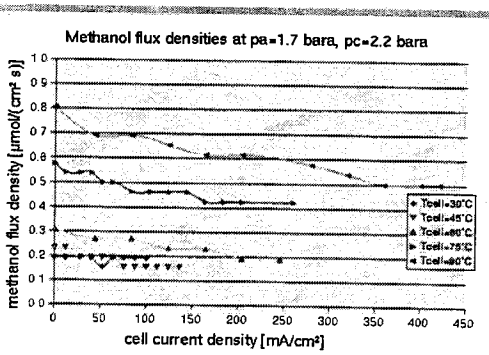

TS

Experimental Results: Water and Methanol Fluxes through a DMFC III

Water fluxes for different pressure differences (T=60°C, pa=1.7 bara)

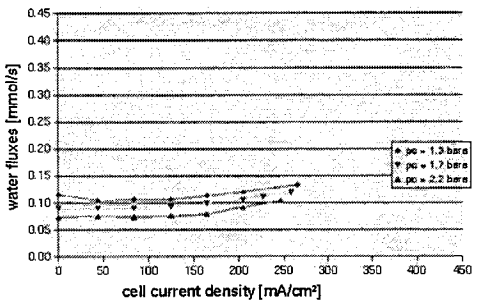

Water fluxes for different pressure differences (T=90°C, pa=1.7 bara)

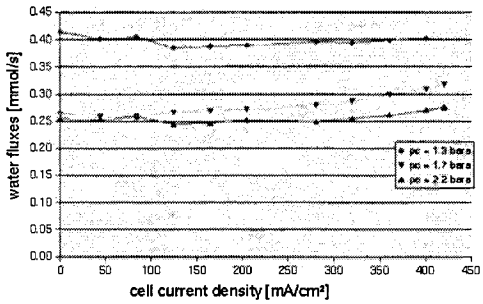

Methanol fluxes for diff. pressure differences (T=60°C, pa=1.7 bara)

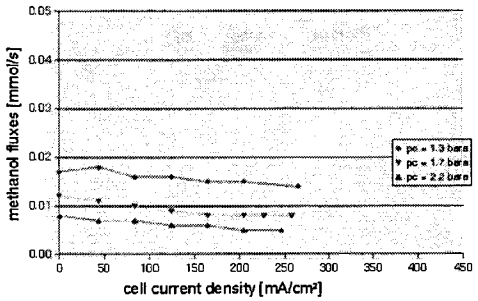

Methanol fluxes for diff. pressure differences (T=90°C, pa=1.7 bara)

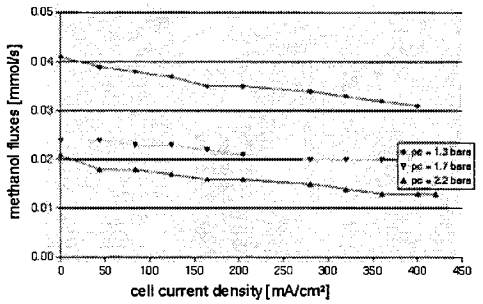

TS

Mass Transport Processes in PEMs for the DMFC: Model Formulation based on the complete Maxwell-Stefan Approach

5 Conclusions

+ M-S offers a very general engineering approach
+ easy to reduce by means of a systematic parameter sensitivity analysis
+ mathematically easy to handle (fast simulation results)
+ for the membrane parameters proven correlations available for many cases

- high number of parameters
- for polymer electrolyte membranes only few data exist for diffusion and activity coefficients
- all 6 binary diffusion coefficients are significant in DMFC
- open question: solvate water versus mobile water ?

Further/actual topics:

- get better parameters (correlations, fit to experimental data, etc.)
- find solution how to treat the protons
- implement M-S PEM model into whole DMFC model

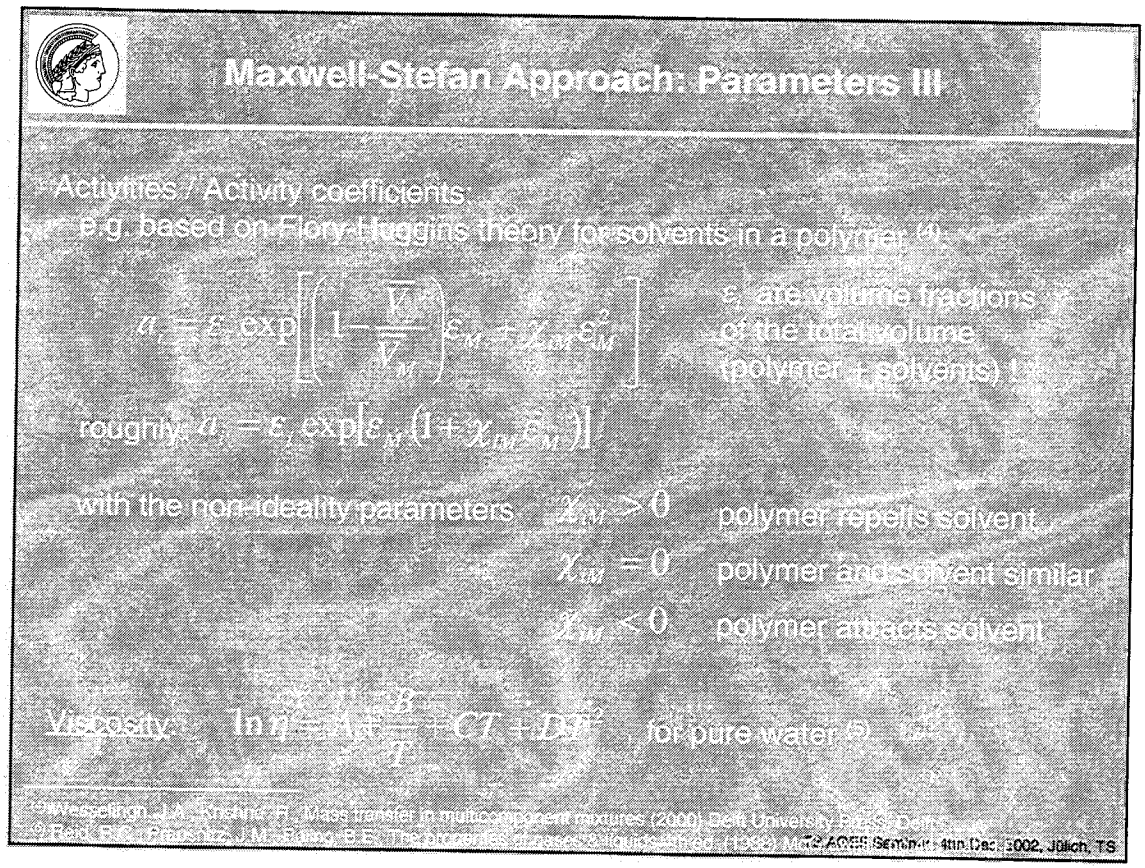
Maxwell-Stefan Approach: Parameters III
Activities / Activity coefficients
e.g. based on Flory-Huggins theory for solvents in a polymer [4]
$a_i = \varepsilon_i \exp\left[\left(1 - \frac{\overline{V}_i}{\overline{V}_M}\right)\varepsilon_M + \chi_{iM}\varepsilon_M^2\right]$
ε_i are volume fractions of the total volume (polymer + solvents) !
roughly $a_i = \varepsilon_i \exp\left[\varepsilon_M (1 + \chi_{iM}\varepsilon_M)\right]$
with the non-ideality parameters
$\chi_{iM} > 0$ polymer repells solvent
$\chi_{iM} = 0$ polymer and solvent similar
$\chi_{iM} < 0$ polymer attracts solvent
Viscosity $\ln \eta = A + \frac{B}{T} + CT + DT^2$ for pure water [5]
[4] Wesselingh, J.A., Krishna, R., Mass transfer in multicomponent mixtures (2000) Delft University Press, Delft
[5] Reid, R.C., Prausnitz, J.M., Poling, B.E., The properties of gases & liquids, 4th ed. (1987) McGraw-Hill, New York
MMT-AG III Seminar, 4th Dec. 2002, Jülich, TS

Proton Transport in Fuel Cell Membranes: Theory and MD Simulations

Eckhard Spohr

Institut für Werkstoffe und Verfahren der Energietechnik

IWV-3, Forschungszentrum Jülich

Motivation

Experiments

models

Results

Conclusions & Outlook

Proton Transfer in PEMs

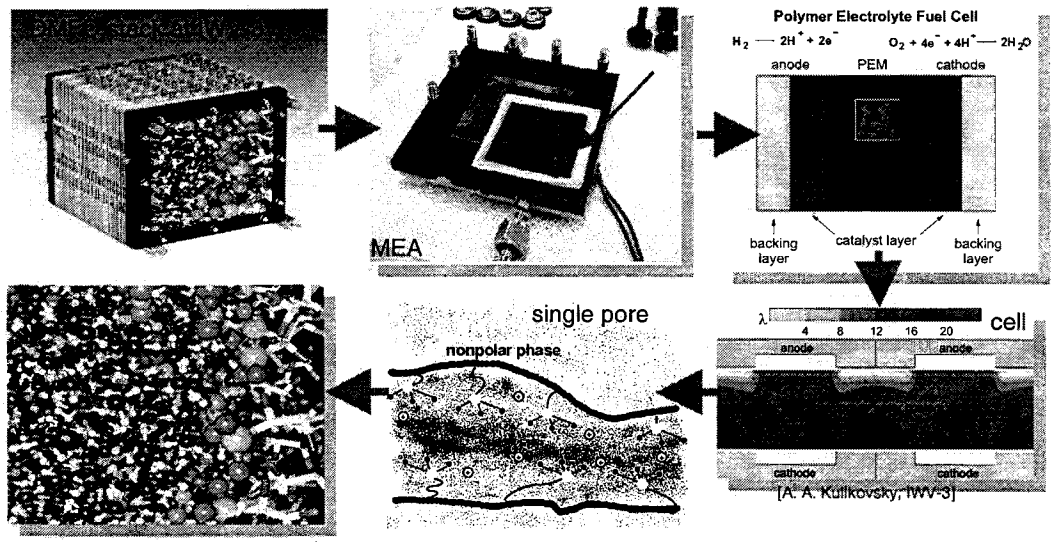

Proton Transfer in PEMs

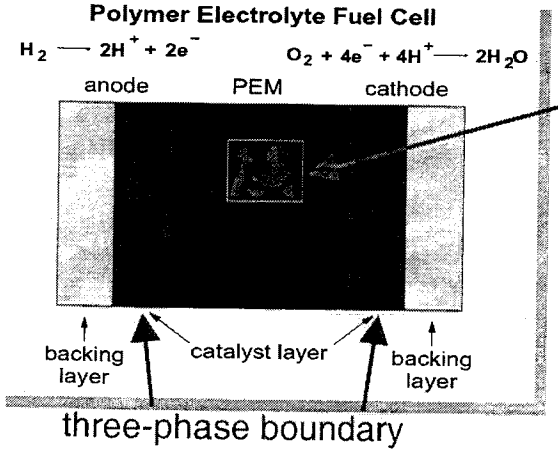

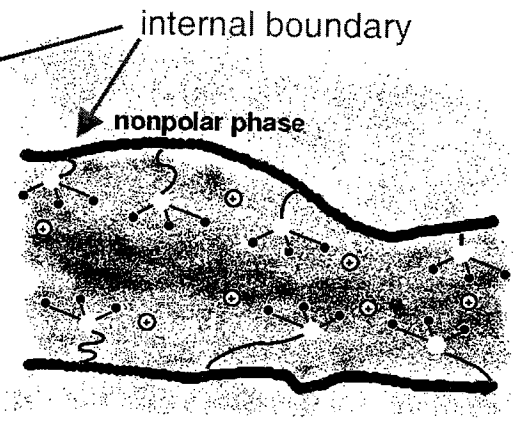

water content and proton mobility**along** internal boundaries (pore surfaces) determine proton conductance of the membrane ⟶ Cell Performance

Goals

modeling of proton conducting polymer electrolyte membranes (PEMs):

- transport mechanism
- structural and dynamic properties (environmental effects) which influence proton conductance
- calculate proton mobility
- as a function of operating parameters such as
  - temperature
  - water content
- Electro osmosis & methanol permeation

neutron scattering on Nafion

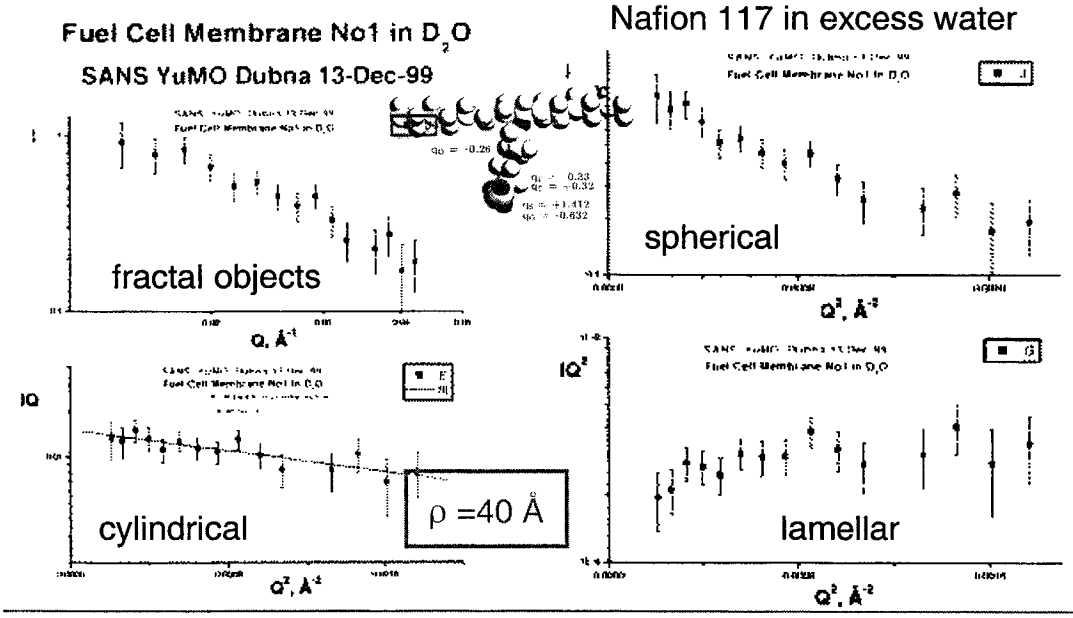

neutron scattering on Nafion

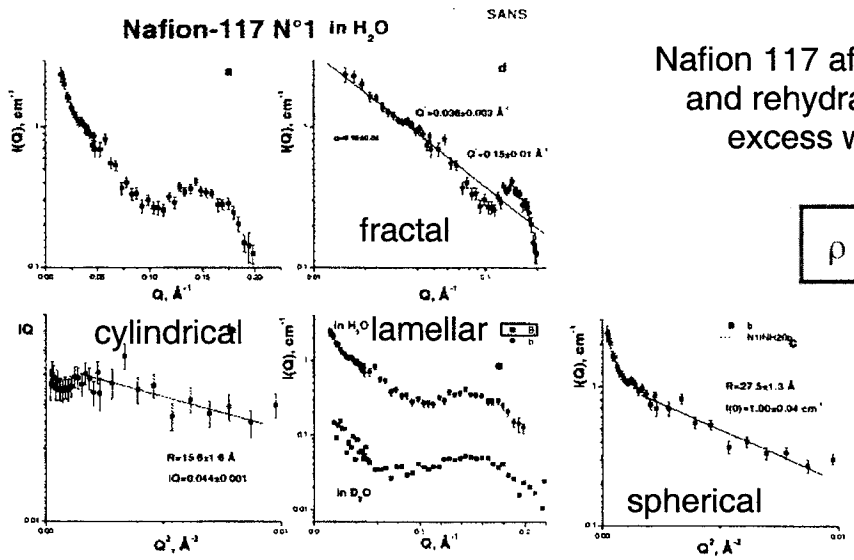

Nafion 117 after drying and rehydrating in excess water

ρ =16-19 Å

[V. I. Gordeliy et al., unpublished]

conductivity of Nafion membranes

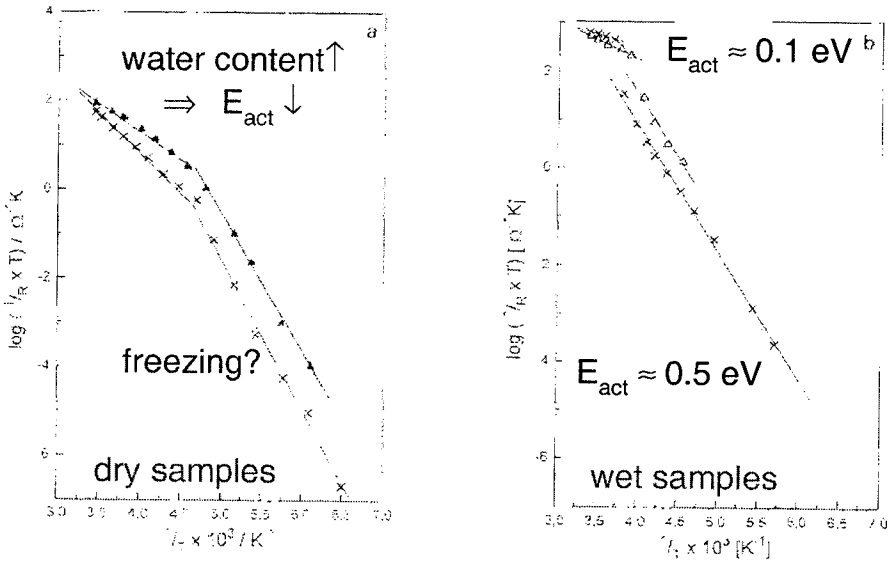

[M. Cappadonia et al., Solid State Ionics 77, 65 (1995)]

Possible Mechanisms

bulk

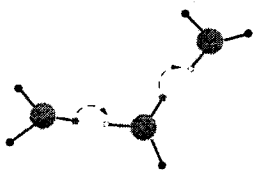

cheap activation
expensive protons

interface

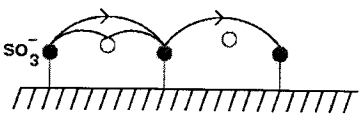

expensive activation
cheap protons

headgroup assisted

Theory: Poisson Boltzmann (PB)

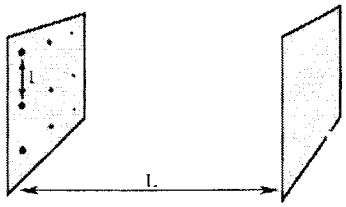

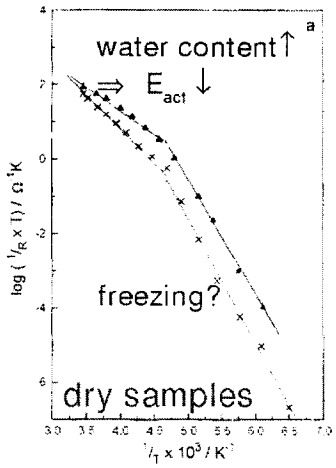

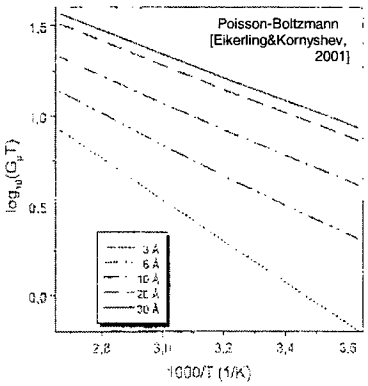

MD Simulations: Challenges

- Nafion membrane in operating fuel cell:
  $\lambda = n_{water} / n_{proton} \approx 20 \Rightarrow$ Model for high concentration
- large systems: 10^4 - 10^5 molecules
- dynamics on time scale ≥ 1 ns
- proton mobility approaches that of bulk water at high water content
  $\Rightarrow$ implementation of 'nonclassical' Grotthus transport

$\Delta x_H \approx 0.4$ Å $\Delta x_+ \approx 2.4$ Å

Car-Parrinello-MD $\leftrightarrow$ empirical valence bond modles

- proton transport assumed adiabatic $\Rightarrow$ classical mechanics
- no background electrolyte $\leftrightarrow$ mean field theory
  (protons are sole free charge carriers)

2-state Empirical valence bond (EVB) model

- Protons are bound to 1 or 2 water molecules:
  Eigen cation $H_3O^+(H_2O)_3$ $\leftrightarrow$ Zundel ion $H_5O_2^+$
- Approximation: proton can be delocalized at most between 2 water molecules
- (adiabatic) state of proton is a superposition of two diabatic basis states

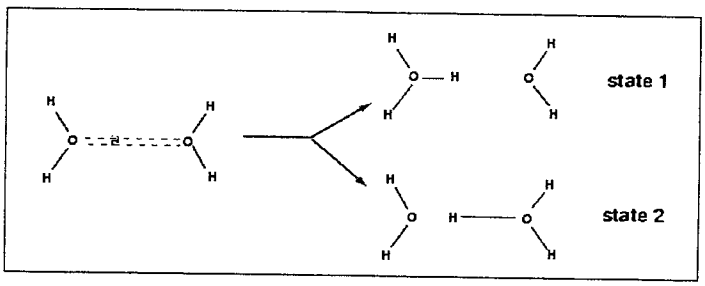

2-state Empirical valence bond (EVB) model

- Energy $E = \{ E_1 + E_2) - [E_1^2 + E_2^2 + 4 V_{12}^2]^{1/2} \} / 2$ and nature of (adiabatic) proton state changes continuously

- implements Zundel proton transfer mechanism
  → reactive, chemical model
- membrane materials differ in
  acidity
  equivalent weight (pore surface charge density)

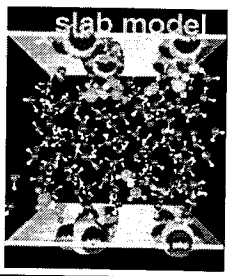

Acid Strength
Models of stationary counter charges

- point charges (q=-e)

- partially charged sulfonate

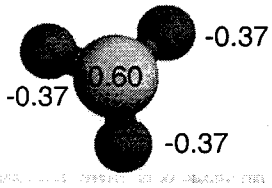

- sulfonate anions

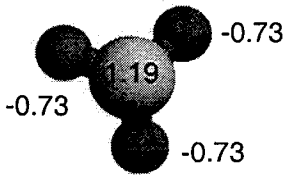

- side chains with partial charges

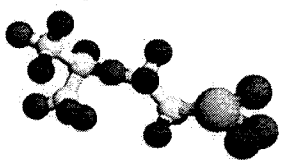

Pore geometry

- pore shape and size varies and depends on pretreatment

⇓

- planar 'slab' pores
- cylinder
- overlapping spheres
- self-organizing

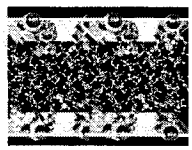

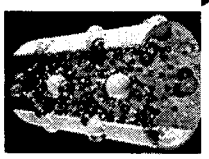

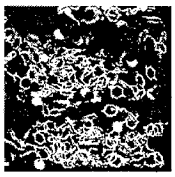

Model: Summary

membrane	⇒ single pore
polymer backbone	⇒ geometric confinement
side chain: mobility, electronic Structure	⇒ mobile / stationary charge, charge distributions
conductivity	⇒ proton diffusion (mobility)
quantum mechanics	⇒ classical mechanics
Grotthus mechanism	⇒ EVB model

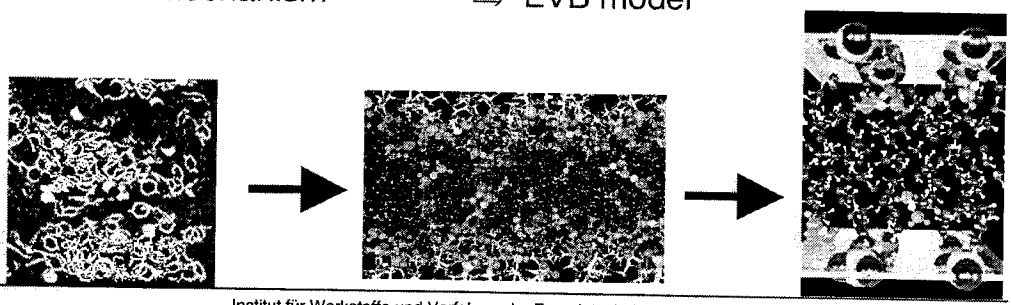

Diffusion Coefficients (300 K)

$$D = \lim_{t\to\infty} \langle [\vec{r}_i(t'+t) - \vec{r}_i(t)]^2 \rangle_{t',i} \,/\, 2ft$$

n_w/n_p	$D/\ 10^{-5}cm^2s^{-1}$	mobile	Model
27:1	0.06(±0.1)	–	point charges
14:1	0.06(±0.1)	–	point charges
27:1	2.4(±0.2)	–	SO_3^- head groups
14:1	0.6(±0.1)	–	SO_3^- head groups
27:1	3.6(±0.3)	+	mobile SO_3^- head groups
14:1	2.4(±0.2)	+	mobile SO_3^- head groups
38:1	4.6(±0.2)	+	flexible molecular sidechains
19:1	3.2(±0.2)	+	flexible molecular sidechains
14:1	1.9(±0.2)	+	flexible molecular sidechains
14:1	0.6(±0.1)	–	SO_3^- head groups
14:1	1.9(±0.2)	–	SO_3^-: partial charges × 0.5

S-H pair correlations

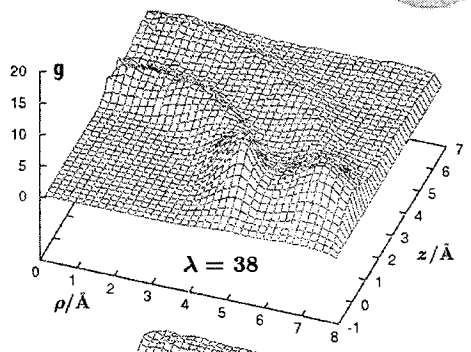

Proton densities

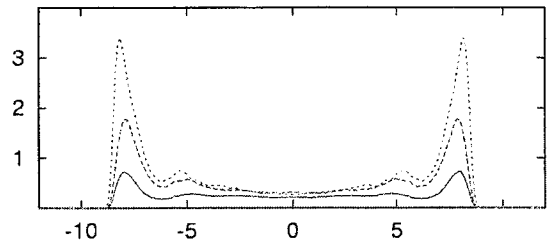

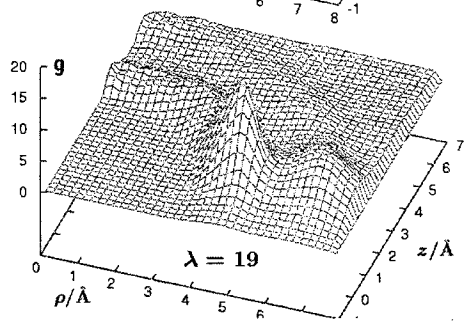

Dependence on equivalent weight & water content

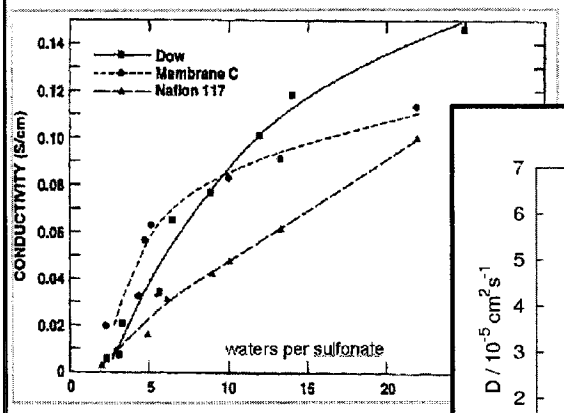

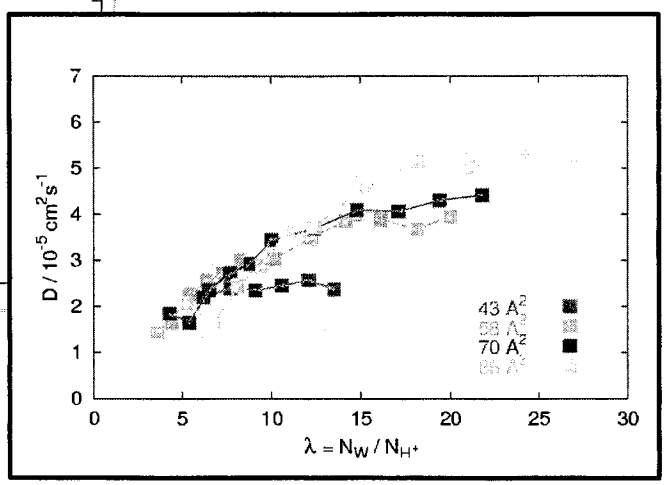

surface charge ↑
D ↓ $\Lambda \propto c\,D$ ↑

Activation Energies

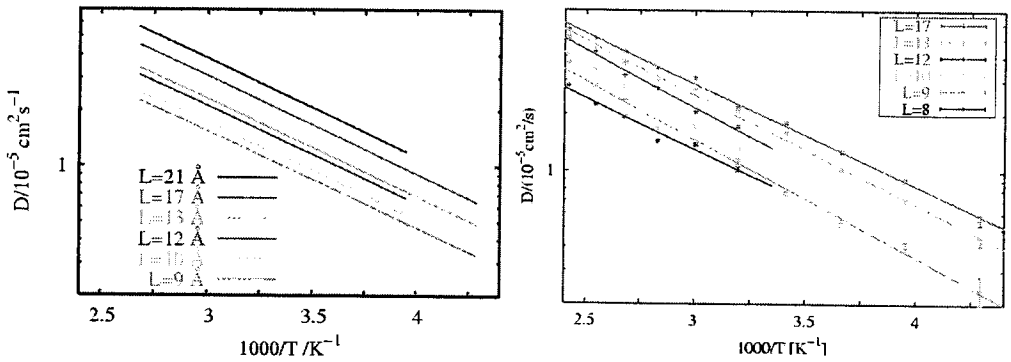

modified theory
- size
- form factor
- Debye Waller factor

simulation

Summary

- proton transfer in PEMs can be interpreted on the basis of the Grotthus mechanism
  - EVB model provides adequate (chemical) description
- strongest environmental effect on H^+ dynamics:
  - delocalization of stationary counter charge (acid strength, electronic effects)
  - flexibility of sulfonate head group and side chain are somewhat less important

Summary

- Conductivity increase with decreasing equivalent weight: double layer thickness ↔ concentration
- Activation energy of diffusion is independent of water content ↔ Poisson-Boltzmann theory
  ↔ Experiment
  3 Modified PB theory

=====>

- tortuosity of pores depends on water content
- pore dynamics

Conclusions

new membrane materials should:

- contain strong acids
  (sulfonic acids → sulfonyl imides)
- electronically stabilize the counter anion
  (PEEK, PEEKK)
- contain high ionic strength, in order to shift proton distribution into the pore interior
  (→ embedding of polar particles)

Who's who?

Alexei

Sean

Michael

Sasha

Jens

Peter

Eckhard

Alexei Kornyshev, Imperial College, London
Sean Walbran, Digital River Inc.
Michael Eikerling, TU München
Alexander Kuznetsov, Frumkin Institute, Moscow
Jens Ulstrup,Technical University Kopenhagen
Peter Commer, Forschungszentrum Jülich

$$: BMWi
CPU: NIC

Forschungszentrum Jülich
in der Helmholtz-Gemeinschaft

Jül-4013
November 2002
ISSN 0944-2952